

✓ CENTER FOR SPACE RESEARCH
MASSACHUSETTS INSTITUTE OF TECHNOLOGY



FACILITY FORM 602

N70-29795 (THRU)

(ACCESSION NUMBER) 314 (CODE) 07

(PAGES) CR-110355

(NASA CR OR TMX OR AD NUMBER)



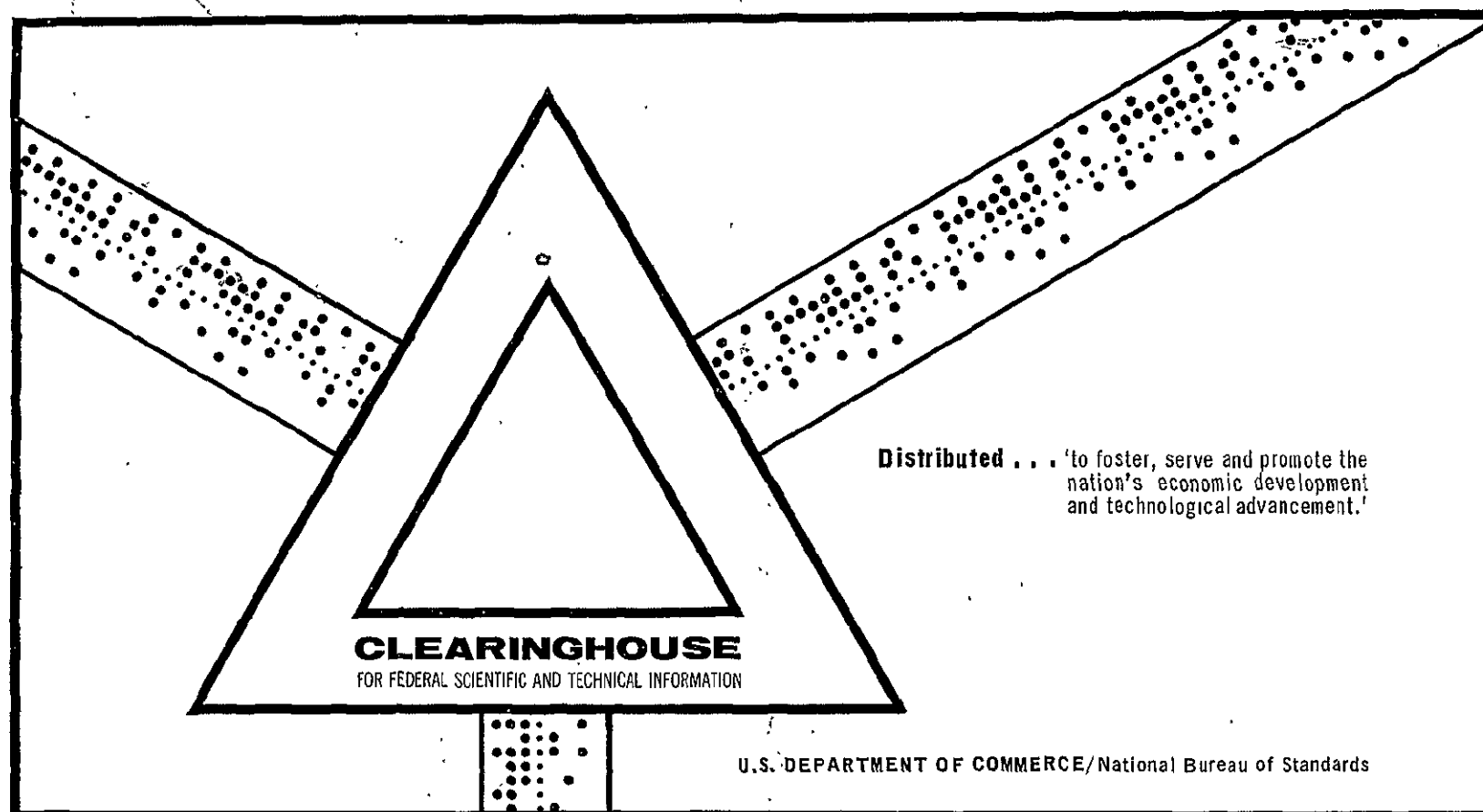
REPRODUCED BY
NATIONAL TECHNICAL
INFORMATION SERVICE
U.S. DEPARTMENT OF COMMERCE
SPRINGFIELD, VA 22161

ANALYSIS OF A COMMUNICATION SATELLITE FOR LUNAR
FAR-SIDE EXPLORATION

Jeffrey R. Kurland, et al.

Massachusetts Institute of Technology
Cambridge, Massachusetts

June 1970



This document has been approved for public release and sale.

NGL-22-009-019

ANALYSIS OF A COMMUNICATION SATELLITE
FOR LUNAR FAR-SIDE EXPLORATION

by

Jeffrey R. Kurland
and
Carl H. Goodwin

CSR T-70-1

June 1970

PRECEDING PAGE BLANK NOT FILMED.

ANALYSIS OF A COMMUNICATION SATELLITE
FOR LUNAR FAR-SIDE EXPLORATION

by

Jeffrey R. Kurland
and
Carl H. Goodwin

Submitted to the Department of Aeronautics and Astronautics
on May 21, 1970 in partial fulfillment of the requirements
for the degree of Master of Science

ABSTRACT

This report presents the feasibility and conceptual design of a communication satellite which provides a real-time, two-way communications link between the Earth and a spacecraft located behind the Moon. This satellite is compatible with the current United States lunar exploration program, Project Apollo, and is capable of relaying color television, voice, high-bit-rate telemetry data, and ranging code from the Command and Service Module and the Lunar Module during all phases of their mission.

The 905-pound satellite has a useful lifetime of four years and is envisioned for launch in the 1973-74 period via a Thrust Augmented Thor-Delta vehicle. A lunar fly-by trajectory places the satellite behind the Moon in a bounded 3500 kilometer radius halo orbit about the Earth-Moon L_2 libration point. This halo orbit affords the satellite a continuous view of both the Earth and the entire lunar back side. However, due to the instability of this orbit, periodic orbit corrections are performed by a set of special thrusters.

The satellite features a ten-foot diameter parabolic antenna and two 40-square foot solar panels. The antenna has two feeds: one feed is fixed and pointed towards the center of the Moon; the other feed is mechanically steerable and points toward the Earth. An antenna pointing accuracy of

+ .25 degrees is achieved by a three-axis attitude stabilization system consisting of momentum wheels and reaction-control thrusters. Moon horizon scanners, Sun sensors, and a Canopus star tracker are used for attitude sensing. The total operational power requirement of the satellite is 471 watts, with an RF power output of 80 watts.

Thesis Supervisor: John V. Harrington

Title: Professor of Aeronautics and Astronautics
Director, Center for Space Research

TABLE OF CONTENTS

I.	GENERAL INTRODUCTION	9
	1.1 Problem Statement	9
	1.2 Proposed Problem Solution	11
II.	APOLLO COMMUNICATION PERFORMANCE ANALYSIS	19
	2.1 CSM/MSFN and LM/MSFN Relay Links	19
	2.2 EVCS/LM/MSFN Relay Links	30
	2.3 ALSEP/MSFN Relay Links	33
	2.4 Apollo Communication Specifications	38
III.	SATELLITE COMMUNICATION PERFORMANCE ANALYSIS	45
	3.1 Frequency Selection	46
	3.2 Link Calculations	50
	3.3 Performance Trade-Off Analysis	51
	3.4 Satellite Communication Specifications	59
IV.	SATELLITE TRAJECTORY AND ORBIT CONTROL	63
	4.1 Launch Specifications	63
	4.2 Earth to L_2 Libration Point Trajectory	66
	4.3 L_2 Libration Point Orbit Control	68
V.	SATELLITE CONCEPTUAL DESIGN	71
	5.1 Design Constraints	71
	5.2 Proposed Configuration	72
	5.3 Equipment Location	77

VI.	SATELLITE SUBSYSTEMS	81
6.1	Communication Subsystem	81
6.1.1	Transponder	83
6.1.2	Power Amplifiers	88
6.1.3	Telemetry and Command	95
6.1.4	Antenna Characteristics	98
6.2	Attitude Control Subsystem	101
6.2.1	Definition of Satellite Axes and Attitude	103
6.2.2	Attitude Disturbance Torques	105
6.2.3	Attitude Sensors	109
6.2.4	Attitude Correcting Torques	111
6.2.5	Operation of the Attitude Control Subsystem	113
6.2.6	Sun Sensors	115
6.3	Power Supply Subsystem	116
6.3.1	Power Requirements	116
6.3.2	Solar Panels	118
6.3.3	Batteries	119
6.3.4	Operation of the Power Supply Subsystem	121
6.4	Structures Subsystem	124
6.4.1	General Description	125
6.4.2	Solar Panel Support and Drive Mechanism	126
6.4.3	Yo-Yo Despin	127

APPENDIX

A.	COMMUNICATION CALCULATIONS	129
A.1	Sample Link Calculation	129
A.2	Effective Antenna Noise Temperature	131
A.3	Effective System Noise Temperature	135
A.4	Parabolic Antenna Size and Beamwidth	139
B.	L_2 LIBRATION POINT ANALYSIS	141
B.1	Definition of Libration Points	141
B.2	Calculation of the L_2 Libration Point Position	143
B.3	Satellite Displacement from the L_2 Libration Point	145
B.4	Equations of Motion about the L_2 Libration Point	147
B.5	Free Motion in the Vicinity of the L_2 Libration Point	155
B.6	Controlled Motion in the Vicinity of the L_2 Libration Point	157
B.7	Periodic and Nonlinear Perturbation Effects	164
C.	LUNAR ORBIT DYNAMICS	167
C.1	Planar Relationships	167
C.2	Lunar Orbit Plane Motion	169
D.	TRAJECTORY ANALYSIS	173
D.1	Description of Computer Program	173
D.2	Lunar Orbit Plane Trajectory	174
D.3	Out-of-Plane Trajectory	179
D.4	Direct Transfer Trajectory	181

E.	POWER SUBSYSTEM CALCULATIONS	183
E.1	Solar Panel Area	183
E.2	Battery Capacity	187
F.	TABLES OF PHYSICAL DATA FOR THE SATELLITE	191
F.1	Launch Vehicle	191
F.2	Weight, Size, and Moments of Inertia	192
F.3	Calculation of Center of Mass and Center of Pressure	192
F.4	Thruster Equipment	192
	REFERENCES	207
	BIBLIOGRAPHY	209

CHAPTER I

GENERAL INTRODUCTION

1.1 PROBLEM STATEMENT

In order to conduct an exploration mission on the far-side of the Moon, a real-time communications capability between the Earth and the Apollo spacecrafts must be provided. The major problem in providing this capability is the spacecraft's inability to have a direct view of the Earth from the lunar back-side. One solution which appears most feasible is the deployment of a specially designed lunar relay communication satellite (LCS) which would be able to view both the lunar back-side and the Earth simultaneously. Such a satellite would relay voice, data, and television from the lunar back-side to the Earth, while also providing voice and data to be transmitted from the Earth to the lunar back-side. This satellite might also be used to provide for navigation of a lunar surface roving vehicle, in addition to assisting in precision landing missions on the lunar front-side.

To interface an LCS into the current and post Apollo Moon exploration programs, the following design constraints must be considered:

- Continuous lunar back-side coverage is required; no front-side coverage is necessary.
- The LCS must be compatible with the existing (or proposed updated) Apollo spacecraft hardware and the existing Manned Space Flight Network ground sites.
- The satellite is to have an operational lifetime of four years.
- The satellite is to be operable on-station for 45 days during an Apollo mission; there will be a maximum of two missions per year.
- Unified S-Band parameters are assumed for all links via the LCS.
- Narrowband color television is required from the lunar back-side.
- Real-time relay of all data and voice is required, including the ALSEP experiment packages.
- Range and range-rate tracking may be achieved via the relay.

- Communications may be initiated from either end of the link.
- No VHF relay is required.

Thus, it is the purpose of this study to investigate the feasibility and conceptual design of an LCS subject to these constraints.

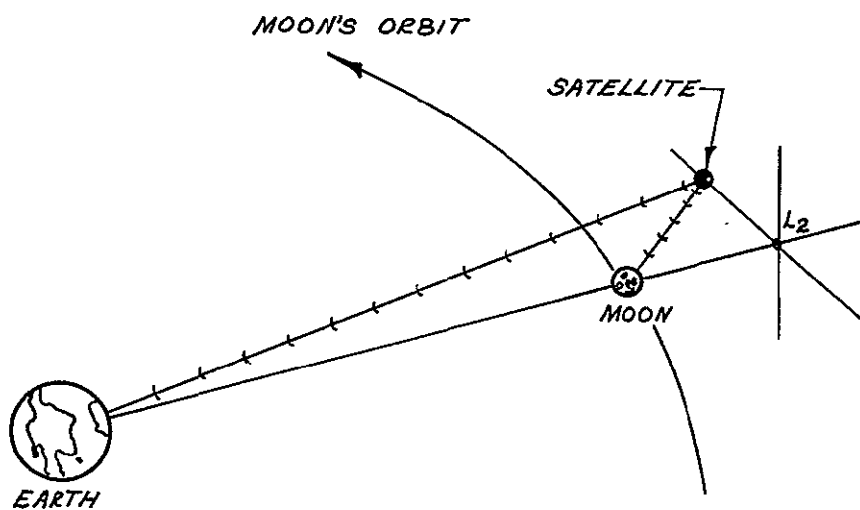
1.2 PROPOSED PROBLEM SOLUTION

Early studies have disclosed two feasible schemes for deployment of an LCS (Reference 1). One scheme suggests a Moon-synchronous LCS located behind the Moon in the vicinity of one of the Earth-Moon libration points (L_2 ; Section B.2). This type of LCS has high station-keeping costs, but is able to maintain a constant direct view of both the lunar back-side and the Earth simultaneously. The other scheme to provide lunar back-side coverage is to deploy a system of LCS satellites in lunar orbit. This system of orbiting satellites is arranged so at least one satellite is always able to provide the desired relay from the lunar back-side to the Earth.

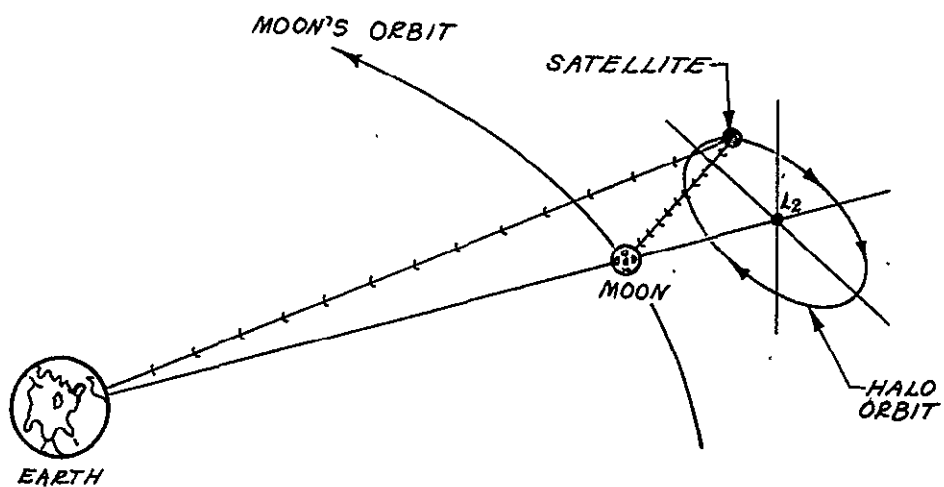
A communication performance evaluation of these two schemes (References 2 and 3) reveals the main advantage of the libration point LCS: that the satellite appears nearly stationary from the Moon and thus is conveniently acquired and tracked by a vehicle on the

surface of the lunar back-side or in orbit about the Moon. This scheme permits the use of a high gain, narrowbeam antenna on the Apollo spacecrafts, thereby providing the necessary performance requirements for the existing Unified S-Band system. For the orbiting scheme, continual acquisition and tracking of the LCS is necessary in order to maintain coverage. This is undesirable because the lunar surface Apollo communication system requires modifications in order to provide its high gain antenna with a tracking capability. Thus, due to communication considerations, a libration point LCS appears most practical.

There are two types of libration satellites which can be deployed. One type of libration satellite, the Hummingbird, maintains itself on-station at a fixed point, offset from L_2 relative to the Earth-Moon line by means of a continuous, low-level thrust (Reference 4). However, at the present time, it is not possible for a chemical thruster to achieve this thrust requirement and so this scheme does not appear feasible. An ion thruster has also been suggested for this application, but it will not be available until the late 1970's. Figure 1.1a shows the geometry of the Hummingbird system. The second kind of libration satellite which has been investigated is the halo orbit satellite (Reference 5). It is aptly named because its motion as viewed from the



(a) HUMMINGBIRD



(b) HALO ORBIT

Figure 1.1 Geometry of Libration Point Relay Satellites

Earth appears as a halo (or circle) which encircles the Moon (see Figure 1.1b). This halo orbit is the result of proper phasing of two simple harmonic motions about the libration point; one motion is in the lunar orbit plane and has a slightly shorter period than the other motion which is normal to the lunar orbit plane. The periods of these two motions are 14.67 and 15.30 days respectively. The proper phasing of the two modes is the principal stationkeeping requirement of the halo orbit satellite propulsion system.

Past studies have sought to examine and analyze the communication and orbital requirements for an LCS capable of meeting the proposed design constraints in Section 1.1. This is due to (i) the limited communication capability between the Apollo vehicles and the LCS which prohibits the transmission of television and high bit-rate telemetry data, and (ii) the high stationkeeping costs required to maintain the halo orbit of the LCS for a period of several years. For the design which is to be presented, it is shown that television and high bit-rate telemetry data can be transmitted by making minor modifications to the existing Apollo communication system. These modifications do not reflect actual or planned design changes to the existing Apollo configuration, but are intended to illustrate how an LCS can fulfill all of the Apollo communication requirements by

applying present state-of-the-art techniques. In addition, stationkeeping costs can be sizeably reduced by keeping the LCS in the halo orbit only during the period of an actual mission; whenever the satellite is not being used, it can be allowed to drift in a bounded orbit about the libration point (Section B.5).

By applying these two assumptions, a practical conceptual design of a lunar libration-point communication satellite has been formulated. Figure 1.2 is a picture of this satellite. The major results of this design are summarized in Table 1.1.

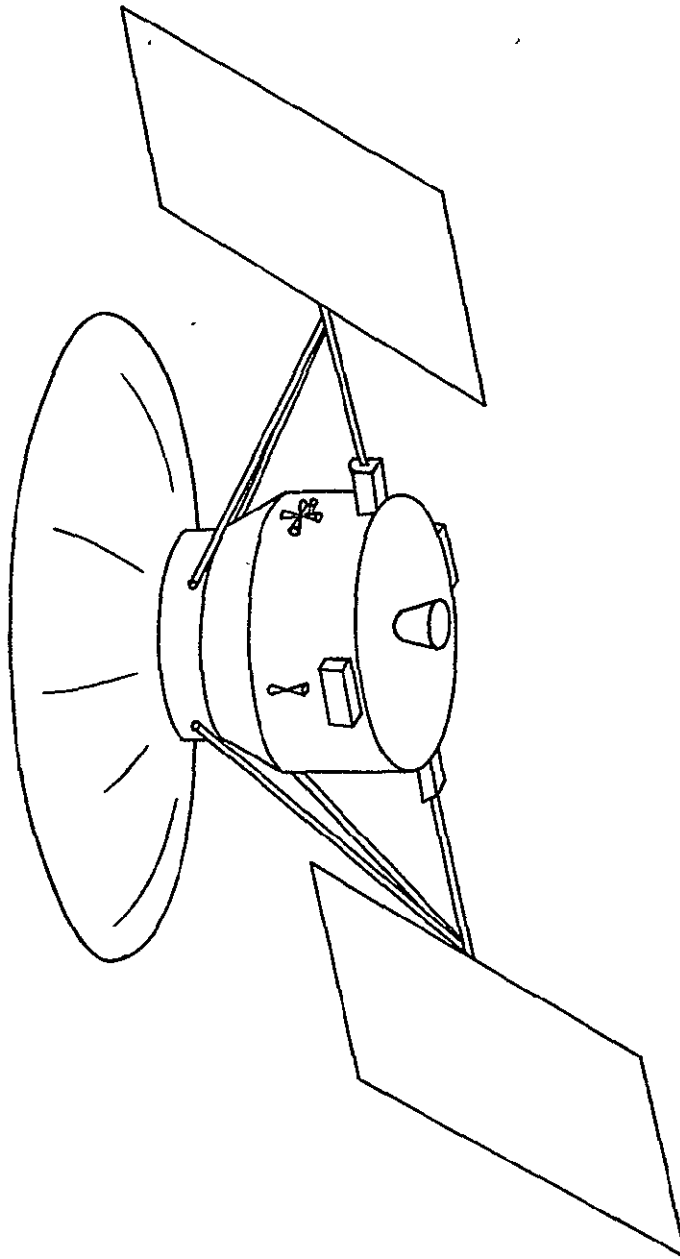


Figure 1.2 Proposed Satellite Conceptual Design

Table 1.1

PROPOSED LCS DESIGN PARAMETERS

PARAMETER	SPECIFICATION
Operational Life	4 years; 8 Apollo missions
Launch Vehicle	Thor Delta (Thrust Augmented)
Overall Dimensions	
Body	
Length	42 inches
Diameter	Maximum: 48 inches
	Minimum: 36 inches
Solar Panels (2)	8 x 5 feet (Silicon Cells)
Weight	
At Launch	905 pounds
On-Station	750 pounds
Communications	
Frequency	S-Band
Data Capability	All modes of Apollo communication system, including color television
Transmitter Power	
To Apollo Spacecrafts	80 watts
To Earth	5 watts
Antennas	
Size	10-foot diameter parabolic (1 fixed feed for lunar coverage and 1 steerable feed for Earth coverage)
Illumination Area	Full illumination of both Earth and Moon
Polarization	Right-hand circular
Electrical Power	
Power Source	
Primary	Solar panels
Secondary	Batteries (NiCad)
Maximum Power Requirement	471 watts
Minimum Power Requirement	251 watts

Table 1.1
CONTINUED

PARAMETER	SPECIFICATION
Attitude Control	
Accuracy Requirement	$\pm .25^\circ$
Torque Source	Momentum wheels, Thrusters
Sensors	Gyros, Moon, and Canopus
Thermal Control	
Equipment	Heat pipes, Electrical heaters

CHAPTER II

APOLLO COMMUNICATION PERFORMANCE ANALYSIS

The Apollo communication system consists of a combination of relay links between the Manned Space Flight Network (MSFN) and the Command and Service Module (CSM), the Lunar Module (LM), the astronaut's Extra-vehicular Communications System (EVCS) used during their walk on the surface of the Moon, and the Apollo Lunar Surface Experiments Packages (ALSEP). In order to effectively describe the communication systems being used in this study, three major relay links are defined: (i) the CSM/MSFN and LM/MSFN relay links, (ii) the EVCS/LM/MSFN relay link, and (iii) the ALSEP/MSFN relay link. The following is a brief description of these links.

2.1 CSM/MSFN AND LM/MSFN RELAY LINKS

The Earth-based Manned Space Flight Network (MSFN) is managed by NASA's Goddard Space Flight Center and consists of many ground stations around the globe, each with the capability of tracking and acquiring data from the Apollo spacecrafts. Every site is equipped

with either an 85-foot or 30-foot parabolic antenna and are referred to as Unified S-Band sites because only one antenna and one system handles all of the communication functions: TV, voice, telemetry, and tracking. In addition to these land-based sites across the United States and in several foreign countries, stations are also located on the sea and in the air in specially designed ships and converted aircraft. All of these stations are tied together by the NASCOM network. This is a combination of radio, satellite, and land-line communication systems that performs the complex task of keeping the MSFN sites linked together so that the transmitted Apollo voice, data, and TV flows uninterrupted into the NASA Manned Spacecraft Center in Houston, Texas.

During an Apollo mission, the Unified S-Band System handles the following communication channels: via the up-link (from Earth to the CSM and LM), voice and up-data; via the down-link (from the CSM and LM to Earth), voice telemetry, television, biomedical data, and emergency key. In addition, range and range-rate information are also provided by this system. Voice includes normal and back-up modes on both links. Telemetry includes real-time and playback PCM data for both high (51.2 Kbps) and low (1.6 Kbps) bit rates. A

summary of the Unified S-Band (USB) capabilities at the MSFN sites is shown in Table 2.1 (Reference 6).

Various combinations of these data channels have been grouped into defined operational communication modes. Throughout a mission, only one mode is transmitted during a particular period of time, for sometimes it is more desirable to maintain strong voice contact rather than to transmit large amounts of telemetry data. A listing of the modes and the services provided by each can be found in the first and second columns of Tables 2.2 through 2.4 (Reference 5).

The modulation techniques employed by the Unified S-Band System are phase modulation (PM) and frequency modulation (FM). Both of these techniques are closely related to each other, since they are examples of angle modulation. PM is used in both the up-links and the down-links, while FM is used only for television transmission to the Earth (on the down-link). The modulation techniques for the different information modes are shown in the third columns of Tables 2.2-2.4. It should be noted that in certain modes, one of the modulating functions is angle-modulated directly onto the carrier, while the remaining functions are angle-modulated onto the sinusoidal subcarrier frequencies.

Table 2.1

UNIFIED S-BAND CAPABILITIES

STATION	VOICE	TLM	TRACKING AND RANGING	UP-DATA	TV ^a	EMERGENCY KEY	30-ft ANTENNA	85-ft ANTENNA	COOLED PREAMP
MILA ^b	X	X	X	X	X	X	X		
BERMUDA	X	X	X	X			X		
GRAND BAHAMA	X	X	X	X			X		
ANTIGUA	X	X	X	X			X		
ASCENSION ^b	X	X	X	X			X		X
CANARY ISLAND	X	X	X	X			X		
GUAM ^b	X	X	X	X			X		X
HAWAII ^b	X	X	X	X			X		X
CARNARVON ^b	X	X	X	X			X		X
GUAYMAS	X	X	X	X			X		
TEXAS	X	X	X	X			X		
CANBERRA ^b	X	X	X	X	X	X		X	X
GOLDSTONE ^b	X	X	X	X	X	X		X	X
MADRID	X	X	X	X	X	X		X	X

Table 2.1
CONTINUED

- a. All 30-foot and 85-foot stations (plus 3 ships) have TV recording capability. Stations which are checked in this column also have the capability for real-time frequencies to Mission Control.
- b. Dual capability (can communicate with CSM and LM simultaneously provided both spacecraft are within the coverage region of the ground antenna).

Table 2.2

APOLLO COMMAND AND SERVICE MODULE
TRANSMISSION CHARACTERISTICS (DOWN-LINK)

CARRIER COMBINATION MODE*	INFORMATION	MODULATION TECHNIQUE
CSM PM Mode 1	Voice 51.2 Kbps	FM/PM PCM/PM/PM
CSM PM Mode 2	PRN Ranging Voice 51.2 Kbps TLM	PM on Carrier FM/PM
CSM PM Mode 3	PRN Ranging Voice 1.6 Kbps TLM	PM on Carrier FM/PM PCM/PM/PM
CSM PM Mode 4	Voice 1.6 Kbps TLM	FM/PM PCM/PM/PM
CSM PM Mode 5	1.6 Kbps TLM	PCM/PM/PM
CSM PM Mode 6	Emergency Key	AM/PM
CSM PM Mode 7	PRN Ranging	PM on Carrier
CSM PM Mode 8	Backup Voice 1.6 Kbps TLM	PM on Carrier PCM/PM/PM
CSM PM Mode 9	PRN Ranging 1.6 Kbps TLM	PM on Carrier PCM/PM/PM
CSM PM Mode 10	Backup Voice	PM on Carrier
CSM FM Mode 1	Playback Voice at 1:1 51.2 Kbps TLM	FM at Baseband PCM/PM/FM

Table 2.2
CONTINUED

CARRIER COMBINATION MODE*	INFORMATION	MODULATION TECHNIQUE
CSM FM Mode 2	Playback Voice at 32:1 1.6 Kbps TLM	FM at Baseband PCM/PM/FM
CSM FM Mode 3	Playback 1.6 Kbps Split Phase TM from LM at 32:1	FM at Baseband
CSM FM	Television	FM at Baseband

* Each mode represents a unique combination of different forms of communications data (i.e., voice, PRN [pseudo random noise] ranging code, 51.2 Kbps and 1.6 Kbps TLM, etc.). During a given time period, only one specific mode is transmitted. The choice of mode is determined according to the form of data which is desired at that particular time.

Table 2.3

APOLLO LUNAR MODULE

TRANSMISSION CHARACTERISTICS (DOWN-LINK)

CARRIER COMBINATION MODE*	INFORMATION	MODULATION TECHNIQUE
LM PM Mode 1	Voice 51.2 Kbps TLM	FM/PM PCM/PM/PM
LM PM Mode 2	PRN Ranging Voice 51.2 Kbps TLM	PM on Carrier FM/PM PCM/PM/PM
LM PM Mode 3	1.6 Kbps TLM	PCM/PM/PM
LM PM Mode 4	Backup Voice 1.6 Kbps TLM	PM on Carrier PCM/PM/PM
LM PM Mode 5	Backup Voice	PM on Carrier
LM PM Mode 6	Emergency Key	AM/PM
LM PM Mode 7	Voice/Biomed 1.6 Kbps TLM	FM/PM PCM/PM/PM
LM PM Mode 8	Backup Voice/ Biomed 51.2 Kbps TLM	PM on Carrier PCM/PM/PM
LM FM Mode 9	Voice/PLSS/Biomed 1.6 Kbps or 51.2 Kbps TLM	FM/FM PCM/PM/FM
LM FM Mode 10	Television Voice/PLSS/Biomed 1.6 Kbps or 51.2 Kbps TLM	FM at Baseband FM/FM PCM/PM/FM

Table 2.3
CONTINUED

* Each mode represents a unique combination of different forms of communications data (i.e., voice, PRN [pseudo random noise] ranging code, 51.2 Kbps and 1.6 Kbps TLM, etc.). During a given time period, only one specific mode is transmitted. The choice of mode is determined according to the form of data which is desired at that particular time.

Table 2.4

MANNED SPACE FLIGHT NETWORK
TRANSMISSION CHARACTERISTICS (UP-LINK)

CARRIER COMBINATION MODE*	INFORMATION	MODULATION TECHNIQUE
MSFN Mode 1	PRN Ranging	PM on Carrier
MSFN Mode 2	Voice	FM/PM
MSFN Mode 3	Up-Data	FM/PM
MSFN Mode 4	PRN Ranging Voice	PM on Carrier FM/PM
MSFN Mode 5	PRN Ranging Up-Data	PM on Carrier FM/PM
MSFN Mode 6	PRN Ranging Voice Up-Data	PM on Carrier FM/PM FM/PM
MSFN Mode 7	Voice Up-Data	FM/PM FM/PM
MSFN Mode 8	Backup Voice	FM/PM

* Each mode represents a unique combination of different forms of communications data (i.e., voice, PRN [pseudo random noise] ranging code, 51.2 Kbps and 1.6 Kbps TLM, etc.). During a given time period, only one specific mode is transmitted. The choice of mode is determined according to the form of data which is desired at that particular time.

The USB System frequency spectrum is centered about 2.3 GHz for the up-links and 2.1 GHz for the down-links. Table 2.5 shows the frequency specifications and the type of information which is transmitted at each frequency for both links. It should be noted that while the CSM transmits PM and FM at separate frequencies, that the LM transmits both PM and FM at the same frequency.

Table 2.5

CURRENT APOLLO COMMUNICATION SPECTRUM

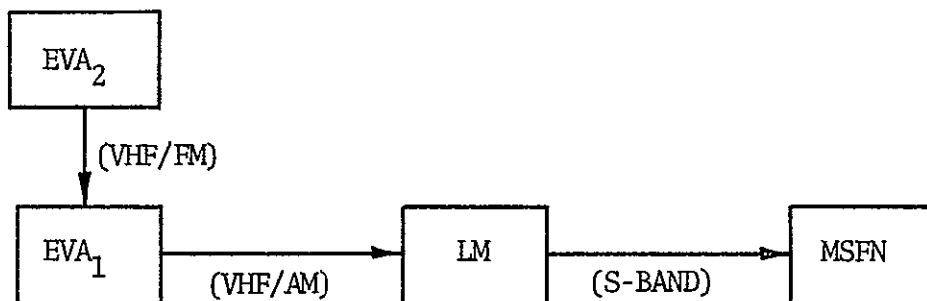
LINK	FREQUENCY	DATA CONTENT
UP-LINK		
Earth-to-CSM (PM)	2106.4 MHz	Telemetry, Voice, Range, Doppler
Earth-to-LM (PM)	2101.8 MHz	Telemetry, Voice, Range, Doppler
DOWN-LINK		
CSM-to-Earth (PM)	2287.5 MHz	Telemetry, Voice, Range, Doppler
(FM)	2272.5 MHz	Television, Telemetry, Voice
LM-to-Earth (PM)	2282.5 MHz	Telemetry, Voice, Range, Doppler
(FM)	2282.5 MHz	Television, Telemetry, Voice

2.2 EVCS/LM/MSFN RELAY LINKS

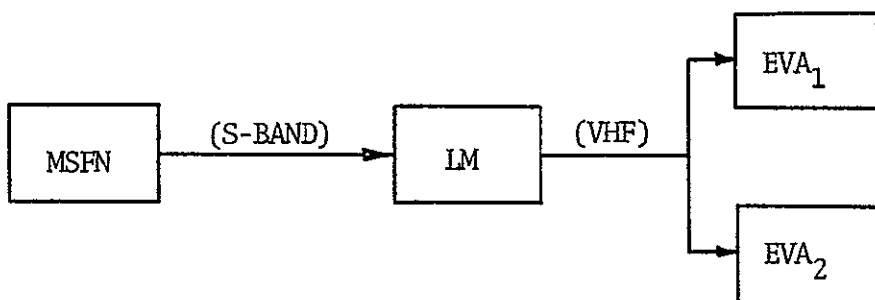
When the astronauts are on the surface of the Moon performing their extravehicular activities outside of the Lunar Module, a specialized and important network is required to maintain communications between the astronauts and the Manned Space Flight Network. This network, called the Extravehicular Communications System (EVCS), relays voice and data simultaneously from the two extravehicular astronauts (EVA's) through the LM to the MSFN. This total relay can be divided into three links: the EVA_2/EVA_1 (VHF/FM), the EVA_1/LM (VHF/AM), and the LM/MSFN (S-Band) links. A flow chart of these links is shown in Figure 2.1 (Reference 6).

The data transmitted from each EVA is of two types. The first is biomedical data supplied in the form of a continuous electrocardiogram (EKG). The second type is Portable Life Support System (PLSS) status data. These data consist of eight critical parameters which are sampled to provide a pulse amplitude modulated (PAM) waveform. In addition, the astronaut's voice is transmitted.

In the EVA_2/EVA_1 link, both the EKG data and the PLSS status data from one astronaut (designated as EVA_2) are modulated onto subcarriers. These two subcarriers and the astronaut's voice are frequency modulated (FM)



(a) DOWN-LINK (EVA₂/EVA₁/LM/MSFN)



(b) UP-LINK (MSFN/LM/EVA₁; MSFN/LM/EVA₂)

Figure 2.1 Block Diagram of Extravehicular Communications System (EVCS)

onto a VHF carrier which is transmitted to the other astronaut (designated as EVA₁). The received carrier from EVA₂ is demodulated in EVA₁'s VHF receiver, thus providing two data subcarriers and voice at baseband. At this point, the EVA₁/LM link begins, where an EKG subcarrier, PLSS status subcarrier, and EVA₁'s voice are added to the demodulated information received from EVA₂. A VHF carrier is amplitude modulated (AM) by the combined information of both EVA's and the carrier is then transmitted to the LM. At the LM, the received AM carrier is demodulated and the voice plus the four data subcarriers are processed for transmission to the MSFN via the LM/MSFN S-Band link. This is accomplished by summing the four EVCS subcarriers and two voice channels onto new subcarriers. Then, they are modulated onto another subcarrier, which is also summed with a PCM telemetry subcarrier from the LM (and sometimes baseband television). This composite signal frequency modulates an S-Band carrier for transmission to the MSFN.

The combination of these data into various modes for transmission to the MSFN from the LM are shown in Table 2.3, Modes 8, 9 and 10. In Mode 9, voice is transmitted from the astronauts while they are in the LM and/or performing their EVA, plus EVCS PLSS status data, and EVA EKG, in addition to both high and low bit rate

telemetry data from the LM. Mode 10 is almost identical to Mode 9 with the exception that television is transmitted simultaneously along with the other data. Both Modes 9 and 10 are FM modes. The LM Mode 8 is a PM mode, designed for use in the event that the subcarrier oscillator in the LM used for the EVA data should fail. In this mode, baseband voice, the EVCS biomedical data, and low bit rate LM telemetry data are summed and the composite signal then PM modulated onto the carrier for transmission to the MSFN.

The frequency spectrum for the EVCS/LM/MSFN relay links is both VHF and S-Band. Table 2.6 shows the frequency specification and the types of information which are transmitted at each frequency for the three links which comprise the total relay.

2.3 ALSEP/MSFN RELAY LINKS

The Apollo Lunar Surface Experiment Package (ALSEP) is a set of scientific instruments and supporting subsystems which are delivered to the lunar surface aboard the Lunar Module. The astronauts place the equipment on the lunar surface, implant sensors, and activate some of the experiments. After the astronauts return to Earth, the ALSEP package is unmanned and self-sufficient with a nuclear-powered electrical system.

Table 2.6

EVCS/LM/MSFN COMMUNICATION SPECTRUM

LINK	FREQUENCY	DATA CONTENT
UP-LINK		
MSFN-to-LM (PM)	2101.8 MHz	VOICE, UPDATA
LM-to-EVA ₂	296.8 MHz	VOICE
LM-to-EVA ₁ (AM)	296.8 MHz	VOICE
DOWN-LINK		
EVA ₂ -to-EVA ₁ (FM)	279.0 MHz	VOICE, DATA
EVA ₁ -to-LM (AM)	259.7 MHz	VOICE, DATA (DATA: EVA ₂ and EVA ₁)
LM-to-MSFN (FM)	2282.5 MHz	VOICE, DATA TELEVISION (DATA: EVA ₂ , EVA ₁ and LM)
CROSS-LINK		
EVA ₁ -to-EVA ₂ (AM)	259.7 MHz	VOICE

The ALSEP measures lunar physical and environmental characteristics and transmits the data to Earth MSFN stations for a period of 1 year (Reference 7). The eight types of experiments in the ALSEP system are

- Passive Seismic Experiment Subsystem
- Magnetometer Experiment Subsystem
- Solar Wind Experiment Subsystem
- Suprathermal Ion Detector Experiment Subsystem
- Active Seismic Experiment Subsystem
- Heat Flow Experiment Subsystem
- Charged Particles Lunar Environment Experiment Subsystem
- Cold Cathode Gauge Experiment

Since weight and volume restrictions on the LM preclude carrying all of the experimental subsystems on any one flight, only two or three of the eight experiments are assigned to a particular flight.

A simplified block diagram of the ALSEP system is shown in Figure 2.2. The data generated by this system are initially in digital and/or analog form. However, before transmission, all of the analog data are converted to digital form at the data subsystem. Then, the experimental data (which is all in digital form) and ALSEP telemetry data are split phase-modulated onto an S-Band carrier for transmission to the MSFN.

There are three bit rates associated with each mode of operation for this system, namely

Contingency Mode	0.530 Kbps
Normal Mode	1.060 Kbps
High Mode	10.600 Kbps

This data is usually transmitted in the normal mode, while the contingency mode serves as a commandable back-up. The high mode data rate is used only when the Active Seismic Experiment is included on a particular mission.

The up-link transmissions from the MSFN-to-ALSEP are to issue commands to any of the experiment packages or the supporting subsystem. These commands are in the form of phase-shift-keyed signals and are received by the ALSEP at S-Band from the MSFN.

Each ALSEP transmits to the MSFN on a different USB frequency. Listed below are the frequency assignments for the first four ALSEP's

ALSEP 1 to MSFN	2276.5 MHz
ALSEP 2 to MSFN	2278.5 MHz
ALSEP 3 to MSFN	2275.5 MHz
ALSEP 4 to MSFN	2279.5 MHz

For the up-link commands, the frequency is 2119.0 MHz for all ALSEP's. This requires that the command format includes a decoder address that identifies which ALSEP is to receive a given command.

2.4 APOLLO COMMUNICATION SPECIFICATIONS

The parameters for the Apollo and ALSEP systems are presented in Table 2.7 and the values represent current Apollo hardware. A modified Apollo system is also presented in Table 2.8. These modifications do not reflect actual or planned design changes to the existing Apollo configuration, but are intended to illustrate a system which could be obtained by application of present state-of-the-art improvements.

The following assumptions were made for the determination of some system parameters.

- Antenna temperature
 - includes all terrestrial and extra-terrestrial noise sources, plus noise contributions inherent to the antenna structure
 - the Apollo spacecraft viewing condition to the LCS is a quiet sky
 - the ground station viewing condition to the LCS is Moon-at-zenith

- the LCS antenna viewing condition to the Apollo spacecrafts is Moon-at-zenith
- the LCS antenna viewing condition to the ground station is Earth-at-zenith
- all antennas are right-hand circular polarized (RCP)
- a cooled parametric amplifier is used at the ground station
- the LCS has a low receiver noise figure due to the use of a low-noise solid-state preamplifier preceding the translation-repeater electronics

Table 2.7

APOLLO COMMUNICATION SYSTEM PARAMETERS

PARAMETER	PARAMETER VALUE	UNITS	COMMENTS
MSFN			
Transmitter Power	10.0	Kw	
Transmit Antenna Gain			
30-foot	43.0	db	S-Band
85-foot	52.0	db	On-Axis
Receive Antenna Gain			
30-foot	44.0	db	S-Band
85-foot	53.0	db	On-Axis
210-foot	61.0	db	
Pointing loss, circuit losses, and polarization loss for 30-ft, 85-ft, and 210-ft antennas	--	--	Included in antenna gain
Receiver Noise Figure	0.8	db	
Effective System Noise Temperature	150.0	°K	Supercooled
CSM			
Transmitter Power	11.2	w	PM mode
	12.6	w	FM mode
Transmit Antenna Gain			
Wide Beamwidth	8.0	db	High Gain Antenna
Medium Beamwidth	18.0	db	S-Band
Narrow Beamwidth	26.7	db	On-Axis
Omnidirectional	0	db	

Table 2.7
CONTINUED

PARAMETER	PARAMETER VALUE	UNITS	COMMENTS
Receive Antenna Gain			
Wide Beamwidth	3.1	db	High Gain Antenna
Medium Beamwidth	22.5	db	S-Band
Narrow Beamwidth	23.0	db	
Omnidirectional	0	db	For 80% Coverage
Transmit Circuit Losses			
High Gain Antenna	6.6	db	All Beamwidths
Omnidirectional	4.5	db	
Pointing Loss			
High Gain Antenna	0.2	db	All Beamwidths
Receiving Circuit Losses			
High Gain Antenna	6.6	db	All Beamwidths
Omnidirectional	4.5	db	
Receiver Noise Figure	13.0	db	
Receiving Antenna Temperature	60.0	°K	
Receiver and Hardware Temperature	290.0	°K	
LM			
Transmitter Power	18.6	w	
Transmit Antenna Gain			
Steerable	20.5	db	S-Band
Erectable	34.0	db	
Omnidirectional	-3.0	db	
Receive Antenna Gain			
Steerable	16.5	db	S-Band
Erectable	33.2	db	On-Axis
Omnidirectional	-3.0	db	85% Coverage
Transmit Circuit Losses			
Steerable	3.8	db	
Erectable	7.8	db	
Omnidirectional	3.4	db	

Table 2.7
CONTINUED

PARAMETER	PARAMETER VALUE	UNITS	COMMENTS
Receive Circuit Losses			
Steerable	5.9	db	
Erectable	9.8	db	
Omnidirectional	5.7	db	
Pointing Loss			
Steerable	0.5	db	
Erectable	2.0	db	
Receiver Noise Figure	13.0	db	
Receiving Antenna Temperature	60.0	°K	
Receiver and Hardware Temperature	290.0	°K	
ALSEP			
Transmitter Power	1.02	w	
Transmit Antenna Gain	15.8	db	
Receive Antenna Gain	15.0	db	On-Axis
Transmit Circuit Losses	2.4	db	
Receive Circuit Losses	2.5	db	
Pointing Loss	3.0	db	
Effective System Noise Temperature	2804.0	°K	

Table 2.8

PROPOSED MODIFIED APOLLO SYSTEM PARAMETERS

PARAMETER	MODIFIED VALUE	UNITS	COMMENTS
Transmitter Power			
CSM	30.0	w	
LM	37.0	w	
Transmit Antenna Gain			
CSM	33.5	db	High Gain (Narrow-beam)
	3.0	db	Omnidirectional
LM	28.5	db	Steerable
	39.1	db	Erectable
	0.0	db	Omnidirectional
Receive Antenna Gain			
CSM	33.0	db	High Gain (Narrow-beam)
	3.0	db	Omnidirectional
LM	24.5	db	Steerable
	38.3	db	Erectable
	0.0	db	Omnidirectional
Transmit Circuit Losses			
CSM	3.0	db	All Antennas
LM	3.0	db	
Receive Circuit Losses			
CSM	3.0	db	All Antennas
LM	3.0	db	
Receiver Noise Figure			
CSM	4.0	db	Addition of solid-state
LM	4.0	db	preamplifier in the receiver

PRECEDING PAGE BLANK NOT FILMED.

PRECEDING PAGE BLANK NOT FILMED.

CHAPTER III

SATELLITE COMMUNICATION PERFORMANCE ANALYSIS

The interfacing of a lunar communication satellite (LCS) into the Apollo Unified S-Band System provides a communication capability between the Apollo spacecrafts and the Earth whenever the spacecrafts are located behind the Moon. This chapter presents the specification and analysis of the LCS communication parameters required to relay television, voice, ranging code, and data from the Apollo vehicles to the Earth, in addition to relaying voice, ranging code, and data from the Earth to the Apollo vehicles.

The weakest links in the CSM/LCS/MSFN and LM/LCS/MSFN communication system are between the LCS and the Apollo vehicles. The reasons for this are:

- The limited radio frequency output power of the LCS and Apollo vehicles.
- The antenna gain constraint at the LCS in order to avoid steering.
- The limited antenna gain at the Apollo spacecrafts due to physical size limitation and spacecraft attitude stability.

- The fact that the LCS is unmanned.
- The inability to employ ultra low noise receivers (20°K effective noise temperature) in conjunction with correlation and integration techniques which require equipment not compatible with spacecraft hardware.

Therefore, the design parameters determined initially for the LCS would provide the same quality signal to both Apollo vehicles and to the MSFN. It is then seen that such a design requires an excessively large antenna on the LCS and, consequently, special electronic equipment for antenna-beam tracking of the Apollo vehicles. A system is finally derived that requires only minor modifications of the current Apollo communication system in order to increase its communications performance, yet one that requires the LCS to have only a single antenna which radiates two beams: one beam wide enough to illuminate the entire lunar back-side; the other beam to illuminate the Earth. This type of system appears to be the most feasible and economical to implement.

3.1 FREQUENCY SELECTION

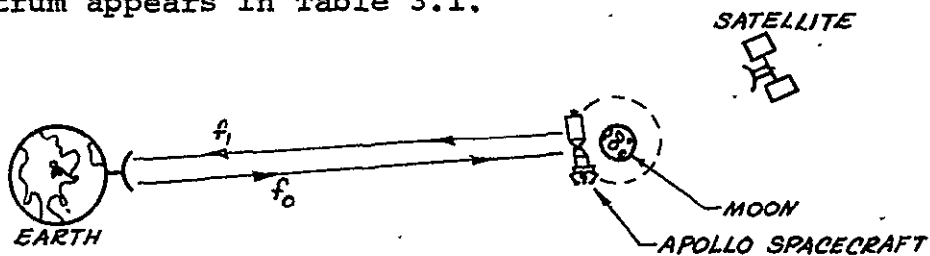
The S-Band frequency spectrum was chosen for this communication system in order to make the LCS compatible

with the existing Apollo Unified S-Band System. Whenever the CSM and LM spacecrafts are in direct view of the Earth, they broadcast directly to the MSFN at frequencies already specified (Table 2.6) for these links. And likewise, when they are on the back-side of the Moon, these same frequencies are used for the CSM/LCS and LM/LCS links. Thus, the frequency spectrum at the Apollo spacecrafts will always remain unchanged.

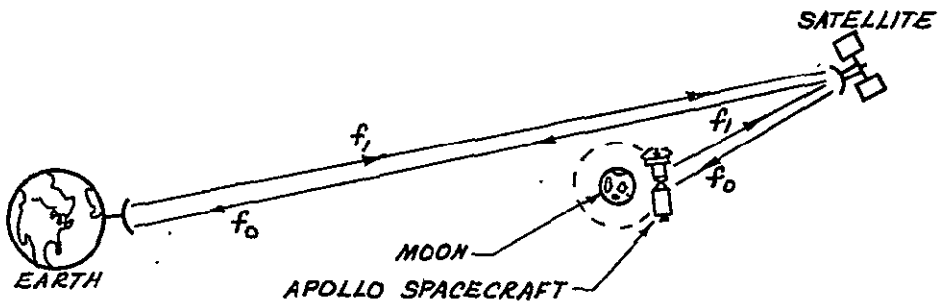
A frequency selection problem does arise, however, for the LCS/MSFN links. This is due to requirements of the signal which is retransmitted by the satellite: that a significant degree of isolation between the received and transmitted signals must exist in order to minimize interference between these two signals. This isolation can be achieved by changing the frequency of the retransmitted signal. This implies that a new set of frequencies must be chosen for the LCS/MSFN links while the CSM/LCS and LM/LCS links operate at their previously specified frequencies. Thus, a problem arises with respect to the selection of frequencies for the LCS/MSFN link.

A very feasible solution is envisioned which requires only minor modifications to the existing MSFN sites. This solution suggests using the same set of frequencies already established for the CSM/MSFN and LM/MSFN links. It is accomplished by making the

down-link frequency from the LCS to the MSFN the same as the up-link frequency from the MSFN to the spacecraft. And, accordingly, the up-link frequency from the MSFN to the LCS is the same as the down-link from the spacecraft to the MSFN. This technique provides a coherent frequency translation at the LCS which is critical for the Unified S-Band pseudo random noise (PRN) ranging technique. This is illustrated in Figures 3.1a and b. A complete description of the LCS frequency spectrum appears in Table 3.1.



(a) MSFN/APOLLO SPACECRAFT LINKS



(b) MSFN/LCS / APOLLO SPACECRAFT LINKS

Figure 3.1 LCS Communication Specifications

Table 3.1

LCS FREQUENCY SPECTRUM

UP-LINK		DOWN-LINK	
CSM			
MSFN-to-LCS (PM)	2287.5 MHz	CSM-to-LCS (PM) (FM)	2287.5 MHz 2272.5 MHz
LCS-to-CSM (PM)	2106.4 MHz	LCS-to-MSFN (PM) (FM)	2106.4 MHz 2092.2 MHz
LM			
MSFN-to-LCS (PM)	2282.5 MHz	LM-to-LCS (PM) (FM)	2282.5 MHz 2282.5 MHz
LCS-to-LM (PM)	2101.8 MHz	LCS-to-MSFN (PM) (FM)	2101.8 MHz 2101.8 MHz
ALSEP			
MSFN-to-LCS (PM)	2119.0 MHz	ALSEP (1)-to-LCS (PM)	2276.5 MHz
		ALSEP (2)-to-LCS (PM)	2278.5 MHz
		ALSEP (3)-to-LCS (PM)	2275.5 MHz
		ALSEP (4)-to-LCS (PM)	2279.5 MHz
LCS-to-ALSEP (PM)	1950.0 MHz	LCS (1)-to-MSFN (PM)	2095.5 MHz
		LCS (2)-to-MSFN (PM)	2097.5 MHz
		LCS (3)-to-MSFN (PM)	2094.5 MHz
		LCS (4)-to-MSFN (PM)	2098.5 MHz

3.2 LINK CALCULATIONS

The three most important parameters in a communication link are the transmitter power, transmit antenna gain, and the receive antenna gain. The extent to which a specified bandwidth of information can be transmitted via a particular link is related to these three parameters by the following relationship:

$$G_T + G_R + P_T = L_T + L_R + L_P + L_S + N_{in} + (S/N)_{in} \quad (3.1)$$

where

- G_T = transmit antenna gain (db)
- G_R = receive antenna gain (db)
- P_T = power amplifier output (db)
- L_T = transmitting circuit losses (db)
- L_R = receiving circuit losses (db)
- L_P = antenna pointing losses (db)
- L_S = space loss (db)
- N_{in} = input noise spectral density at receiver terminals (db)
- $(S/N)_{in}$ = required RF signal-to-noise power ratio at the receiver for a particular function (db)

Some of the values of the parameters appearing in Equation (3.1) are specified in Section 2.4 or are calculated according to fundamental communication equations

(Appendix A). The only parameters which must be evaluated are G_T , G_R , and P_T at the LCS for both the up-links and down-links. By using Equation (3.1), the minimum required values of these parameters are determined. The results are presented in Table 3.2 and a complete sample calculation appears in Section A.1.

3.3 PERFORMANCE TRADE-OFF ANALYSIS

The weakest link in the Apollo/LCS/MSFN system is the Apollo spacecraft-to-LCS link. Since the transmitter power and transmit antenna gain at each Apollo spacecraft is fixed, the maximum required gain at the LCS is determined by Equation (3.1). These results are presented in Table 3.2. For each value appearing in that table, a corresponding parabolic antenna diameter and -3db beamwidth is calculated. The equations used to compute these values plus a sample calculation appears in Section A.4, while the complete results are in Table 3.3.

In order for the LCS to be capable of receiving narrowband color television (and consequently, all other down-link modes), only the employment of the CSM's high gain antenna and the LM's steerable and erectable antenna appear feasible. This is because the use of an omni-directional antenna at the Apollo spacecrafts

Table 3.2

MINIMUM REQUIRED VALUES AT THE LCS

	CURRENT APOLLO	MODIFIED APOLLO
LINK	G_R (db)	
CSM-to-LCS		
High Gain	41.4	26.7
(Omnidirectional)	(65.8)	(57.0)
LM-to-LCS		
Steerable	42.9	33.1
Erectable	34.9	22.0
(Omnidirectional)	(66.0)	(59.6)
MSFN-to-LCS	4.0	--

	CURRENT APOLLO	MODIFIED APOLLO
LINK	$ERP = G_T$ (db) + P_T (db)	
LCS-to-CSM		
High Gain	53.4	44.3
(Omnidirectional)	(74.3)	(74.3)
LCS-to-LM		
Steerable	69.2	52.8
Erectable	46.4	39.2
(Omnidirectional)	(78.5)	(77.3)
LCS-to-MSFN	29.3	--

Note: The Apollo omnidirectional antennas are not to be used during normal operation of the LCS.

Table 3.3

MINIMUM REQUIRED RECEIVE ANTENNA VALUES AT THE LCS

LINK	CURRENT APOLLO		MODIFIED APOLLO	
	ANTENNA DIAMETER (FT)	BEAMWIDTH (DEG)	ANTENNA DIAMETER (FT)	BEAMWIDTH (DEG)
CSM-to-LCS				
High Gain (Omni)	23.9 (397.0)	1.39 (.08)	4.41 (144.0)	7.57 (.23)
LM-to-LCS				
Steerable	26.0	1.17	9.2	3.6
Erectable (Omni)	11.3 (407.0)	2.95 (.08)	2.57 (195.0)	12.7 (.17)
MSFN-to-LCS	.32	104.0	----	----

Note: The Apollo omni-directional antennas are not to be used during normal operation of the LCS.

requires the LCS to have an enormously large receiving antenna which cannot be feasibly deployed. Thus, it is seen from Table 3.3 that for the current Apollo design, a parabolic receiving antenna with a diameter of 26.0 feet will provide adequate receiving gain (42.9 db) at the LCS for reception of signals transmitted via the CSM's high gain antenna and the LM's steerable and erectable antenna. However, an examination of the relative geometries between the LCS, the Moon, and the Earth, as shown in Figure 3.2, reveals that an LCS antenna must have a -3 db beamwidth of

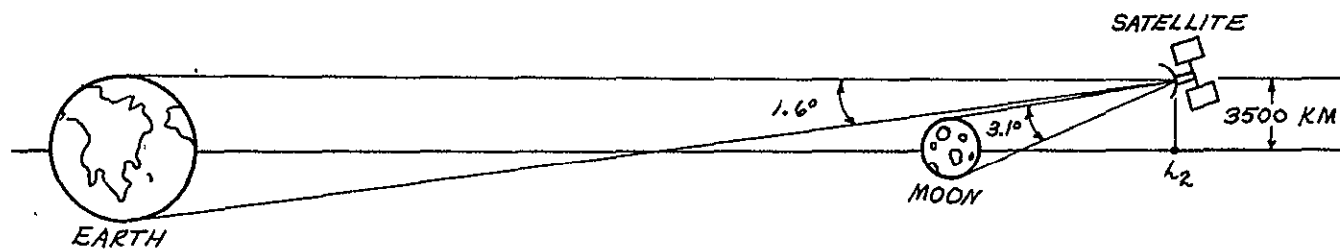


Figure 3.2 L_2 Libration Point Communication Geometry

3.1 degrees in order to use a single beam to achieve full coverage of the lunar backside from the L_2 libration point. Since a 26-foot parabolic antenna has only a -3db beamwidth of 1.17 degrees, it is obviously not sufficient to provide complete lunar coverage. This problem can be solved possibly by using an electronically steerable feed on the LCS antenna which is capable of achieving a ± 1.93 degree pointing variation of the antenna beam. This will enable the beam to illuminate any specified area on the back-side lunar surface.

There are several disadvantages which result from the deployment of this type of antenna. One problem occurs with attitude control. An antenna whose beamwidth is only 1.17 degrees must have a $\pm .12$ degree pointing accuracy. To achieve this accuracy requires a sophisticated satellite attitude control system and one which would be impractical to implement on a satellite which is to be designed for a lifetime of four years. Secondly, since the CSM and/or LM vehicles traverse the entire lunar back-side while in a parking orbit around the Moon, the narrow-beam LCS antenna must be capable of continuously tracking these vehicles during that period of time. To provide the LCS antenna with this capability would add extreme complexity to the overall satellite design. In addition, it would not be possible to

illuminate both vehicles simultaneously if they are at opposite ends of the lunar back-side.

A simple solution to overcome the problems created by the deployment of such a narrow-beam antenna is to merely increase the size of the beamwidth. If an antenna with a -3db beamwidth of 3.1 degrees were used, it would be able to fully illuminate the entire surface of the lunar back-side, thereby eliminating the need for beam steering and pointing. In addition, a pointing accuracy of only $\pm .25^\circ$ would be required. According to Equations (A.9) and (A.10), a narrower beamwidth would result in a smaller antenna and less gain; a parabolic antenna with a 3.1° beamwidth has a gain of 34.6 db and a reflector diameter of 10.0 feet. However, the amount of gain achieved by this antenna is 8.3 db less than that which could be achieved by the 26.0-foot antenna and is, therefore, 8.3 db below the minimum required gain necessary to receive narrowband television from either the CSM or the LM (utilizing the current Apollo system). However, this would not be the case if a modified Apollo system is used. The largest value of the minimum required gain for the LCS antenna using a modified Apollo is 33.1 db (employing the LM's steerable antenna as shown in Table 3.2). So, a margin of 1.5 db exists when the 10.0-foot antenna is used with the modified Apollo. Therefore,

it appears most practical to modify the existing Apollo communication system to implement this smaller antenna on the LCS. Use of this antenna permits continuous coverage of the entire lunar back-side while requiring only present state-of-the-art attitude control techniques to achieve the necessary degree of antenna pointing accuracy. As mentioned in Section 2.4, modifications of the existing Apollo communication system involves uprating its equipment by increasing the RF power, increasing the size of its antenna, and reducing the receiver noise figure and other system losses. It is, therefore, assumed throughout the remainder of this study that a modified Apollo system will be implemented.

The next part of this trade-off analysis derives the required LCS transmitter power for the LCS-to-Apollo link. In Table 3.3, the minimum required values of the LCS effective radiated power ($ERP = G_T + P_T$) are specified. Again neglecting the omni-directional antennas on both the CSM and LM and assuming a modified Apollo system, the largest value of required ERP is 52.8 db (for the LM's steerable antenna). Since the LCS receiving antenna is also used for lunar transmission, the transit antenna gain (G_T) for this 10-foot parabolic reflector is 33.8 db (a decrease of .8 db because the LCS-to-Apollo frequency is less than the Apollo-to-LCS frequency). The required LCS transmitter power simply becomes

$$P_T = ERP - G_T \quad (3.2)$$

$$= 52.8 - 33.8$$

$$= 19.0 \text{ dbw or } 80.0 \text{ watts}$$

where, for the LCS-to-Apollo links

P_T = required LCS transmitter power

ERP = minimum required LCS effective radiated
power

$$= 52.8 \text{ dbw}$$

G_T = required LCS transmitter antenna gain

$$= 33.8 \text{ dbw (10-foot parabolic antenna)}$$

Thus, a minimum of 19.0 dbw or 80 watts of RF power is required by the LCS in order to provide all up-link modes of communications to either the LM and/or the CSM.

Thirdly, the antenna sizes and transmitter power for the LCS/MSFN link is determined. Again, referring to Table 3.3, the minimum required effective radiated power for the LCS-to-MSFN link is 29.3 dbw. If the same 10-foot parabolic antenna which is used for the LCS/Apollo links is employed for the LCS/MSFN links (by implementing a second feed on the antenna), then the LCS transmitter power for the LCS-to-MSFN link is from (3.2)

$$P_T = 29.3 - 33.8$$

$$= -4.5 \text{ dbw} = 3.5 \times 10^{-5} \text{ watts}$$

where, for the LCS-to-MSFN link

P_T = required LCS transmitter power

ERP = minimum required LCS effective radiated
power

$|$ = 29.3 dbw

G_T = required LCS transmit antenna gain

= 33.8 db

As expected, less than one-watt of transmitter power is required. This is due to the high gain receiving antenna and low noise system temperature at the MSFN, and the relatively low transmitting losses at the LCS. However, to provide a significant margin for this link, a transmitter power of 5 watts (.7 dbw) is specified.

Use of the LCS 10-foot antenna also provides adequate gain for the reception of signals transmitted to the LCS from the MSFN. According to Table 3.2, a receiving antenna gain of only 4.0 db is required for this link. Thus, a very significant margin of over 30 db is achieved.

3.4 SATELLITE COMMUNICATION SPECIFICATIONS

The complete LCS communication specifications are shown in Table 3.4. The values for the transmitter power, receive antenna gain, and transmit antenna gain were derived in Section 3.3. Most of the other values

relate to specific hardware and reflect mid-1970 developments. Further clarification is provided by Figures 3.3 and 3.4.

Table 3.4

PROPOSED LCS COMMUNICATION SPECIFICATIONS

PARAMETER	PARAMETER VALUE	UNITS	COMMENTS
Transmitter Power			10-foot
LCS-to-MSFN	5.0	w	Parabolic
LCS-to-Apollo	80.0	w	Antenna at
Transmit Antenna Gain			the LCS for
LCS-to-MSFN	33.8	db	Transmitting
LCS-to-Apollo	33.8	db	and Receiving
Receive Antenna Gain			Via Modified
MSFN-to-LCS	36.4	db	Apollo
Apollo-to-LCS	34.6	db	System; See
Transmit Circuit Losses			Section 3.4
LCS-to-MSFN	3.0	db	
LCS-to-Apollo	3.0	db	
Receive Circuit Losses			
MSFN-to-LCS	3.0	db	
Apollo-to-LCS	3.0	db	
Pointing Loss			
LCS-to-MSFN	0.7	db	
LCS-to-Apollo	0.7	db	
Receiver Noise Figure			
MSFN-to-LCS	4.0	db	
Apollo-to-LCS	4.0	db	
Receiving Antenna Temperature			
MSFN-to-LCS	116.0	°K	
Apollo-to-LCS	116.0	°K	
Receiver and Hardware Temperature	314.0	°K	

LCS SPECIFICATIONS

ANTENNA

10-FOOT DIAMETER PARABOLIC

DUAL FEEDS (1 FIXED, 1 STEERABLE)

TRANSMITTER POWER

TO APOLLO - 80 WATTS

TO MSFN - 5 WATTS

RECEIVER NOISE FIGURE = 686° K

BANDWIDTH = 4 MHz

S/N _{in} = 8 db

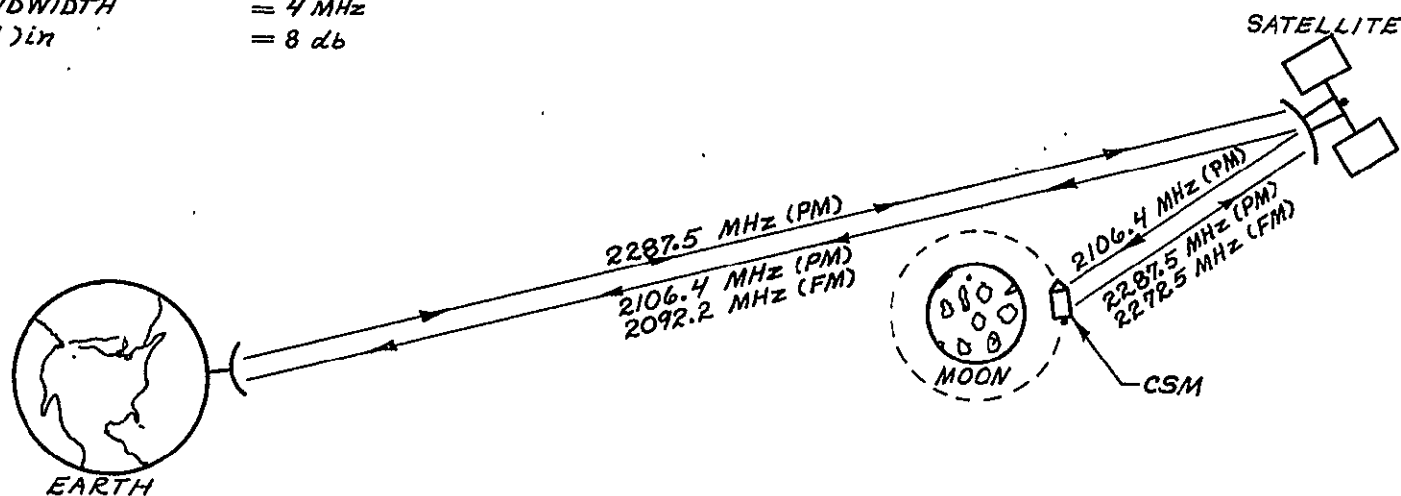


Figure 3.3 MSFN/LCS/CSM Link Summary

LCS SPECIFICATIONS

ANTENNA

10-FOOT DIAMETER PARABOLIC

DUAL FEEDS (1 FIXED, 1 STEERABLE)

TRANSMITTER POWER

TO APOLLO - 80 WATTS

TO MSFN - 5 WATTS

RECEIVER NOISE FIGURE = 486° K

BANDWIDTH = 4 MHz

S/N 17 = 8.26

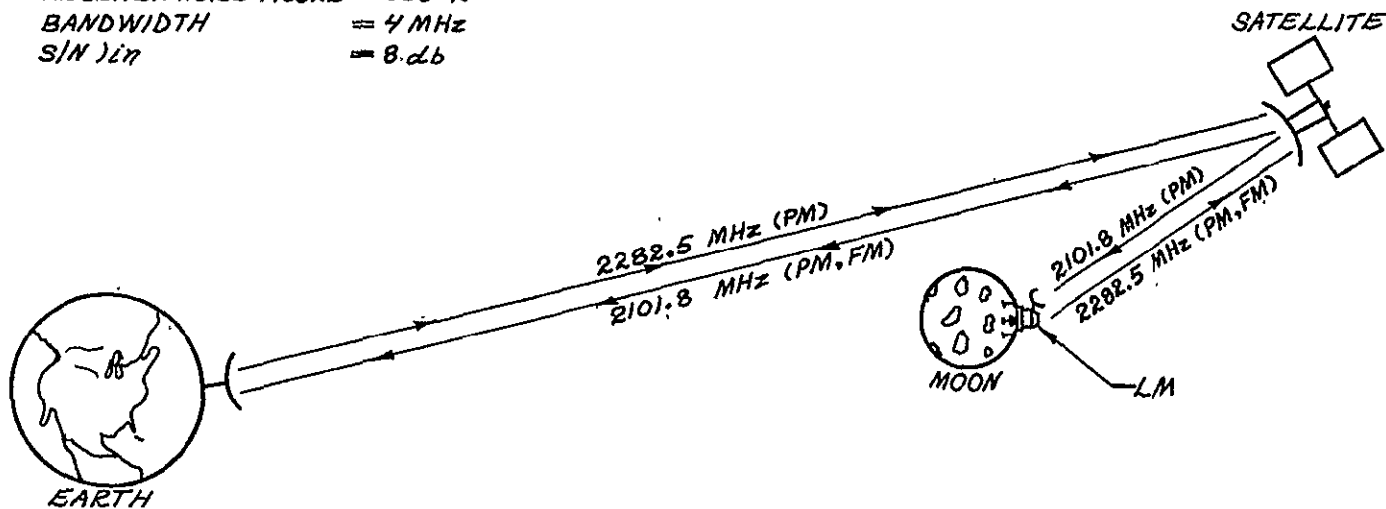


Figure 3.4 MSFN/LCS/LM Link Summary

CHAPTER IV

SATELLITE TRAJECTORY AND ORBIT CONTROL

In this chapter, the motion and motion control of the LCS is discussed from the time the satellite is launched, throughout its proposed four-year lifetime.

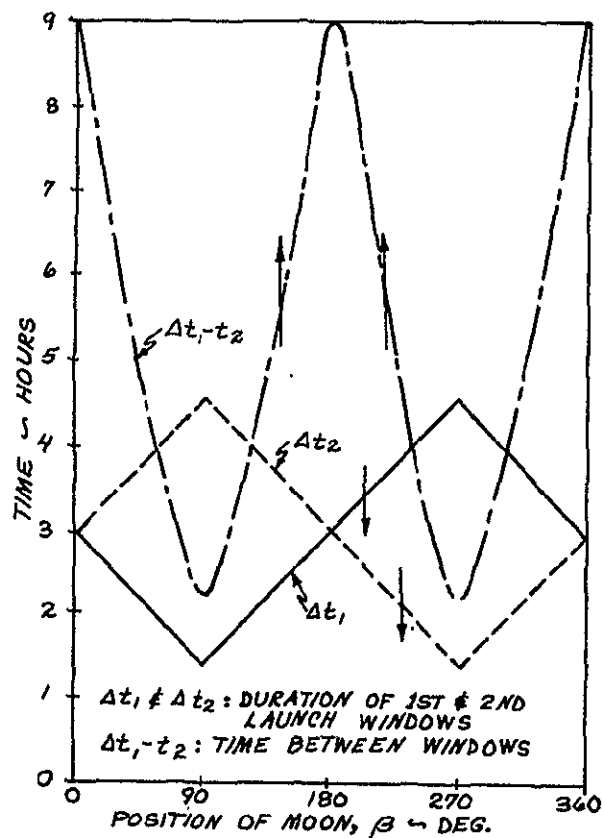
The following topics are included:

- Launch
- Earth-to- L_2 trajectory
- Stationkeeping
- Attitude control

Background information in these areas is provided by Appendices B and C.

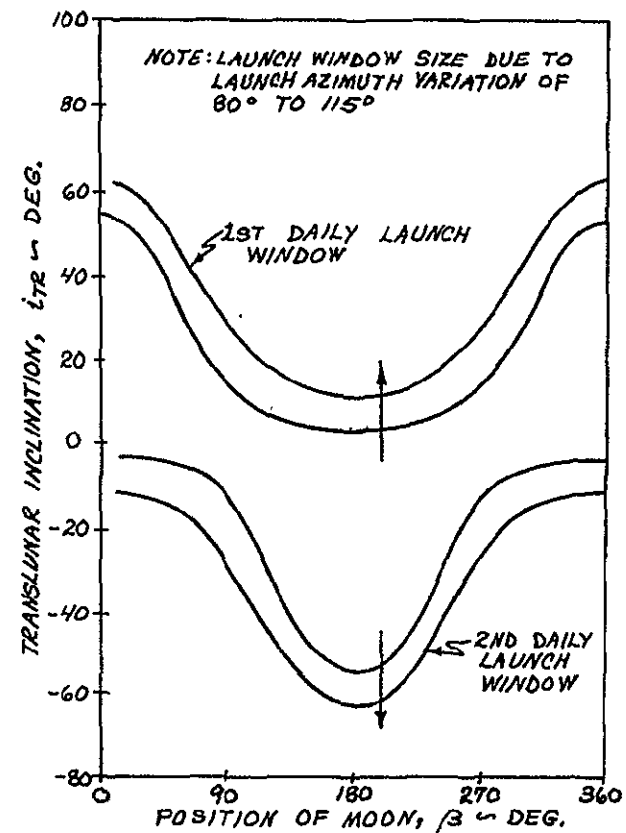
4.1 LAUNCH SPECIFICATIONS

Launch of the LCS is envisioned for the 1973-74 period. An approximate spacecraft weight of 905 pounds would presently require the use of a Titan 3X launch vehicle. However, since a new family of Thrust Augmented Delta (TAD) vehicles is expected to be operational by 1973 (Reference 5), this appears to be a more appropriate choice. The particular vehicle chosen for the LCS is a three stage Delta with nine-castor strap-on thrust



(a) LAUNCH TIMES VS MOON POSITION

NOTE:
 ARROWS INDICATE
 MOVEMENT FOR
 INCLINATION BETWEEN
 EQUATOR AND LUNAR
 ORBIT OF $\gamma 26^\circ$



(b) TRAJECTORY INCLINATION VS MOON POSITION

Figure 4.1 Launch Windows

augmenters. This vehicle has an escape payload capacity of 940 pounds and costs about half as much as the Titan 3X. The launch would be made from the Eastern Test Range at Cape Kennedy.

The following factors are to be considered when defining a launch window.

- The launch point is at a fixed latitude on the Earth's surface ($28^{\circ}28'$).
- The lunar orbit plane is inclined relative to the Earth's equatorial plane (varies from $18^{\circ}18'$ to $28^{\circ}36'$ over a period of 18.6 years; Section C.2).
- The Moon orbits the Earth once every 27.3 days.

A study (Reference 5) has been made of launch windows for a lunar-orbit-plane inclination of 26° , for this will occur in January, 1974 (Section C.2). The results of this study are shown in Figure 4.1 for a simplified (circular) lunar orbit, where β is measured in the Moon's orbit plane and is equal to zero at the ascending node on the Earth's equatorial plane. The use of an Earth parking orbit allows two launch times per day. If variable launch azimuths are considered, these launch times become launch windows. Assuming that the satellite does not change its orbital plane while being injected into

the Earth-to- L_2 trajectory, the inclination of the parking orbit with respect to the lunar-orbit-plane is changing from day to day and from window to window during a particular day. It is noted that the 26° angle increases to $28^\circ 36'$ by 1989 and the arrows in Figure 4.1 show the movement of the curves for this increase. Overall, the values shown do not increase significantly.

4.2 EARTH-TO- L_2 LIBRATION POINT TRAJECTORY AND NAVIGATION

A direct trajectory from Earth to L_2 was considered, but was discarded due to the high ΔV (3400 ft/sec) requirements at L_2 . A lunar fly-by technique is used instead in order to get an increase in velocity from the Moon. The details of the trajectory analysis appears in Appendix E, and a summary of critical parameters is presented below:

Velocity change from parking orbit to	
trajectory	10,900 ft/sec
Time to closest approach to the Moon	
(perilune)	5.5 days
Velocity change at perilune	700 ft/sec
Time to injection into halo	
orbit	8.8 days

Velocity change to initialize halo	
orbit	500 ft/sec
Midcourse correction velocity	
changes	70 ft/sec

These are only representative values because the exact numbers are dependent upon the initial inclination of the trajectory.

The third stage of the Delta launch vehicle uses spin stabilization for injection accuracy, so the satellite must be despin after ejection from the third stage. Due to its high spin rate (≈ 100 rpm), a large fuel weight is required if attitude control thrusters are used for despin. Therefore, a yo-yo despin technique is considered to be the solution to this problem (Section 6.4.3). A small residual roll rate usually remains after despin, and this is corrected by the attitude control thrusters. After this operation, the solar panels and high gain antenna are deployed.

Once the LCS is in the proper trajectory and coasting towards L_2 , the Sun is acquired by means of sensors on the solar panels. This aligns the satellite's pitch and yaw axes. A star tracker is then used to align the roll axis by sighting and locking onto the star Canopus. This is accomplished through a 360° programmed roll maneuver which provides a star map from the tracker.

Ground controllers then identify Canopus and command the tracker to maintain a fix on this star. Thus, the LCS is stabilized about all three of its axes during this portion of its flight. This technique of stabilization has been used successfully by Mariner spacecrafts.

From this point, rotation rate information is provided by a three-axis gyro package in the rate mode. To position the LCS for midcourse correction, perilune, and halo orbit insertion burns, the gyro package is first switched from the rate to the position mode. The star and Sun sensors are then taken out of the attitude control loop, and programmed yaw and pitch maneuvers are performed. After each burn, the spacecraft is again returned to its original orientation and controlled by the sensor system.

4.3 L_2 LIBRATION POINT ORBIT CONTROL

An analysis using linearized equations of motion about L_2 (Appendix B) shows that a 3500 km halo orbit is a feasible method for providing constant communication between the Earth and the LCS. Stationkeeping costs for a continuous halo are found to be about 387 ft/sec-year (362 ft/sec for double Z-axis period control and 25 ft/sec for perturbations and nonlinear effects). However, a controlled halo need only be maintained for about 45 days per Apollo mission (this is the initial

period in which an ALSEP is monitored). The remainder of the time, the LCS is allowed to drift into its free Lissajous motion (Section B.5), although the halo orbit can be reinitialized at any time by ground controllers. This mode of operation results in a significant saving of stationkeeping fuel, for only 25 feet per second is required during these drift periods. By assuming two Apollo missions per year and a four year lifetime (Section 1.1), the total stationkeeping requirement is 462 feet per second.

On-station attitude sensing is performed by a Canopus sensor on a two degree-of-freedom gimbal and a set of electronic lunar horizon scanners (Reference 8). Control torque is provided by three momentum wheels which are unloaded at torque stall by a hydrazine thruster system.

After the L_2 insertion burn, the LCS is crudely positioned. By using the gyro package and the onboard computer in conjunction with the sensors, a more precise attitude is obtained. The solar panels are then oriented using the Sun sensors.

PRECEDING PAGE BLANK NOT FILMED.

CHAPTER V

SATELLITE CONCEPTUAL DESIGN

This chapter presents the procedure which was used to establish the conceptual design configuration of the LCS. Primary mission objectives provided the guidelines for a logical design solution (Section 1.1).

5.1 DESIGN CONSTRAINTS

There are three basic design requirements which must be met if the satellite is to perform satisfactorily. First, a ten-foot diameter high gain parabolic antenna (Section 3.4) must be pointed with a high degree of accuracy towards the Moon. Second, the satellite must be maintained in a nominal halo orbit. Finally, adequate power must be provided to operate the satellite communication system.

The first requirement is met with (i) a system of attitude sensors which detect any pointing errors of the high-gain antenna, and (ii) a set of small-torque generating devices (momentum wheels and thrusters) which reorient the satellite to correct the pointing errors.

Ordinary stationkeeping and a special Z-axis period control technique (Section B.6) are used to maintain the satellite in its halo orbit. This is accomplished by periodic velocity changes produced by a thruster system.

Adequate power could be supplied by either of two systems, a nuclear reactor or a combination of solar cells and batteries. Due to the high cost of nuclear power sources, solar cells and batteries constitute a more realistic solution to the power requirement.

5.2 PROPOSED CONFIGURATION

The first item which is determined is the location of the spacecraft body with respect to the parabolic antenna. The body must provide adequate support for the antenna, but yet be properly shaped to allow the antenna to be folded so the satellite fits inside the launch vehicle fairing. Since the antenna makes up a large percentage of the exposed surface area of the satellite, the center of pressure of the antenna greatly affects the center of pressure of the LCS. Thus, to minimize the disturbance torque due to solar radiation pressure, the spacecraft body is placed at the center of the parabolic antenna.

Moon edge trackers are a simple, reliable, and accurate means for sensing pitch and yaw attitude errors

(see Figure 5.1 for axis definitions). Since the spacecraft body is behind the antenna, the Moon sensors are placed on the lip of the antenna. This constraint introduces no new problems because these trackers are lightweight and have no moving parts.

Roll attitude is not necessary for maintaining antenna pointing, but is required because of the unique stationkeeping requirements (Z-axis period control) of the LCS. A Canopus star sensor is a proven method for providing this roll information. Therefore, a sensor is placed where an unobstructed view is obtained of the South ecliptic pole region (where Canopus is located). Since the yaw and pitch attitudes are continuously changing while the LCS is on station, the sensor is mounted on gimbals to provide two-degrees-of-freedom to locate and track Canopus.

The attitude errors of the LCS are corrected by a set of momentum (or inertia) wheels. These wheels are accelerated or decelerated in order to exert a torque on the body of the satellite, which results in the satellite's reorientation. Whenever the maximum or minimum angular velocities of these wheels are reached, stall torque occurs, which implies that the wheels can no longer be accelerated (if they are at their maximum angular velocity) or decelerated (if they are at their

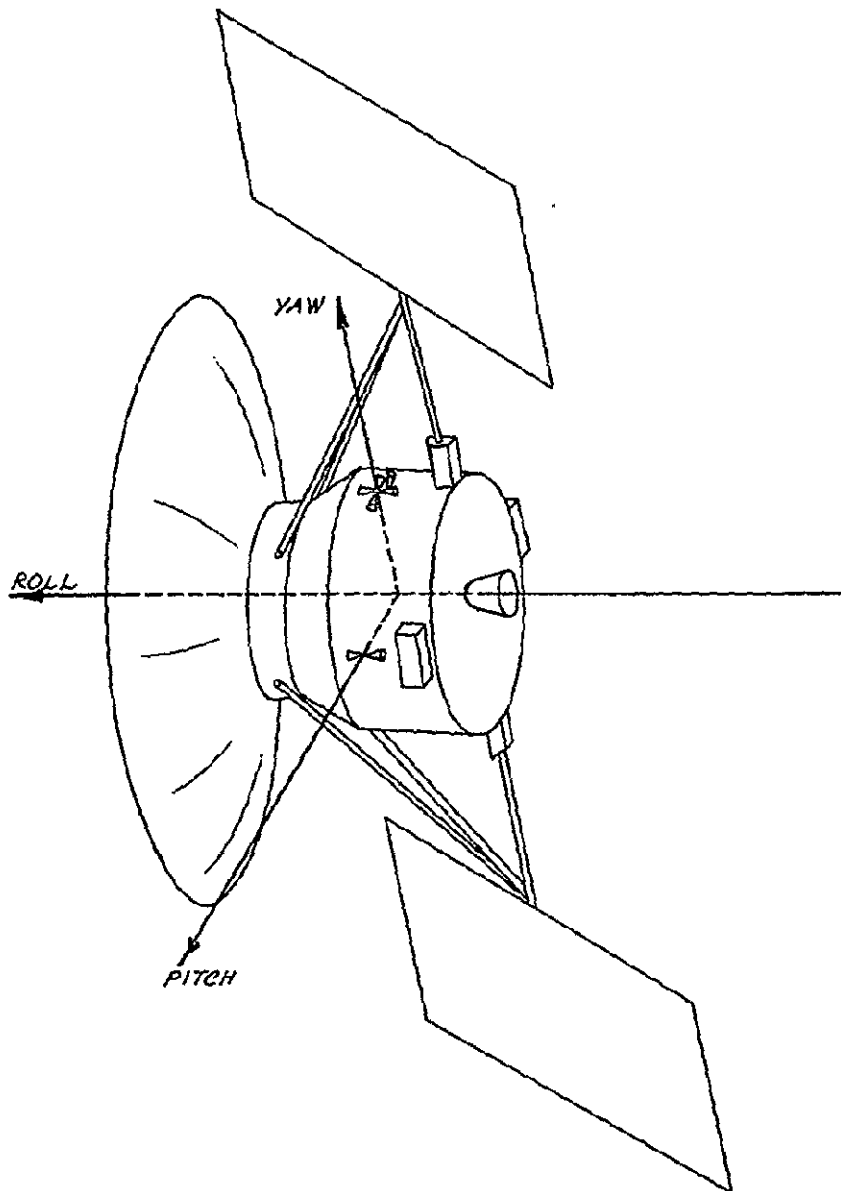


Figure 5.1 Satellite Axes Definitions

minimum angular velocity). To overcome this problem, the total angular momentum of the wheels must be reduced or increased. This is accomplished by a system of thrusters (see Section 6.2.4). There are a total of twelve thrusters proposed for LCS attitude control system. Pitch and roll jets (4 sets of 2 per set) are located on the positive and negative yaw axes of the spacecraft body. Two pair of yaw jets are similarly spaced along the pitch axis. An attempt is made with the non-cylindrical shape of the satellite body to avoid proximity of the thrusters to the antenna. Since the thrusters are positioned along the satellite's principal axes, the resultant shape, as shown in Figure 5.1, allows the center of gravity to be moved away from the antenna.

While the LCS is in the halo orbit, its roll axis is constantly coning about the negative X-axis (Section 6.2.1) with a cone angle of $3^{\circ}07'$ (this happens because antenna is kept pointing towards the Moon). If attitude control thrusters are used for the Z-axis period control burns, the LCS is required to be pitched $3^{\circ}07'$ every 7.33 days (as it crosses the positive and negative Z-axes (Section B.6). This would cause the communications operation of the satellite to be interrupted while the stationkeeping burn is performed. Therefore, it is proposed to include an extra pair of thrusters for the specific

purpose of avoiding this situation. Each of these thrusters is located on the spacecraft body near the pitch and roll jets. Their thrust vectors are misaligned $3^{\circ}07'$ with respect to the yaw axis and pass through the center of mass of the LCS. The thrust levels for these jets is low enough to allow the momentum wheels to correct for any satellite misorientation which might occur during their firing.

Body mounted solar cells are not feasible because (i) a large satellite body is not needed to house the equipment subsystems, and (ii) the Sun angle with respect to the LCS is constantly varying. Thus, to obtain maximum power from the solar cells, maneuverable panels are used. These panels present a nearly constant area of cells normal to the Sun. This is done by rotating the panels 360° every synodic month (29.53 days). Since the LCS is essentially traveling in the lunar-orbit-plane, it can be considered in the plane of the ecliptic (the actual angle between the two planes is $5^{\circ}09'$). Thus, the panels rotate about the satellite's yaw axis and are never shadowed by the body of the satellite. Sun sensors are placed on the panels to provide pointing information. These panels are located as far as possible from the antenna to help shift the center of mass towards the aft end of the satellite.

The star Canopus is located on the celestial sphere with an hour-angle of 6h 23m and a declination of $-52^{\circ}41'$ (Figure 5.2). This implies that during the lifetime of the LCS, a field of view with a half cone angle of about 23 degrees must be provided. This viewing requirement creates a unique problem for the configuration just described, because a Canopus sensor placed anywhere on the spacecraft will have its field of view periodically blocked by a solar panel. Thus, it is proposed to use two star trackers, so that one tracker will view Canopus whenever the other tracker cannot (Figure 5.3). It is noted that there is ample time when both sensors can see Canopus to provide easy switching.

5.3 EQUIPMENT LOCATION

Some of the major equipment subsystems have preferred positions in the LCS. These are:

- Communication subsystems are near the parabolic antenna to minimize the feed losses
- Attitude control and stationkeeping fuel tanks are placed symmetrically about the center of mass of the satellite to maintain the position of the center of mass as fuel is used. Also, they should be

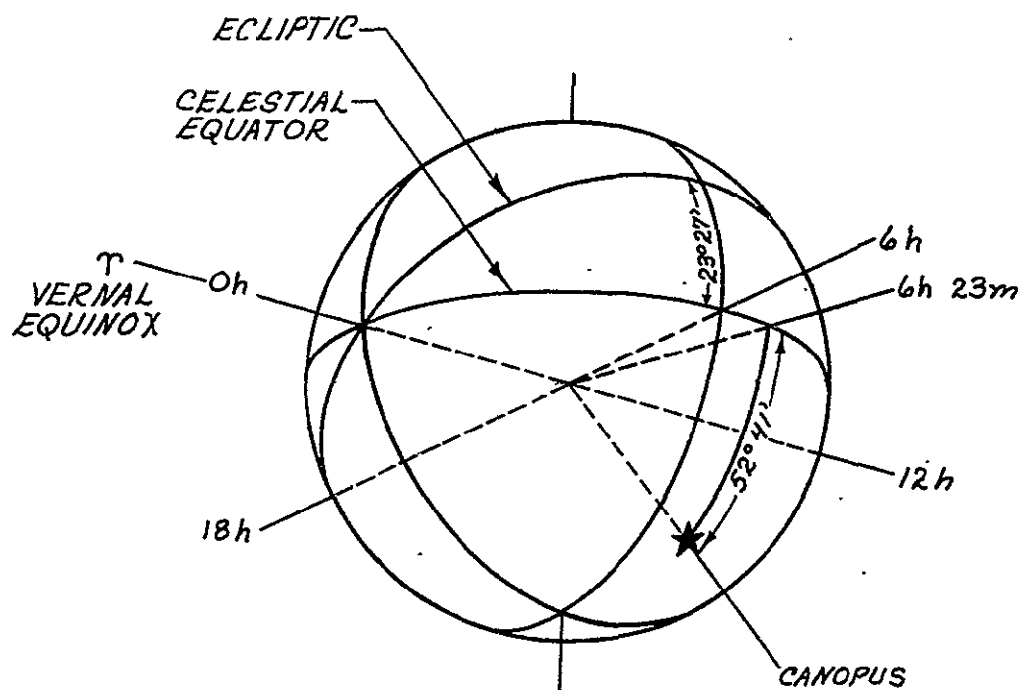


Figure 5.2 Position of the Star Canopus on the Celestial Sphere

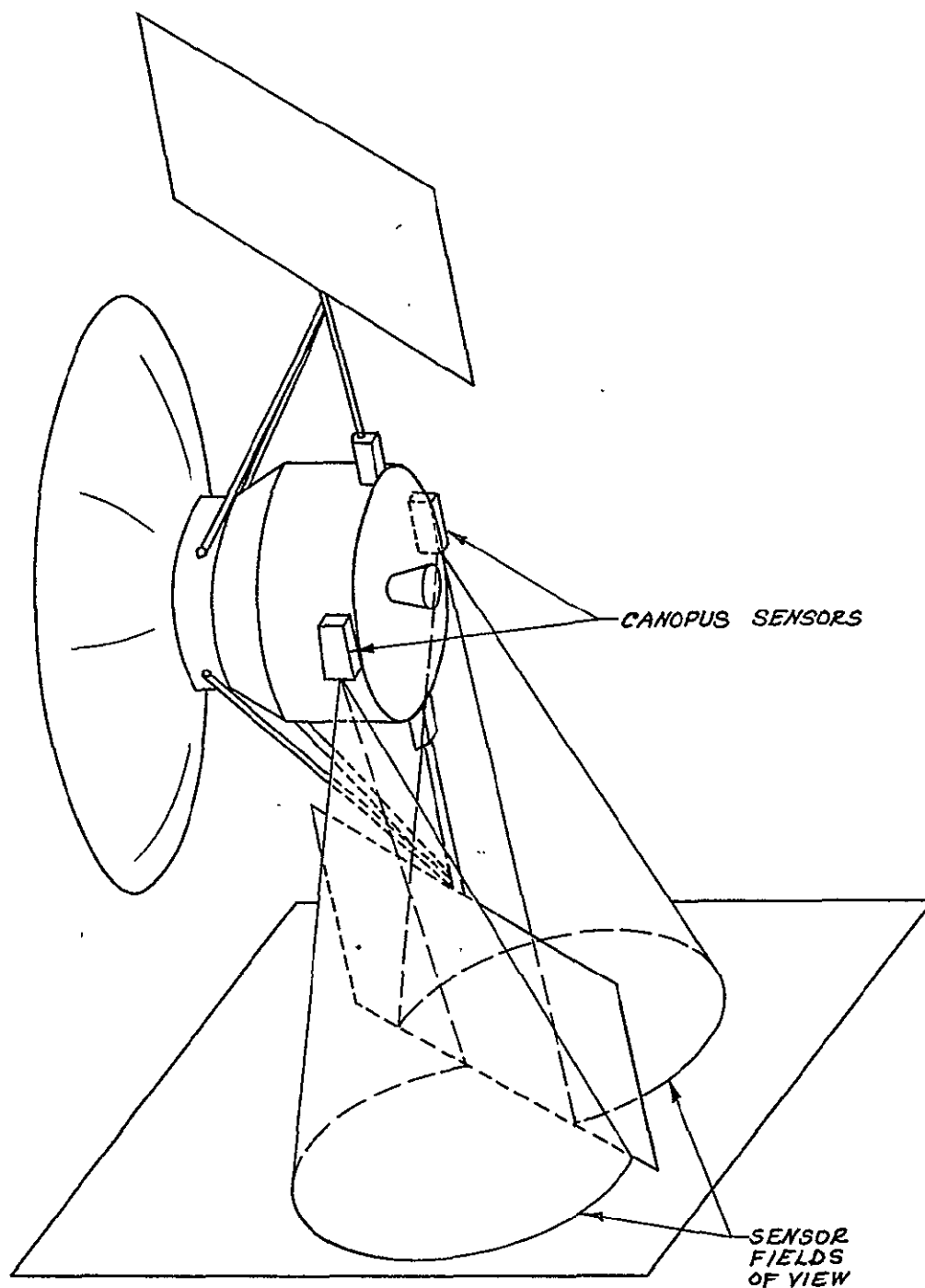


Figure 5.3 Fields of View of Canopus
Star Trackers

near the thrusters to minimize the length of fuel lines.

The momentum wheel package is located at the satellite's center of mass to prevent nutation and coning when they are accelerated or decelerated.

CHAPTER VI

SATELLITE SUBSYSTEMS

This chapter presents a preliminary discussion of the major subsystems needed to complete the conceptual design of the LCS outlined in Chapter V. The following subsystems are presented:

- Communications
- Attitude control
- Power supply
- Structures
- Yo-yo despin

The analysis of these subsystems is not exhaustive, for a more detailed design depends upon the specifications of the actual hardware.

6.1 COMMUNICATION SUBSYSTEM

The LCS communication subsystem must perform the following functions:

- Relay transmissions from the Manned Space Flight Network to the Apollo spacecrafts.

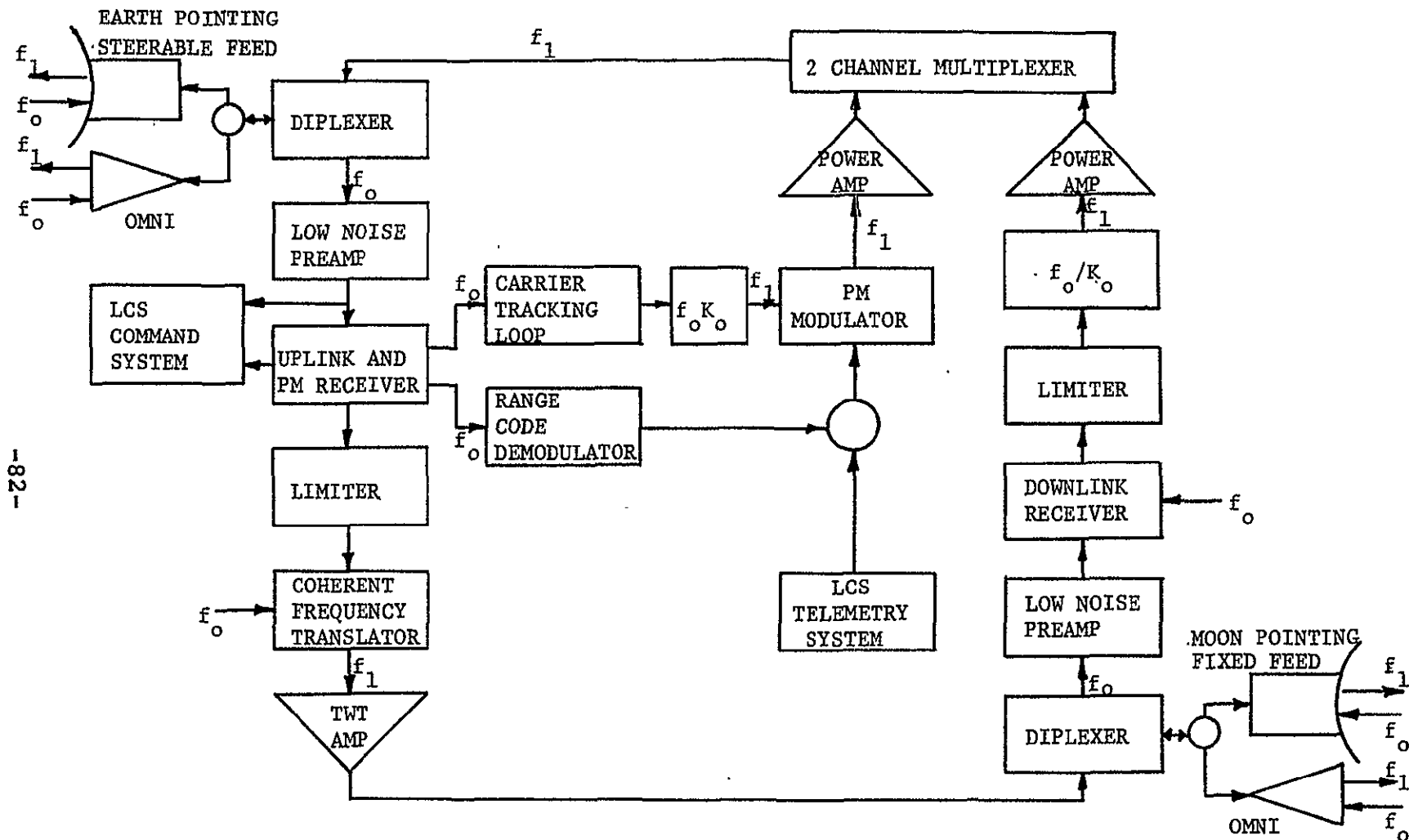


Figure 6.1 LCS Communication System Block Diagram (No Redundancy Shown)

- Relay transmissions from the Apollo spacecrafts to the Manned Space Flight Network.
- Provide a receiver for commands from the Manned Space Flight Network.
- Provide a telemetry transmitter for satellite monitoring data, housekeeping data, and ranging code to the Manned Space Flight Network.

In addition, this system must also be compatible with the existing Apollo Unified S-Band system and be able to provide for range and range-rate tracking of the Apollo spacecrafts (as specified in Section 1.1).

The complete LCS communication subsystem consists of four basic components: the transponder, the power amplifier, the LCS telemetry and command system, and the on-board antennas (high-gain directional antenna and omnidirectional antenna). A complete block diagram of the communication subsystem is shown in Figure 6.1. The remainder of this section presents an in-depth discussion of these four basic components.

6.1.1 Transponder

The main purpose of the transponder is to achieve a coherent frequency translation of signals received at the LCS from the MSFN and the Apollo spacecrafts. This

translation is necessary due to the requirement that the received and retransmitted signals must have a significant degree of isolation in order to minimize interference between these two signals. This isolation is achieved by changing the frequency of the retransmitted signal. Thus, the up-link signals are multiplied by the translation ratio of 240:221, while the down-link signals are multiplied by the translation ratio 221:240. In addition, this translation must be coherent in order to achieve Carrier Doppler tracking of the LCS and the Apollo spacecrafts. Coherency is obtained by phase-locking the oscillators of the entire MSFN/LCS/Apollo spacecraft communication loop to the frequency of the up-link carrier. The tracking carrier loop which appears in Figure 6.1 is the device which generates the up-link frequency at the LCS.

The main components of the carrier tracking loop are a phase detector, loop filter, and voltage control oscillator (VCO). As shown in Figure 6.2, the tracking loop resembles a simple feedback control system.

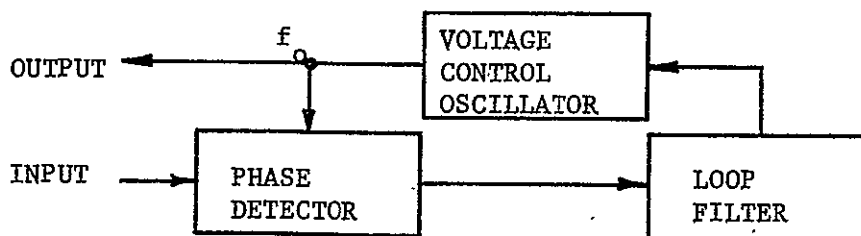


Figure 6.2 Carrier Tracking Loop

The input to this loop is a phase-modulated RF carrier whose center frequency has been slightly shifted as a result of the relative motion between the LCS and the MSFN. The output is a pure unmodulated sinusoidal signal generated by the VCO. The frequency of this signal, f_o , is identical to the initial center frequency of the RF carrier when transmitted at the MSFN. It is the frequency of this output signal which is used to provide a reference for the oscillators in the transponder shown in Figure 6.1.

The up-link RF signals are received from the Earth via the steerable feed on the LCS parabolic antenna. These signals are then routed by a diplexer to a special low noise, solid-state preamplifier. From the preamp, the signals enter the up-link receiver shown in Figure 6.3. After leaving the receiver front end, the signals are split into two branches: (i) the horizontal branch which leads to the carrier tracking loop to generate the communication subsystem reference signal, f_o ; and (ii) the vertical branch which leads to an IF limiting amplifier. The output of the VCO is used in the receiver to provide a reference signal for the receiver front end and the wideband detector. The output of the IF limiting amplifier is fed into the wideband detector which produces an output consisting of a coherent PRN ranging

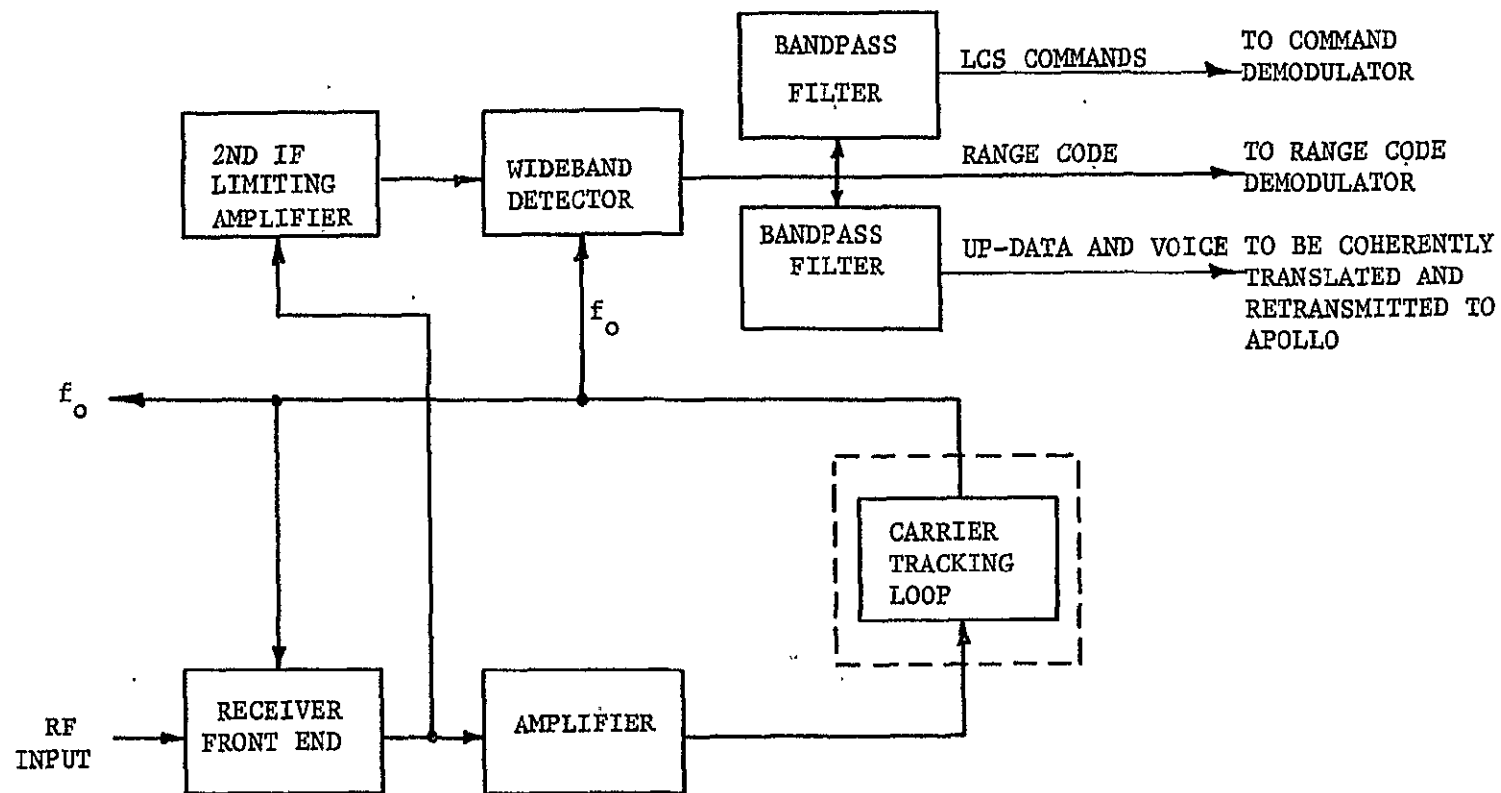


Figure 6.3 Diagram of LCS Up-Link S-Band Receiver

code, the commands for the LCS, and the up-data and voice for the Apollo spacecrafts.

The remainder of the transponder provides modulation, demodulation, and frequency translation of the RF signal. Again referring to Figure 6.1 for the up-link, the LCS command signals are demodulated and interpreted by a special command demodulator and decoder. The demodulated ranging code is summed with the LCS telemetry data and phase modulated onto a coherently translated carrier ($f_o \times k_o = f_o \times \frac{240}{221}$) for transmission to Earth. The up-data and voice signals go into a special limiter, after which the frequency of the carrier is coherently translated for amplification and transmission to the Apollo spacecrafts.

The RF signals, which comprise the down-link, are received from the Apollo spacecrafts via the fixed feed of the LCS parabolic antenna. These signals may be phase modulated or frequency modulated onto the RF carrier depending upon the type of data being transmitted (as described in Section 2.1). The receiver signals are routed from the diplexer through a special low noise, solid-state preamplifier (similar to the one used in the up-link). From the preamp, they pass through the down-link receiver (whose oscillators are coherently locked) and a limiter. The carrier frequency is then translated

to the lower frequency ($f_o \times \frac{1}{k_o} = f_o \times \frac{221}{240}$) after which the RF signal is amplified by a 5-watt solid-state power amplifier. This amplified signal is then multiplexed with a phase modulated carrier containing the demodulated LCS ranging code (from the up-link) and the LCS telemetry data. The total multiplexed RF signal is finally transmitted to Earth via the steerable feed of the LCS parabolic antenna.

6.1.2 Power Amplifiers

The LCS communication subsystem contains two types of power amplifiers: (i) a solid-state amplifier for down-link transmissions from the LCS to the MSFN, and (ii) a traveling wave tube (TWT) amplifier for up-link transmissions from the LCS to the Apollo spacecrafts. For the down-link, the LCS transmitter power level is mainly a function of the satellite antenna gain. In Section 3.4, it was derived that approximately five watts of RF power would be sufficient for this operation. For the up-link, the LCS power level is determined by the effective gain of the LCS transmitting antenna and the signal strength required by the Apollo spacecrafts for reception of an acceptable quality signal. Since a narrow-beam parabolic transmitting antenna is being used, whose effective gain is about 33.8 db, then an RF power

of 19.0 dbw or 80 watts must be supplied to the satellite antenna in order to provide acceptable reception.

There are two main categories of highly reliable devices capable of producing the desired power outputs. These are the electron beam interaction devices (power tubes) and the solid-state devices. The choice of device is primarily dependent upon efficiency because it relates directly to: (i) prime power requirements (and, therefore, solar panel size); and (ii) thermal control (since the excess waste energy must be radiated into space in order to keep the spacecraft temperature at its operating level).

The solid-state devices appear attractive for supplying only the down-link RF power, since their maximum output is limited to 15 watts. In this category, only varactor multipliers and phase controlled Gunn-effect oscillators can operate at a reasonable efficiency. By assuming an efficiency of 40% for a varactor multiplier, approximately 25 watts of prime power (for two amplifiers) will be required for this link. However, when considering the up-link, solid-state devices do not appear feasible. In order to obtain 80 watts of RF power, it would be necessary to parallel many amplifiers. This mode of operation is undesirable when using Gunn-effect oscillators because of the difficulties

anticipated in maintaining identical phase characteristics over the wide bandwidths in several parallel amplifiers. In addition, the varactor multiplier is also undesirable because of its low efficiency. Thus, the electron beam interaction devices are the best choice of power amplifiers for the up-link because of their high efficiency.

In choosing the power tube best suited for the needs of the LCS, the following parameters were considered: efficiency, gain, bandwidth, output power capability, and lifetime. The requirements which govern the limits of these parameters are:

- A power output of at least 40 watts per tube.
- A power gain of at least 19 db per tube (the input signal to the tube will be on the order of 1 watt).
- An operating frequency of 2 GHz.

There are essentially four types of microwave power tubes which have the necessary power-handling capability. These are: (i) a triode, (ii) a traveling wave tube (TWT), (iii) an amplatron, and (iv) a klystron. The triode would be very impractical because it cannot operate at frequencies above 1 GHz. Above this frequency, its power output, gain, and efficiency diminishes

rapidly. In addition, the efficiency of the triode is inversely proportional to its operating lifetime, so it would not be able to operate effectively for a mission of four years. The amplatron and klystron tubes also do not appear feasible because it is only possible for them to achieve a high gain by passing a small percentage of the bandwidth, namely 1-2 per cent for the amplatron and 0.1-0.3 per cent for the klystron at gains of 17 db and 45 db respectively. In addition, the klystron has only a maximum operating lifetime of about 2-1/2 years, as compared to slightly more than 1/2 year for the amplatron. Thus, the best choice appears to be the traveling wave tube. The TWT which would be used in the LCS has an efficiency on the order of 40% with a gain of 19 db at a bandwidth in excess of 50 per cent. Its operating life would be able to exceed four years at these conditions.

It should be noted that traveling wave tubes operate with a maximum efficiency near full power output. Thus, it is desirable to drive this type of amplifier at a constant power level. This can be accomplished by using a hard-limiter just prior to the RF amplifier. An ideal hard-limiter is a device which has the transfer function

$$\begin{aligned} e_o &= -A && \text{when } e_i < 0 \\ e_o &= 0 && \text{when } e_i = 0 \end{aligned}$$

$$e_o = +A \quad \text{when } e_i > 0$$

where e_i = limiter input (volts)

e_o = limiter output (volts)

The output of this limiter, in the absence of an input signal, is a set of pulses of constant amplitude and random phase. However, this is an undesirable output, which can be avoided only by employing a modulation scheme which assures that an input signal is present at all times. This is achieved by angle modulation schemes (phase and frequency) such as those used in the Unified S-Band System.

In actual operation, it is necessary to have two TWT's. These tubes are connected in parallel in order to produce the required power output of 80 watts. A block diagram of the TWT amplifiers is shown in Figure 6.4. During an actual mission, the filaments of both TWT's are always on and the driver signal and DC plate power are applied to both tubes. This does not provide for any redundancy, but if one tube should fail, only a 3 db loss would occur which is not extremely critical for the continued operation of the LCS. Whenever the satellite is not being used, the DC plate power is shut off to both TWT's. However, the filaments are always left on in order to avoid thermal cycling and reliability degradation.

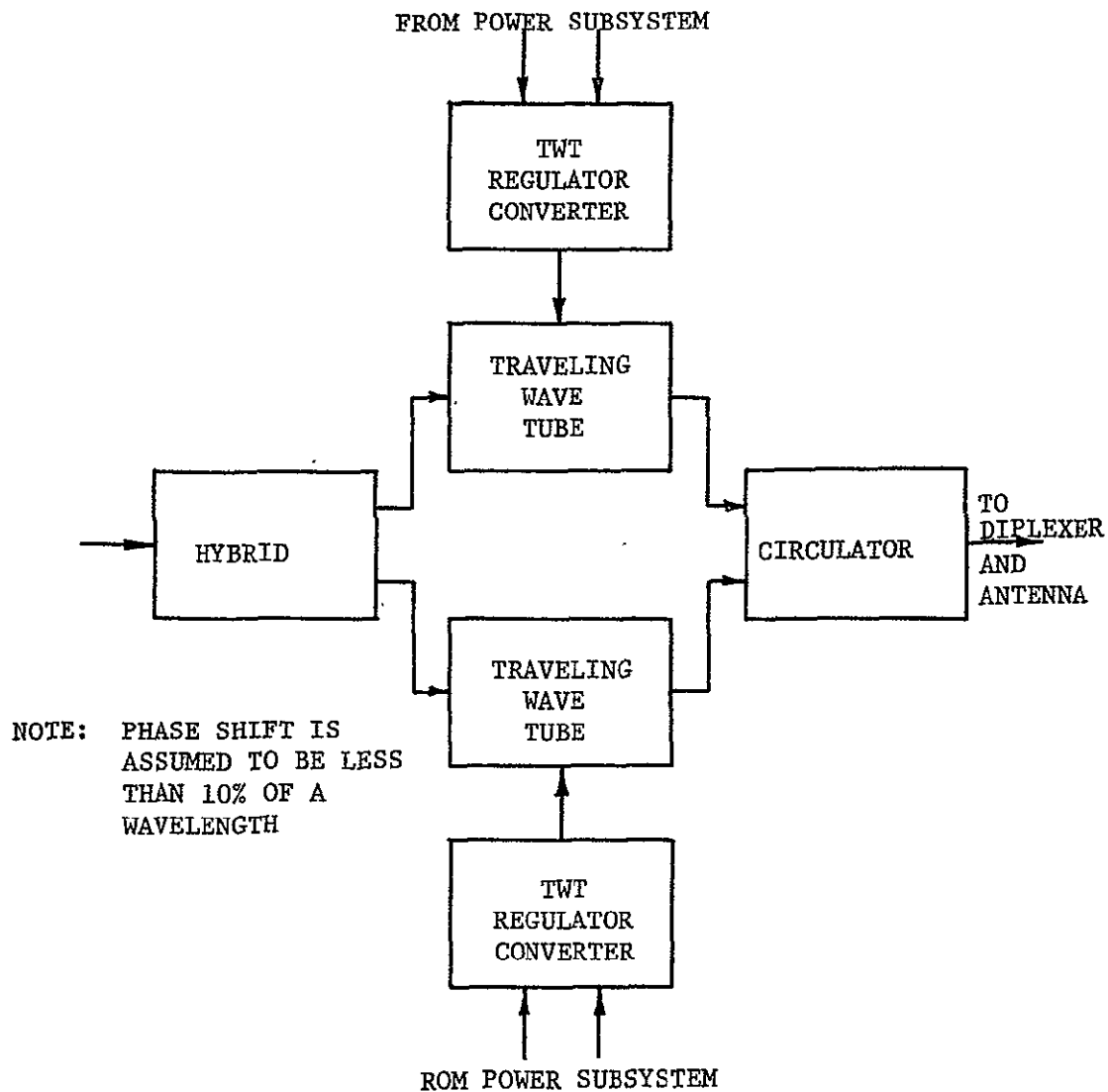


Figure 6.4 Traveling Wave Tube Amplifier Block Diagram

The power requirements for the TWT amplifiers in full operation is 220.0 watts. The proposed distribution is 105.0 watts for the plate of each TWT and 5.0 watts

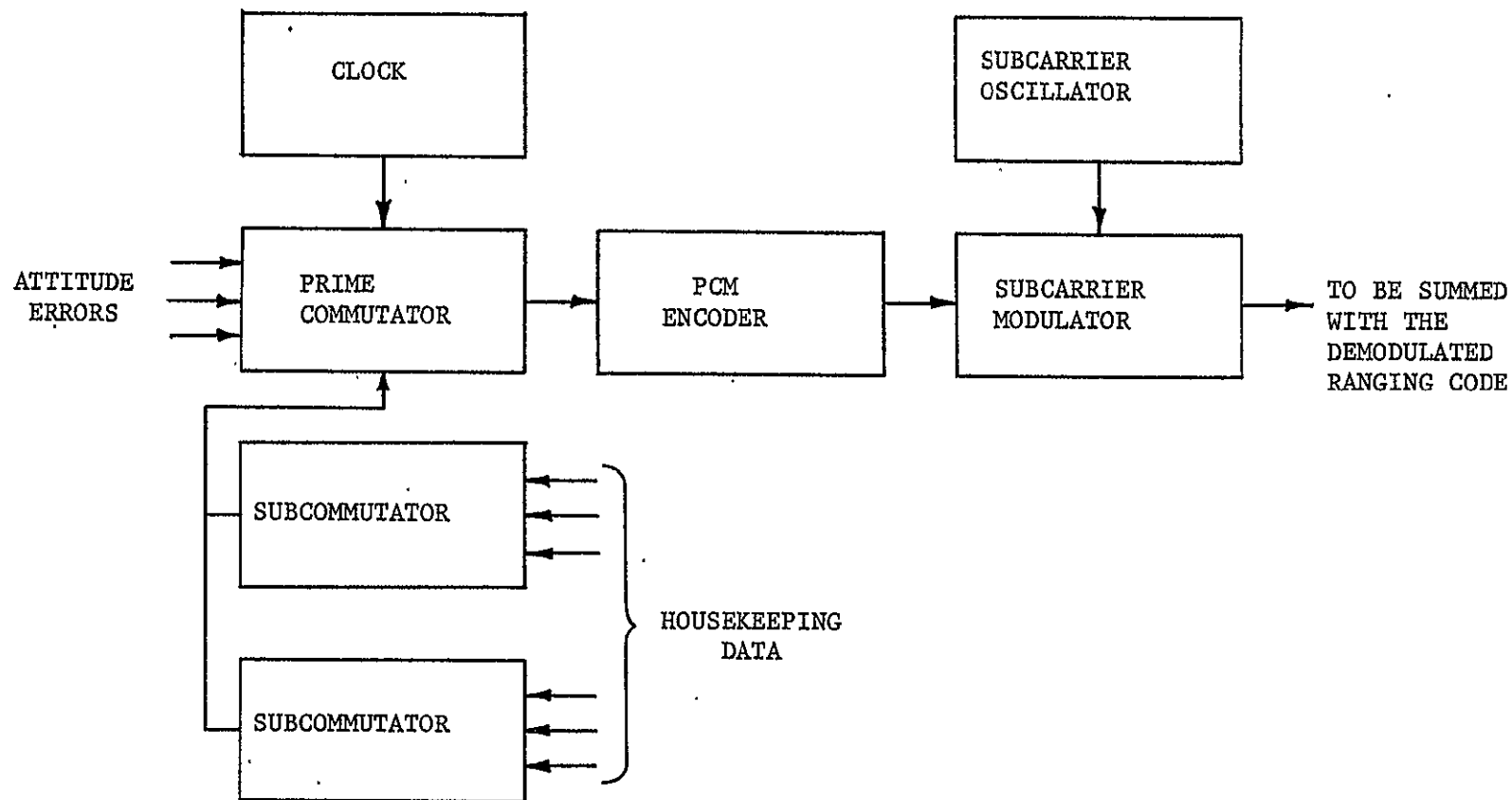


Figure 6.5 LCS Telemetry System Block Diagram

for their respective heaters. Assuming an efficiency of 40% for the TWT's and a 95% efficiency for the regulator/converter, the required 80.0 watts for the up-link power level is obtained.

6.1.3 Telemetry and Command

The function of the telemetry system in the LCS is reporting housekeeping data and verifying receipt of commands. At this initial stage of design, twenty-six commutator channels are proposed where each channel may be assigned to a specific function. The actual number of total channels may be increased at a later stage of design by employing more subcommutators. The weight and power requirements of the telemetry would increase due to such a change, but the bandwidth would be unaltered as long as the prime commutator remains at its present number of channels and sampling rate. A block diagram of the telemetry system is shown in Figure 6.5.

The commutators specified here are:

- 1 ten-channel prime commutator with a sampling rate of 2 samples/second
- 2 ten-channel subcommutators each with a sampling rate of 0.2 samples/second.

Since each channel contains 6 bits of information, the prime data rate is 120 bps (bits per second). If

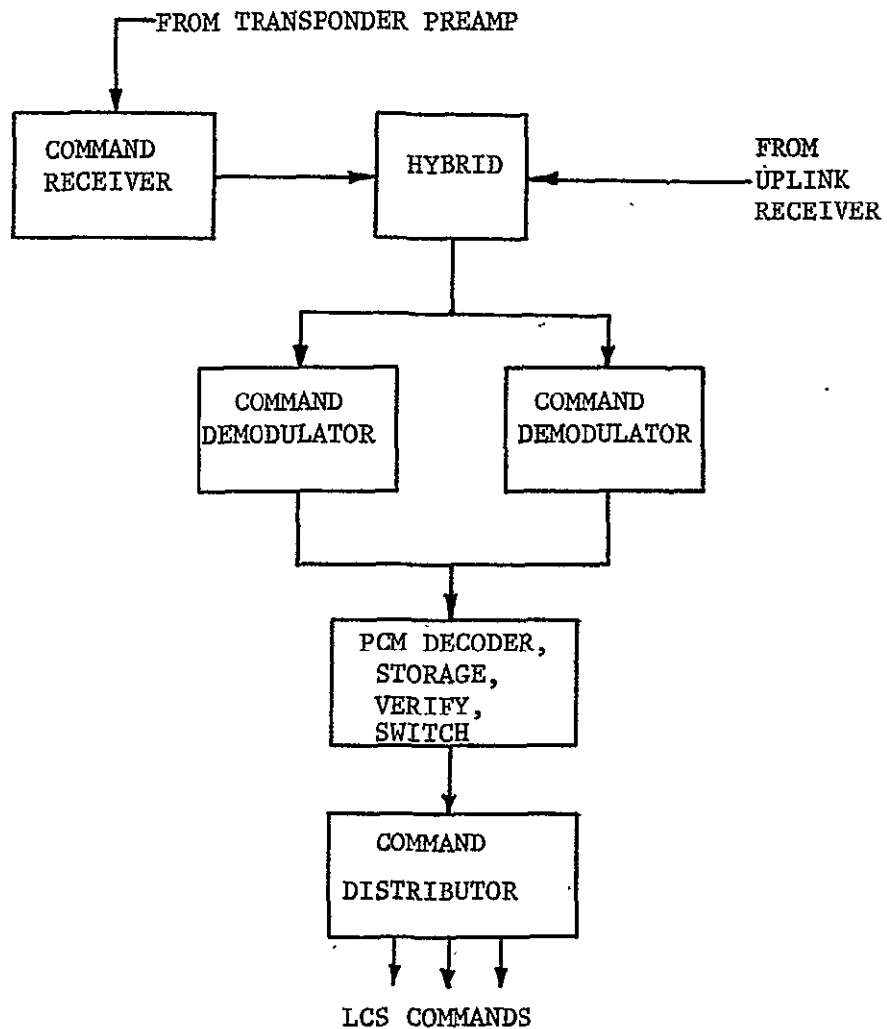


Figure 6.6 LCS Command System Block Diagram

necessary, this data rate may be easily modified to 128 bps to be compatible with existing ground and satellite equipment. The two ten-channel subcommutators are assigned to functions which vary slowly with time, such as fuel pressure, temperatures, and status of operation (on or off) of various on-board devices. The prime commutator handles all of the attitude control data. In addition, two channels are used for synchronization with the two subcommutators, while a third channel transmits time information from an on-board clock.

The command up-link is most vital for the operation of the LCS. Although many spacecraft functions operate automatically, ground control is essential in some cases and an override capability must accompany all automatic functions. Since the loss of command ability of the LCS at an early stage in the mission could result in a complete mission failure, most of the command system must be redundant. Thus, two command receivers are used. One receiver is part of the up-link receiver as shown in Figure 6.3 and the other receiver is part of the telemetry subsystem shown in Figure 6.6. In addition, two command demodulators are used to provide further redundancy.

Commands are given in a three step sequence to prevent stray signals from being interpreted as commands

by the command system. The command sequence is (i) enable, (ii) command, and (iii) execute.

- An enable command prepares the command decoder/storage to accept the operational command.
- A command is sent by the ground station after telemetered verification of the receipt of the enable command. A command may be considered operational because its execution results in the operation of some spacecraft subsystem or component.
- An execute command is sent after telemetered verification of the receipt of the operational command. The execute command unlocks the operational command decoder and thus permits the execution of a command.

This type of command system has been successfully operated in space on several communication satellites, namely ATS and Early Bird.

6.1.4 Antenna Characteristics

The satellite antenna system consists of three antennas: (i) a 10.0-foot diameter high gain parabolic

reflector with one fixed feed and one steerable feed, and (ii) two omnidirectional antennas. The parabolic antenna is used to relay signals for the MSFN/LCS/Apollo spacecraft links. The specifications of this antenna are determined according to beam illumination and effective gain requirements which are necessary in order to achieve satisfactory reception of signals transmitted from the Apollo spacecrafts (see Section 3.4). The omnidirectional antenna is used primarily for the reception and transmission of command signals between the LCS and MSFN, especially during all stages of flight of the LCS until the satellite is on-station in its halo orbit. The two omnidirectional antennas are located on the LCS in the following positions: one is mounted on the fixed feed of the parabolic antenna and pointing along the reflector axis; the other is mounted on the bottom of the vehicle and pointing along the roll axis of the LCS. Since this latter antenna is exposed immediately after the fairing of the launch vehicle is removed, it will be used during the early stages of the flight prior to the deployment of the parabolic antenna (when the other omnidirectional antenna is exposed). The omnidirectional antenna on the feed is mainly a back-up for the high gain antenna whenever its narrow beam is in error and not pointing at the center of the Moon.

The important design characteristic of the parabolic antenna is its two feeds; one feed is fixed and Moon pointing, while the other feed is steerable and Earth pointing. The Earth pointing feed generates a beam which is angularly displaced from the beam for the Moon link. The amount of beam offset is a function of the lateral distance from the LCS to the L_2 libration point as shown in Figure 6.7.

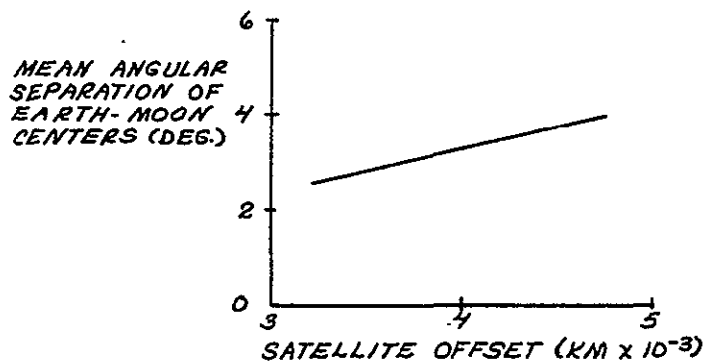


Figure 6.7 Beam Displacement vs. Satellite Offset

It is desirable for these two feeds to be physically and electrically separate. The feed design and focal length-to-diameter ratio may be chosen to meet the beam displacement requirements for a satellite offset of 3500 kilometers. The deployment and packaging of polarizers and circuitry become simpler for a larger offset, but these savings are counterbalanced by the additional fuel required to maintain this larger offset (Section B.6).

The feed for the Moon-directed beam is placed on the reflector-axis so that maximum antenna performance will be realized for the initial LCS/Apollo spacecraft links. The feed for the Earth-directed beam is located off-axis. Since the antenna axis is pointed at the center of the Moon, the Earth-directed beam must precess around the antenna axis at the orbital rate of the LCS. This is done by rotating the feed or by electronically switching between a cluster of feeds. Of these alternatives, mechanical rotation appears more attractive.

The phased array antenna was considered as an alternative to the parabolic antenna to eliminate the steerable feed. Its use on the LCS was studied as both a total phased array and as a reflector antenna with a small phased array feed. However, it was concluded that either type of antenna would be enormously large (and, hence, impractical) if it were to achieve the gain required at the LCS to receive signals from the Apollo spacecrafts.

6.2 ATTITUDE CONTROL SUBSYSTEM

The attitude of a satellite is defined as the vehicle's orientation relative to a specific reference frame. Often there are disturbing torques acting on the vehicle to produce a change in this orientation. Thus,

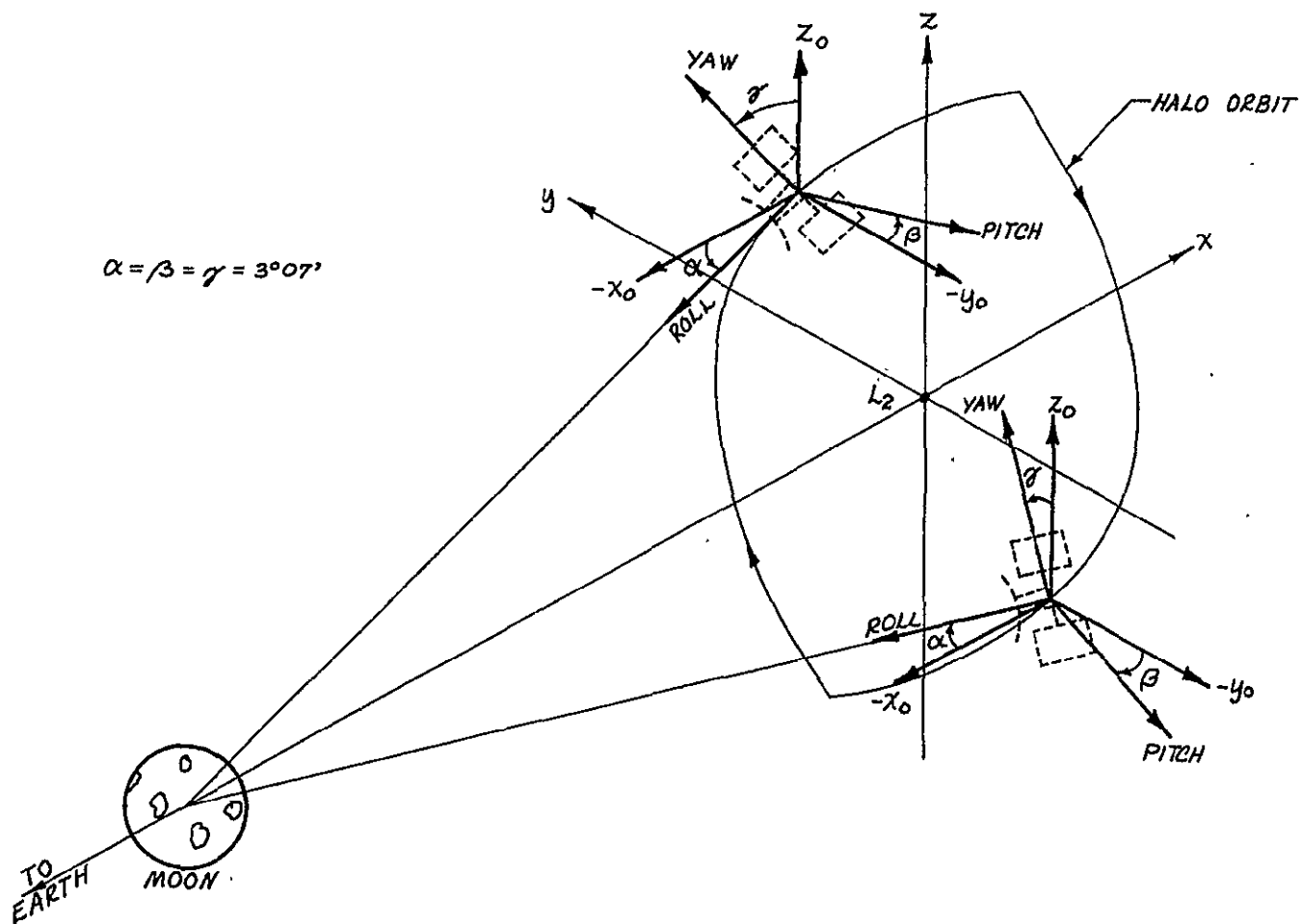


Figure 6.8 Orientation of Satellite Body Axes Relative to Orbital Axes

attitude control is the ability of the orbiting satellite to retain a specified orientation while being subjected to these disturbing torques. The attitude control system of the LCS operates in the following manner:

- Determines the attitude of the LCS with respect to a fixed reference.
- Evaluates and processes any attitude errors into a form usable by the attitude correcting devices, namely momentum wheels and hydrazine thrusters.

This section presents the components and operation of the complete LCS attitude control subsystem.

6.2.1 Definition of Satellite Axes and Attitude

The attitude of the LCS is described by specifying the angles of rotation between two coordinate systems. One coordinate frame is the body frame (B-frame) which is fixed to the body of the satellite as shown in Figure 6.8. The other frame is the orbital frame (O-frame) to which the B-frame is referred. The origins of both the B-frame and the O-frame are located at the center of mass of the LCS (Section F.3) and the axes of the B-frame are in the direction of the satellite's principal axes. Thus, the attitude of the LCS is defined as the

orientation of the B-frame relative to the O-frame. The axes of these two frames are defined as follows:

<u>Orbital Frame</u>	<u>Body Frame</u>
X_0 : parallel to Earth-Moon line	Roll: coincident with feed axis of the parabolic antenna; points toward the center of the Moon.
Z_0 : normal to Earth-Moon plane	Yaw: parallel to the longitudinal axes of the solar panels
Y_0 : orthogonal to X_0 and Z_0 ; lies in Earth-Moon plane	Pitch: perpendicular to roll and yaw.

When the LCS travels around the L_2 libration point in the desired orbit, the roll axis is always pointing towards the center of the Moon. Since the X_0 -axis is parallel to the Earth-Moon line, a cone is described as the roll axis rotates around the X_0 -axis with the apex located at the center of mass of the LCS. This has a half cone angle of $3^\circ 07'$. Since the remaining O-frame axes are mutually perpendicular to the X_0 -axis, and the remaining B-frame axes are mutually perpendicular to the roll axis, a coning motion will also occur about the Y_0 and Z_0 axes with a similar cone angle of $3^\circ 07'$. This is shown in Figure 6.9. Therefore, it is the

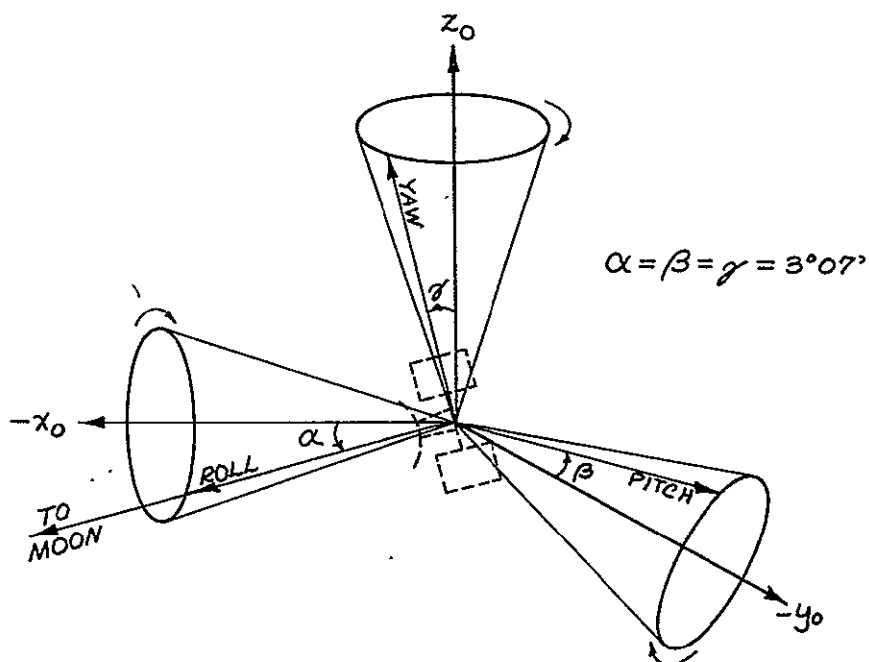


Figure 6.9 Coning Motion of Satellite Body Axes Around Orbital Axes

function of the LCS attitude control subsystem to constantly maintain these cone angles at $3^{\circ}07'$ in the presence of disturbing torques.

6.2.2 Attitude Disturbance Torques

Once the desired attitude of the satellite is obtained, it must be maintained in the presence of disturbing torques. The external torques that act on the LCS are due to:

- Solar radiation pressure
- Thruster misalignment

- Solar panel cable unwind
- Gravity gradient
- Cross-coupling resulting from the LCS angular velocity in the presence of the other four torques

Solar pressure affects the attitude of the yaw axis of the LCS because a disturbance torque is generated as a result of the misalignment of the satellite's center of pressure with its center of mass. Since the center of pressure to center of mass offset of the LCS is 13.65 inches (Section F.3) the maximum disturbance torque is

$$\begin{aligned}
 \text{Solar pressure torque} &= (\text{Solar pressure}) & (6.1) \\
 & \quad (\text{LCS surface area}) \\
 & \quad (\text{CM-CP offset}) \\
 &= (9.65 \times 10^{-8} \text{ lbs/ft}^2) \\
 & \quad (100 \text{ ft}^2) \left(\frac{13.62 \text{ in}}{12 \text{ in/ft}} \right) \\
 &= 1.07 \times 10^{-7} \text{ ft-lbs.}
 \end{aligned}$$

The magnitude of this torque has a sinusoidal variation with a period of approximately 28 days. This variation is due to the revolution of the satellite around the Earth which causes the angle of the Sun's rays against the body of the LCS to vary 360 degrees every 28 days.

Thruster misalignment creates the largest disturbance torque experienced by the LCS. This torque

results because the thrust vector may not pass through the center of mass of the satellite. The torque reaches a maximum during burns for Z-axis period control when the thrust level is the greatest. The maximum torque is calculated by assuming that the thrust vector is offset from the center of mass by .25 inches. Thus, the resultant torque is:

$$\begin{aligned}
 \text{Thruster misalignment} & & (6.2) \\
 \text{torque} & = (\text{Thrust level}) \\
 & \quad (\text{Thrust vector-CM offset}) \\
 & = (1.0 \text{ lbs}) \left(\frac{.25 \text{ in}}{12 \text{ in/ft}} \right) \\
 & = 2.08 \times 10^{-2} \text{ ft-lbs.}
 \end{aligned}$$

This torque has its greatest effect on the attitude of both the roll and pitch axes.

The disturbance torque created by unwinding the solar panel cables occurs every synodic month (see Section 6.2.4) and effects the attitude of the yaw axis. The magnitude of this torque is proportional to the time required for the cables to be unwound. Thus, this torque is reduced by unwinding the cables during a twenty minute period. The resulting disturbance torque is small and the resulting motion can be corrected by LCS attitude correcting devices.

A gravity gradient disturbance torque occurs only if the following exist:

- The LCS has large differences in principal moments of inertia.
- The angle between the local vertical to the Moon and the roll axis is not zero.
- The angle between the direction of motion of the Earth-Moon system and the pitch axis is not zero.
- The angle between the angular velocity vector of the Earth-Moon system and the yaw axis is not zero.

The resultant torques produced when these conditions exist are proportional to the square of the satellite angular velocity with respect to the orbital-frame. Since the maximum torque due to gravity gradient occurs about the pitch axis and has an order of magnitude of 10^{-10} ft-lbs, it can be easily corrected.

Finally, cross coupling or gyroscopic disturbance torques are considered to be minimal. This is due to the small angular velocities of the satellite in inertial space and with respect to the orbital frame (which is the coning motion) and are 10^{-6} and 10^{-7} radians/sec respectively.

6.2.3 Attitude Sensors

The effect of pitch and yaw axis disturbance torques is determined by four Moon horizon scanners. One pair of scanners sense pitch attitude and another pair sense yaw attitude. These scanners are located on the lip edges of the LCS high-gain parabolic antenna and view the horizon circle of the Moon as shown in Figure 6.10. Each scanner contains four arrays of thermopile elements which generate an electrical signal. These signals are compared to each other to give pitch and yaw information. When the same number of elements of each scanner view the horizon, their output signals are equal. This implies that both the pitch and yaw axes are at the proper attitudes. If the output signals are not equal, then a corrective torque must be applied to the satellite until these signals are equal. The accuracy of the Moon scanners is $\pm 1^\circ$, which is sufficient to satisfy the $\pm 0.25^\circ$ design requirement of the LCS.

The roll attitude of the LCS is determined by star trackers (Section 5.2) which locate and lock onto the star Canopus. These sensors are light sensitive devices with a 10° field of view and are mounted on two degree-of-freedom gimbal systems. One star tracker is used initially during trans-lunar flight when its gimbals are locked and the LCS is rolled until Canopus is sighted.

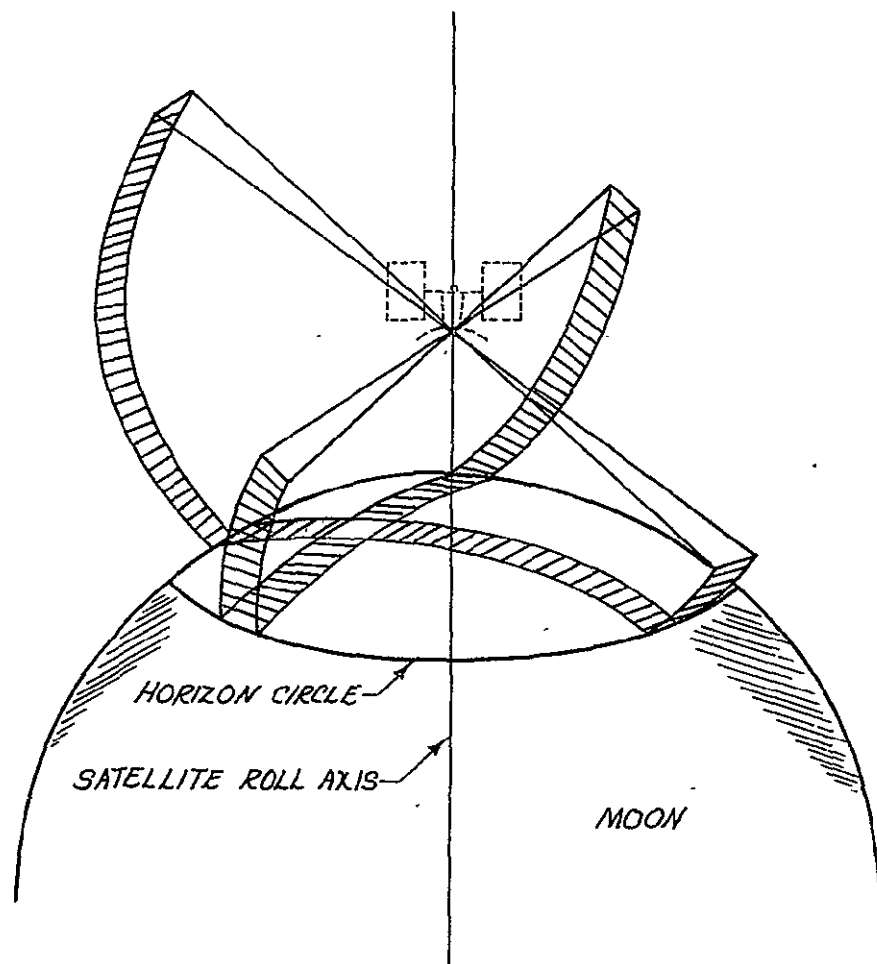


Figure 6.10 Tracks of Moon Horizon Scanner

This fixes the attitude of the satellite roll axis during this phase of the mission. Once the LCS is on-station in the halo orbit, the gimbals are commanded from the Earth in order to provide the proper alignment of the roll axis. Precession of the gimbal angles is needed because the yaw axis of the LCS is coning around the line of sight from the sensor to Canopus with a cone angle of 15-20 degrees along the entire path of the orbit. Information to these gimbals should be updated periodically throughout the flight of the LCS. However, this creates a severe operational problem and it is suggested that other techniques be developed.

6.2.4 Attitude Correcting Torques

Once the attitude error of the LCS is known, a torque must be applied to the satellite body in order to correct this misorientation. The torque is generated by accelerating or decelerating a rotating wheel inside the satellite. This technique utilizes a system of three momentum (or inertial) wheels which are driven by brushless DC motors (Reference 9). A wide range of torque levels is obtainable by using gears between the wheels and the drive motors. Appendix F gives an estimate of the size and weight of the momentum wheel package which is located at the center of mass of the LCS to prevent

cross coupling torques caused by misalignment of the wheel spin axes and the principal axes of the LCS.

It should be noted that a momentum wheel has a maximum or minimum angular velocity. When this extreme condition occurs, the wheel reaches a stall torque, implying that it can no longer be accelerated (if it is at its maximum angular velocity) or decelerated (if it is at its minimum angular velocity) to create a torque on the satellite body. To overcome this problem, the total angular momentum of the wheel must be reduced or increased, which can only be accomplished by a mass expulsion system, namely, reaction control thrusters. These thrusters similarly create torques on the satellite body. However, the sense of this torque is determined according to whether the momentum wheel is at its maximum or minimum angular velocity. Assuming that the wheel is rotating with a positive sense and is at its maximum angular velocity, a positive thrust is required to allow the wheel to decelerate without affecting the attitude of the satellite. Similarly, if the wheel is at its minimum angular velocity, a negative thrust is necessary to allow the wheel to accelerate.

6.2.5 Operation of the Attitude Control Subsystem

The complete attitude control subsystem is shown in Figure 6.11. The effect of a disturbance torque on the satellite body causes a change in the orientation of the satellite. The magnitude and sense of this angular displacement is measured by either the Moon horizon scanners or the Canopus star trackers and a signal is then sent to the on-board computer. The corresponding momentum wheel is accelerated (or decelerated) to create a torque on the satellite body which rotates the satellite back into its desired orientation. However, the satellite may be properly oriented and yet have a rate error. A rate gyro is used to make this measurement, since the output of the rate gyro is proportional to the angular velocity (or rotational rate) of the body axes of the satellite. So, the computer again activates the momentum wheel until a sensor indicates that the satellite is properly orientated and the rate gyro shows that the satellite has the correct angular velocity. The speed of the momentum wheel is measured by a tachometer and the computer activates the proper thrusters whenever their minimum or maximum angular velocities are reached.

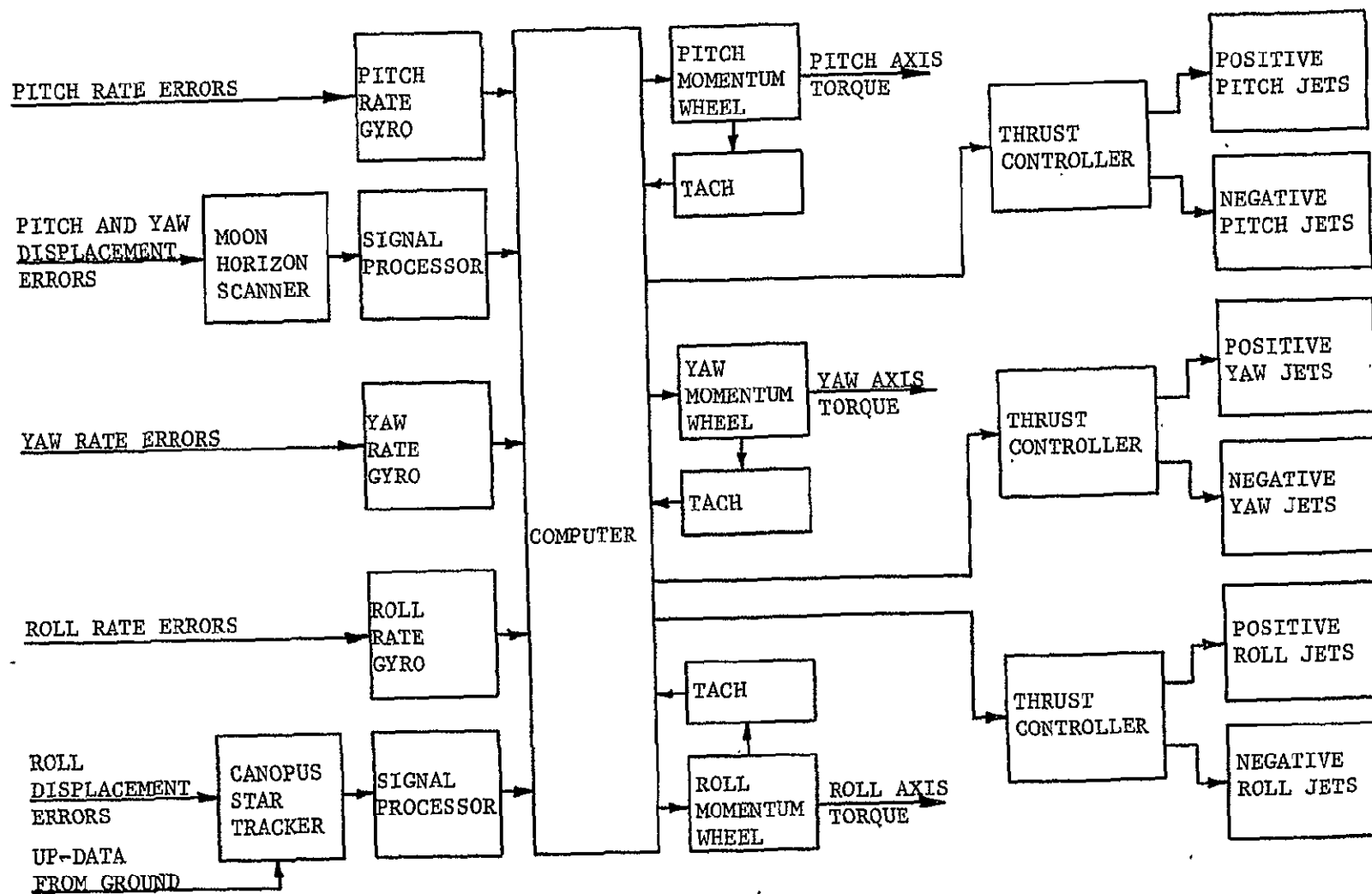


Figure 6.11 Block Diagram of Attitude Control Subsystem

6.2.6 Sun Sensors

Sun sensors align the LCS during the trajectory and orient the solar panels while in halo orbit. These sensors are extremely simple, reliable, and lightweight, although their accuracy may decrease with age. Each consists of two light sensitive cells on either side of a shield (Figure 6.12). The two cells are part of a bridge network which senses voltage differences. The spacecraft attitude is corrected until the voltages generated by the cells are equal. During the trajectory, these sensors can be used to align two axes of the spacecraft.

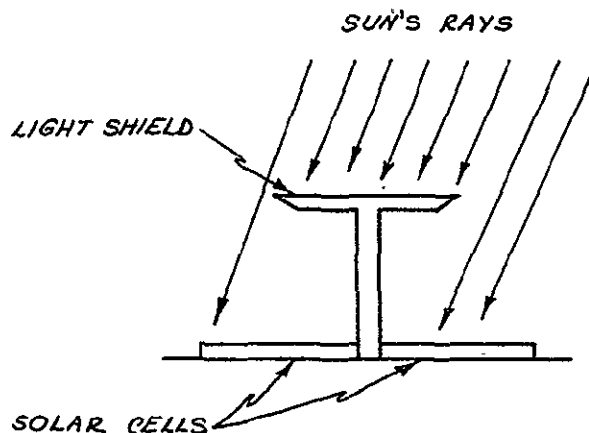


Figure 6.12 Sun Sensor

6.3 POWER SUPPLY SUBSYSTEM

Primary electrical power for the LCS is supplied by solar cells mounted on two independently orientable panels; secondary power is provided by a nickel cadmium battery. Both the primary and the secondary sources can be used separately or together in parallel. During the early stages of flight of the LCS, the battery is the only source of electrical power. Once the fairing of the launch vehicle is removed and the LCS is despun, the solar panels are deployed and become operational. The battery is also needed whenever the panels are shaded from the Sun or if the primary source should fail.

6.3.1 Power Requirements

The main consideration used in designing the power system is the amount of power required for complete operation of the LCS. Table 6.1 shows the operational prime power requirements. Whenever the LCS is operating during an Apollo mission, 471 watts are needed. During periods between missions, only 251 watts are necessary, because neither the high gain communication amplifiers (TWT's) or high gain parabolic antenna (with its feed drive) are used. Eclipse periods are estimated to last a maximum of 2.75 hours and to occur no more than 10 times during the four year life of the satellite. In order to minimize

Table 6.1

LCS OPERATIONAL PRIME POWER REQUIREMENTS

EQUIPMENT	WATTS
Antenna	
Feed Drive	10.0
Communications	
Transponder	6.0
Telemetry and Command	25.0
TWT Amplifiers	210.0
TWT Heaters	10.0
Down-link Amplifiers	25.0
Power Supply	
Charge Regulator	6.0
Panel Drive Motors	10.0
Control Systems	
Attitude Control	100.0
Stationkeeping	<u>70.0</u>
Total Wattage	471.0

the size of the battery needed to power the LCS, it is recommended that a mission not be flown if an eclipse is to occur any time during the mission. Thus, the batteries are sized to provide minimum required power during eclipse periods and maximum power if the primary power source should fail.

6.3.2 Solar Panels

Primary power is delivered from solar cell arrays mounted on a single side of each of two panels. During launch, the panels are folded around the body of the LCS (see Figure F.3) and are deployed by a spring mechanism immediately after the vehicle is despun during translunar flight. At this time, Sun sensors are used to properly orient the panels so that they are normal to the Sun-line. This orientation is maintained by continuously rotating the panels about an axis parallel to the yaw axis (approximately normal to the ecliptic). Power is transferred from the panels to the satellite body by means of a wrap-around cable. The use of this cable allows maximum transfer of power, but requires that the panels be rotated once every synodic month in order to unwind the cable (a further discussion of this cable is in Section 6.4).

The type of cells being used are 2x2 centimeter N/P ohm-centimeter silicon cells of .014 inch thickness. They are chosen because of their slow rate of degradation. A .006 inch microsheet coverglass covers the cells to protect them from solar flare radiation. In addition, a blue-red filter is used to restrict absorption of energy in the solar cell sensitive regions. The cells are mounted on two 8x5 foot aluminum honeycomb panels. (The derivation of the solar panel area is in Section E.1). A thin sheet of glass epoxy is used to bond the cells to the panels and to provide electrical insulation between the aluminum and the cells.

6.3.3 Batteries

Secondary power is provided from a nickel-cadmium battery. This type of battery is chosen because it has the highest survivability and longest cycle life of any space qualified battery. This is a very important criteria because of the four year lifetime of the LCS.

The sizing of the battery is dependent upon several conditions. One is the possibility of the LCS failing to receive power from the solar cells during an actual landing mission on the lunar back-side. In this emergency situation, the satellite must remain fully operational long enough for the astronauts to safely

about the lunar excursion portion of their mission and immediately lift-off from the lunar surface. Thus, the battery is expected to provide full power to the LCS for a period of 1.75 hours. The second condition occurs whenever the solar cells are shaded from the Sun by either the Moon or the Earth. These eclipse periods are estimated to last for a maximum of 2.75 hours and to occur no more than 10 times during the four-year operational lifetime of the satellite. In order to minimize the total amount of electrical power needed during an eclipse period, it is recommended that a mission not be flown if an eclipse is expected to occur anytime during the mission. Thus, the TWT amplifiers and the high gain antenna feed drive motor will be off, reducing the LCS power requirement to 251 watts.

In Section E.2, the calculations for determining the battery size are shown. The battery consists of 168 cells, each cell having an output of 1.28 volts DC at 6 amp-hours. It has seven banks of cells connected in parallel to provide a total of 42 amp-hours of current, and each bank contains 24 cells in series to provide a nominal 30 volts DC. In emergency operation, the cells can be 90 per cent discharged to provide for the safety of the astronauts. However, during eclipse periods, the cells will be discharged only 75%. The total battery weight is 84 pounds.

6.3.4 Operation of the Power Supply Subsystem

A power control system is used to match the varying requirements of the LCS's loads and to provide current protection in case of power overloads. This system is designed to provide 30 volts DC to operate the satellite subsystems. A block diagram of the complete power supply system is shown in Figure 6.13.

During periods of full sunlight, the battery is charged by power from the solar array. Silicon diodes, placed in series with each string of solar cells, are used to prevent the battery from discharging into the cells whenever they are not being illuminated. The battery is controlled by the battery charge regulator which keeps it from reaching a predetermined overcharge temperature. The battery temperature is monitored to determine when this overcharge temperature is approached, at which time the charging current is reduced to a minimum of 0.33 amperes for a fixed period of time. At the end of this period, the battery resumes normal charging until the critical temperature is again reached.

Another problem occurs whenever the communications equipment is not operating, for the power supplied by the panels exceeds the power required by 220 watts. This is solved by dissipating the excess power with resistors on the solar panels. A shunt regulator controls this function.

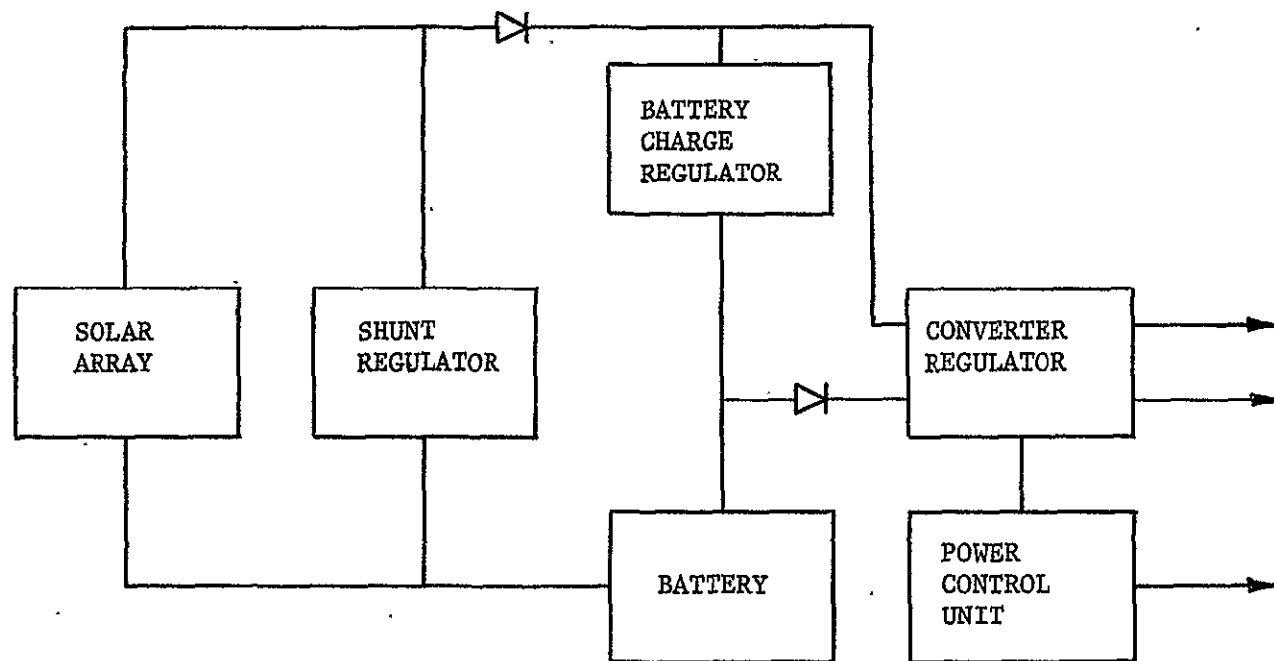


Figure 6.13 LCS Power Supply Subsystem Diagram

The power control unit is used to regulate and distribute the solar array power and to provide telemetry outputs on the performance of the power supply subsystem. It also performs the following functions:

- Regulates the main power bus voltage.
- Provides automatic disconnect and reconnect of the TWT's as dictated by the power capability of the solar array.
- Provides telemetry monitoring of current, voltage, and temperature to permit operational analysis of the subsystem.

The main regulator provides 30 volts DC, although the solar panels are sized to deliver 35 volts, allowing five volts for losses (two volts through lines and diodes and three volts through regulators). This regulator also provides adequate control for the range of voltages from the battery (23.5 volts to 33.5 volts, depending on the ambient temperature and current). There are two outputs from the regulator: one output is connected to the TWT power regulator through a filter to minimize feedback of unwanted ripple; the other output is for the remainder of the electronic components and is connected through an additional filter section. A DC converter is also incorporated in this regulator and furnishes the heater, anode, helix, and collector voltages for the TWT's as derived

from the 30 volt DC supply. The converter has an efficiency of 85% and is unregulated.

6.4 STRUCTURES SUBSYSTEM

The LCS structure is designed to provide an adequate support system for the spacecraft subsystems at a minimum cost and weight. Aluminum is chosen as the prime material because of its low density and ease of fabrication. Honeycomb sandwich material is also used whenever possible, since it possesses excellent vibration damping characteristics.

The major structural design problem is the provision of adequate support and rotational movement for the solar panels, which must extend beyond the high gain parabolic antenna. The physical size of the launch vehicle fairing also presents an additional problem of folding the panels and its support arms.

Another problem arises with the transfer of electrical power from the solar panels to the spacecraft body because continuous rotation of the panels necessitates the use of slip rings. The slow rotation of these metal to metal contacts would eventually cold weld within the four-year lifetime of the LCS.

6.4.1 General Description

The main structural members are two cylindrical support tubes which carry and transmit the launch loads and to which all other members are attached as shown in Figure 6.14a. The larger, four-foot diameter tube contains two honeycomb equipment platforms (one at each end) and a crossing network of stiffened support panels as shown in Figure 6.14b. The three-foot diameter tube has

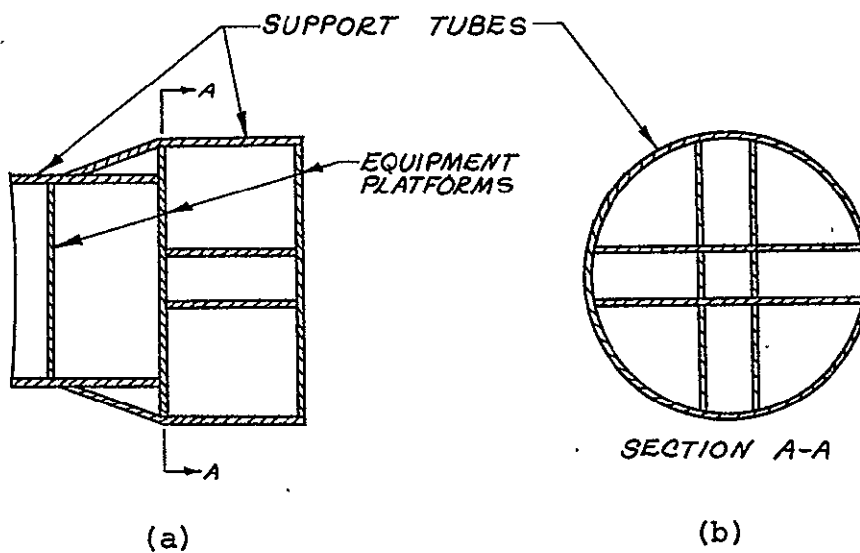


Figure 6.14 LCS Structure

one equipment platform and mounting brackets to support the high gain antenna.

6.4.2 Solar Panel Support and Drive Mechanism

At launch, the solar panels and their supports are folded inside the launch vehicle fairing (note each panel is hinged along its center line; Figure F.3). After despin, they are unfolded and form a rigid structure which can be easily rotated. The unfolded configuration with two support members per panel is shown in Figure 1.2.

Each panel driveshaft is connected to the spacecraft by a universal joint. This allows the shaft to be folded at launch and provides free rotation of the panel in case of incomplete deployment. Figure 6.15 is a schematic of this attachment.

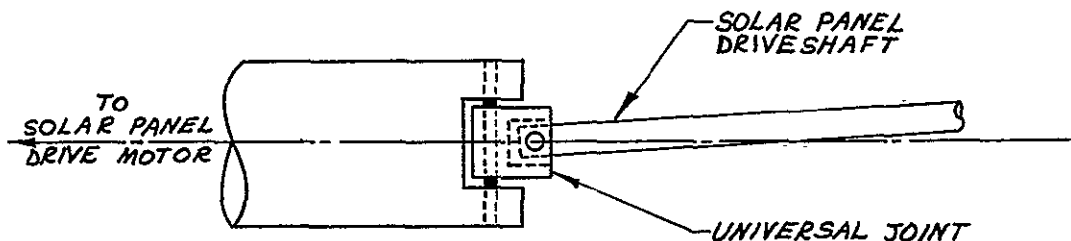


Figure 6.15 Solar Panel Drive Mechanism Schematic

The two support members are three sections of telescoping tubes which are spring loaded to extend when the yo-yo despin collar (Section 6.4.3) is released. A

simple locking mechanism for these rods is pictured in Figure 6.16.

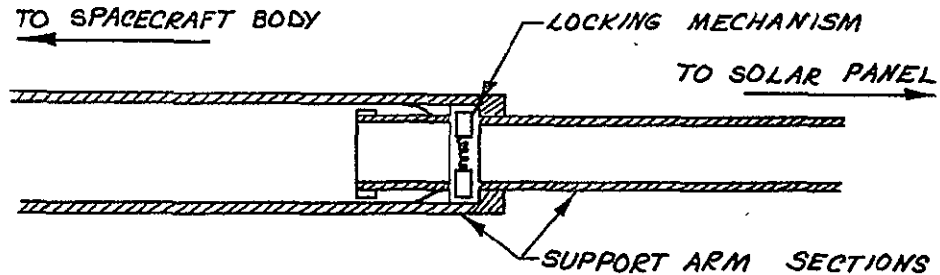


Figure 6.16 Support Arm Locking Mechanism Schematic

To avoid cold welding of slip rings, a direct cable attachment is used between panels and body. This necessitates an unwinding maneuver of the cable every synodic month (29.53 days).

6.4.3 Yo-Yo Despin Mechanism

The Delta third stage ejects the LCS into space with a spin rate of about 100 rpm. Yo-yo despin is a common technique for eliminating most of this spin. This despin mechanism consists of a circular U-channel at the center of mass of the folded spacecraft (Figure F.3; Section F.3). Two cables are attached to this channel at opposite ends of a diameter and wrapped around the satellite body one and a half times. A small weight is attached at the extreme end of each cable and is

released by the firing of two pyrotechnic bolts on command from the ground. Thus, the cables unwind and, thereby, decrease the rotation rate of the LCS. Once the cables are fully extended, they are released and the U-channel is jettisoned, allowing the solar panels to deploy.

The size of the small weights can be calculated using the equation

$$M = \frac{I}{(l + r)^2 - r^2} \quad (6.3)$$

where M = mass of each weight

I = LCS spin moment of inertia (folded)

l = length of each cable

r = radius of the U-channel

Substituting from Appendix F,

$$M = \frac{62 \text{ slug-ft}^2}{[(25 + 2.7)^2 - 2.7^2] \text{ ft}^2} = 0.079 \text{ slug}$$

or 2.55 pounds each.

APPENDIX A

COMMUNICATION CALCULATIONS

A.1 SAMPLE LINK CALCULATION

The following is the procedure used to determine the minimum required antenna gain at the LCS for the LM/LCS link. Rewriting Equation (3.1),

$$G_R = L_T + L_R + L_P + L_S + N_{in} + (S/N)_{in} - G_T - P_T \quad (A.1)$$

The values for the above parameters are

- L_T = LM transmit circuit losses
 - = 3.4 db, for the steerable antenna;
current Apollo
 - = 3.4 db, for the omnidirectional antenna;
current Apollo
 - = 3.0 db, for the steerable and omnidirectional
antennas; modified Apollo
- L_R = LCS receive circuit losses
 - = 3.0 db
- L_P = LM antenna pointing loss
 - = 0.5 db, for the steerable antenna.

L_S = Space loss

$$= 37.8 + 20 \log R + 20 \log f$$

where R = maximum separation distance between the LM and the LCS

$$= 37,770 \text{ nm}$$

f = transmission frequency

$$= 2282.5 \text{ MHz}$$

$$= 37.8 + 20 \log (37770.0) + 20 \log (2282.5)$$

$$= 195.6 \text{ db}$$

N_{in} = Noise input spectral density at LCS receiver terminals

$$= 10 \log (KT_e B_{IF})$$

where K = Boltzmann's constant

$$= 1.38 \times 10^{-23} \text{ w/(Hz} \cdot \text{ } ^\circ\text{K)}$$

T_e = overall effective noise temperature at receiver input (derived in Section A.3)

$$= 686 \text{ } ^\circ\text{K}$$

B_{IF} = RF bandwidth

$$= 4 \times 10^6 \text{ Hz, maximum value of this system for television transmission}$$

$$= 10 \log [(1.38 \times 10^{-23}) (686) (4 \times 10^6)]$$

$$= -134.8 \text{ db}$$

$(S/N)_{in}$ = 8.0 db, for television

G_T = LM transmit antenna gain

$$= 20.5 \text{ db, for the steerable antenna; current Apollo}$$

= -3.0 db, for the omnidirectional antenna;
current Apollo

= 28.5 db, for the steerable antenna;
modified Apollo

= 0.0 db, for the omnidirectional antenna;
modified Apollo

P_T = LM transmitter power

= 18.6 watts = 12.7 dbw; current Apollo

= 37.0 watts = 15.7 dbw; modified Apollo

Thus, substituting these values into Equation (A.1), we have the following results

G_R = 42.9 db, for steerable antenna;
current Apollo

= 68.0 db, for omnidirectional antenna;
current Apollo

= 33.1 db, for steerable antenna;
modified Apollo

= 59.6 db, for omnidirectional antenna;
modified Apollo

These values of G_R represent the minimum values of the receiving antenna gain which are necessary in order to obtain the desired signal strength at the LCS receiver.

A.2 EFFECTIVE ANTENNA NOISE TEMPERATURE

The antenna noise temperature, T_a , represents the noise power radiated into the antenna plus the thermal noise generated directly at the antenna. An antenna

whose entire beam is intercepted by the Moon has a noise temperature of

$$T_a = T_1 = 220^\circ\text{K}$$

where T_1 = lunar radio noise temperature at 2. GHz.

Similarly, an antenna whose entire beam is intercepted by the Earth has a maximum noise temperature of

$$T_a = T_2 = 290^\circ\text{K}$$

where T_2 = Earth radio noise temperature at 2 GHz.

The noise temperature for an antenna on the LCS whose beam is intercepted by both the Moon and the Earth is

$$T_a = T_1 \left(\frac{\alpha}{\theta}\right)^2 + T_2 \left(\frac{\beta}{\theta}\right)^2 \quad (\text{A.2})$$

where β = maximum angular antenna coverage of the Earth

$$= 1.9^\circ$$

α = maximum angular coverage of Moon

$$= 3.25^\circ$$

θ = -3db antenna beamwidth

$$= 5.2^\circ$$

Thus, we get

$$T_a = 220 \left(\frac{3.25}{5.2}\right)^2 + 290 \left(\frac{1.9}{5.2}\right)^2 = 116^\circ\text{K}$$

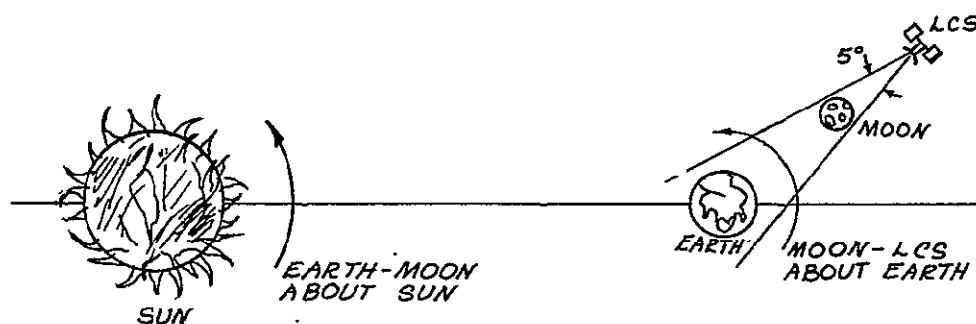


Figure A.1 Illumination of the Sun
by the LCS Antenna

The LCS antenna directly views the Sun for approximately 9 hours per month. As shown in Figure A.1, the Moon has an approximate period of revolution about the Earth of 28 days per month or 13 degrees per day and the LCS antenna has a -3db beamwidth of 5 degrees. Thus, it will intercept the Sun for only 5/13 of a day (9.2 hours). However, the maximum solar noise pick-up (which is approximately 1000°K neglecting Earth occultation) is achieved only during the passage of the -1.5 db antenna beamwidth points. The -1.5 db beamwidth is given by

$$\theta = \left(\frac{K_{db}}{3} \right)^{1/2} \theta_{3db} \quad (A.3)$$

where θ = angular width of main lobe for decay of K_{db}

$$K_{db} = 1.5$$

$$\theta_{3db} = -3db \text{ beamwidth of LCS antenna}$$

$$= 5.2^\circ$$

Substituting these values into (A.3),

$$\theta = \left(\frac{1.5}{3} \right)^{1/2} \quad (5.2)$$

$$= 3.5^\circ$$

Thus, the antenna effectively faces the Sun for only 6.5 hours per month.

The antenna noise temperature of the LCS is effected when the antenna directly views the Sun. Since the Sun subtends approximately 0.5 degrees whether viewed from the Earth, the LCS, or from a point near the Moon, the effective LCS noise temperature can be expressed as

$$T_{a_s} = \left(\frac{2.0 \times 10^{14}}{f} \right) \left(\frac{0.5}{\theta} \right)^2 \quad (A.4)$$

where T_{a_s} = antenna noise attributed to a direct view of the Sun

f = RF frequency of the signal

= 2.1 GHz

= 2.1×10^9 Hz

θ = -3db antenna beamwidth

= 5.2°

$$\text{Thus, } T_{a_s} = \left(\frac{2.0 \times 10^{14}}{2.1 \times 10^9} \right) \left(\frac{.5}{5.2} \right)^2$$
$$= 1000^\circ\text{K}$$

In Section A.3, it is shown that the effective system noise temperature is hardly changed as a result of this increased value of T_a when the antenna views the Sun.

A.3 EFFECTIVE SYSTEM NOISE TEMPERATURE

The total noise at the receiver terminal is due primarily to three separate sources: the antenna noise as received from sources external to the receiving system; the noise introduced by the lossy transmission line and

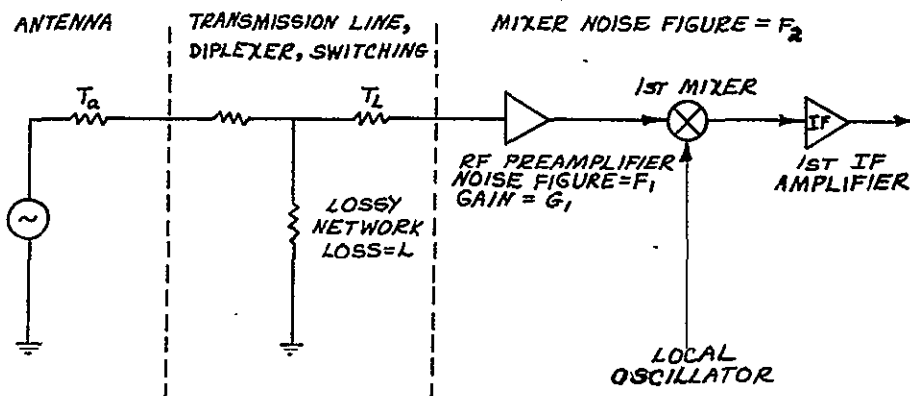


Figure A.2 Primary Parameters Affecting Receiver Noise

associated RF hardware connecting the antenna to the receiver input; and the noise generated at the receiver input terminals. Referring to Figure A.2, the overall effective noise temperature at the receiver IF amplifier is given by

$$T_e = \frac{T_a}{L_R} + T_L \left(1 - \frac{1}{L_R}\right) + \left(F_1 + \frac{F_2 - 1}{G_1} - 1\right) T_r \quad (A.5)$$

where T_e = overall effective system noise temperature at the receiver input

T_a = effective antenna noise temperature

T_L = transmission line temperature

T_r = receiver temperature

L_R = receiving circuit losses

F_1 = preamplifier noise figure

F_2 = mixer noise figure

G_1 = preamplifier gain

In order to reduce the receiver noise figure, an RF preamplifier can be employed, in which case

$$F = F_1 + \frac{F_2 - 1}{G_1} \quad (A.6)$$

where F = overall receiver noise figure.

Thus, combining (A.5) and (A.6), we get

$$T_e = \frac{T_a}{L_R} + T_L \left(1 - \frac{1}{L_R}\right) + (F-1)T_r \quad (A.7)$$

Now, let $T_o = T_L = T_r$, so (A.7) becomes

$$T_e = \frac{T_a}{L_R} + T_o \left(F - \frac{1}{L_R}\right) \quad (A.8)$$

Solving (A.8) for the example in Section A.1, we have the following values at the LCS:

$$T_a = 116^\circ\text{K}$$

$$T_o = 314^\circ\text{K}$$

$$F = 4.0 \text{ db}$$

$$= 2.5$$

$$L_R = 3.0 \text{ db}$$

$$= 2.0$$

Thus, the overall effective system noise temperature at the LCS according to (A.8) is.

$$T_e = \frac{116}{2.0} + 314 \left(2.5 - \frac{1}{2.0} \right)$$

$$= 686^\circ\text{K}$$

It is this value of T_e which is used in the calculation of the noise input at the receiver terminal.

For the special case when the LCS antenna is viewing the Sun, the effective system temperature becomes

$$T_{e_s} = \frac{T_{a_s}}{L_R} + T_o \left(F - \frac{1}{L_R} \right) \quad (\text{A.9})$$

where T_{e_s} = effective system noise temperature when the antenna is viewing the Sun.

T_{a_s} = antenna noise attributed to a direct view of the Sun

= 1000°K (from Section A.2)

So, this becomes

$$T_{e_s} = \frac{1000}{2.0} + 314 \left(2.5 - \frac{1}{2.0} \right)$$

$$= 1128^\circ\text{K}$$

Thus, when the LCS antenna directly views the Sun, the effective system noise temperature increases by approximately 2.1 db. It should be noted that if the receiver preamplifier is not used, the receiver noise figure is

13 db (instead of 4 db) and the effective system noise temperature would increase only .38 db when the Sun is viewed.

A.4 PARABOLIC ANTENNA SIZE AND BEAMWIDTH

The gain of an antenna is primarily a measure of its concentration of radiated power. Thus, the gain of a parabolic antenna is given by

$$G = 20 \log f + 20 \log D - 52.6$$

where G = parabolic antenna gain (db)

f = carrier frequency (MHz)

D = diameter of the parabolic reflector (feet)

The relationship between beamwidth and gain is quite simple for the ideal case where all of the radiated power is concentrated in a single narrow-beam lobe. For a parabolic antenna, this beam is conical in shape, so we have

$$\theta = \frac{7 \times 10^4}{(f)(D)} \quad (A.11)$$

where θ = -3db beamwidth (degrees)

f = carrier frequency (MHz)

D = diameter of the parabolic reflector (feet)

As an example, consider a single beam transmitted at a frequency of 2100.0 MHz and radiated from a parabolic antenna with a diameter of 5.0 feet. The resulting gain and -3db beamwidth from Equations (A.10) and (A.11) are

$$\begin{aligned} G &= 20 \log (2100.0) + 20 \log (5.0) - 52.6 \\ &= 27.8 \text{ db} \end{aligned}$$

$$\begin{aligned} \theta &= \frac{.7 \times 10^4}{(2100.0)(5.0)} \\ &= 6.67 \text{ degrees} \end{aligned}$$

While the above discussion shows the inter-relationship between transmitting antenna gain, diameter and beamwidth, it should be noted that the same relationships are also applicable when the antenna is receiving. Thus, for a given frequency and antenna size, the radiation and absorption patterns of a properly terminated antenna are the same.

APPENDIX B

L₂ LIBRATION POINT ANALYSIS

B.1 DEFINITION OF LIBRATION POINTS

There are five equilibrium solutions to the restricted three body problem. That is, five points in the vicinity of two finite bodies in space at which an infinitesimal third body will have zero relative velocity.

These five points are called libration points, and their existence was discovered by Lagrange in 1772. Physically, these points represent locations at which centrifugal and gravitational accelerations balance each other while the third body orbits the center of mass of the system with a period equal to that of the primary bodies. Three of these points lie along the line joining the primaries. The last two form equilateral triangles with the finite bodies and lie in the orbit plane. The libration points for the Earth-Moon system are shown in Figure B.1 and the conventional numbering system should be noted.

$$D = 3.84 \times 10^5 \text{ KM}$$

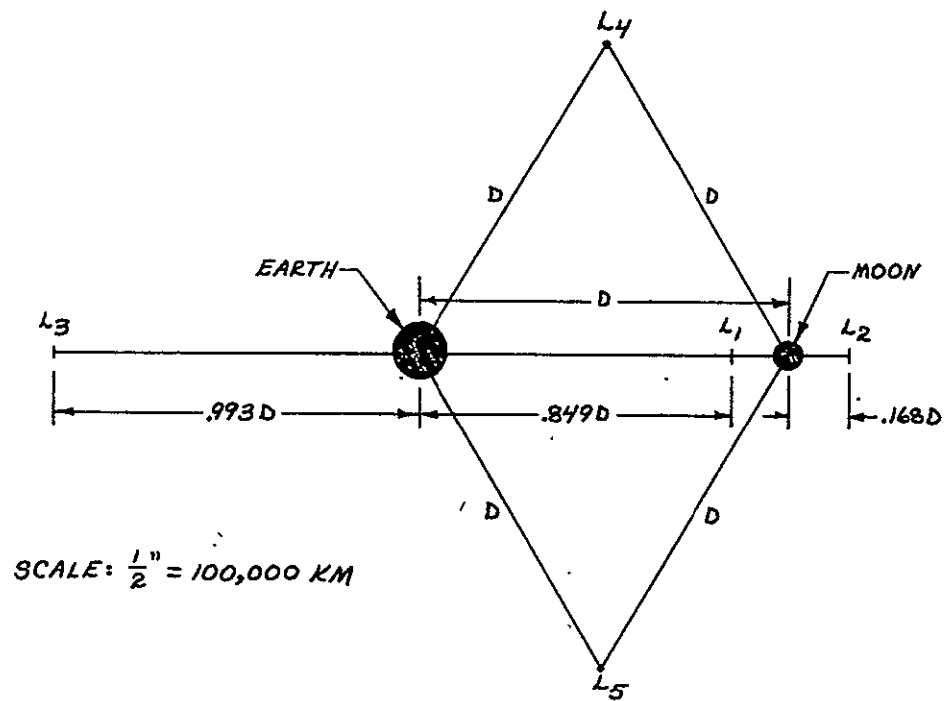


Figure B.1 Positions of the Earth-Moon Libration Points

B.2 CALCULATION OF THE L_2 LIBRATION POINT POSITION

The second libration point (L_2) is of particular interest because it provides a constant view of the lunar far-side. The position of L_2 is found by equating the centrifugal and gravitational forces acting on a body at an arbitrary distance (d) beyond the Moon. Let

D = Earth-Moon distance
 d = Moon-libration point distance
 G = Universal Gravitation Constant
 M_e = mass of the Earth
 M_m = mass of the Moon
 M = mass of the third body
 T = orbital period of the Moon
 V = orbital speed of the third body

It is assumed that

- the Earth and Moon are both spherically symmetrical
- the Earth, Moon, and third body are in circular orbits about the Earth-Moon center of mass
- the mass of the third body is small and has no effect on the orbit of the Earth and Moon.

Equating the centrifugal and gravitational forces,

$$GM \left[\frac{M_e}{(D+d)^2} + \frac{M_m}{d^2} \right] = \frac{MY^2}{\left(d + \frac{M_e D}{M_e + M_m} \right)} \quad (B.1)$$

Substituting $d = kD$

$$u = \frac{M_e}{M_e + M_m}$$

$$V = \frac{2\pi \left(d + \frac{M_e D}{M_e + M_m} \right)}{T}$$

into (B.1), we get

$$G \left[\frac{M_e}{D^2 (1+k)^2} + \frac{M_m}{k^2 D^2} \right] = \frac{4\pi^2}{T^2} D(k+u) \quad (B.2)$$

Now, define $A = \frac{GT^2}{4\pi^2 D^3}$ and substitute this in (B.2) to get,

$$k^5 + (u+2)k^4 + (2u+1)k^3 + (u-A(M_e+M_m))k^2 - 2AM_m k - AM_m = 0 \quad (B.3)$$

Using the normalization factors $M_e + M_m = 1$ and $p = M_m$ (which yield $1 - p = M_e$) along with the equation

$T = 2\pi \sqrt{\frac{D^3}{G(M_e+M_m)}}$ in (B.3), we see that A becomes unity and

$$k^5 + (3-p)k^4 + (3-p)k^3 - pk^2 - 2pk - p = 0 \quad (B.4)$$

The roots of this equation are (with $p = 0.012$)

$$-1.498 \pm i .865$$

$$-.0854 \pm i .131$$

$$.167$$

For the values $D = 3.84 \times 10^5$ kilometers and $k = .167$ (the real root of B.4), we find that $d = 6.45 \times 10^4$ kilometers. It is interesting to note that the value for k is dependent only upon the masses of the two primary bodies.

B.3 SATELLITE DISPLACEMENT FROM THE L_2 LIBRATION POINT

The Earth, Moon, and L_2 libration point lie in a straight line. Therefore, communications from Earth to a satellite at L_2 cannot be achieved unless the satellite is displaced from L_2 in a direction perpendicular to the Earth-Moon line. This section establishes the minimum distance (X) which will allow direct visual sighting of a satellite from Earth.

Let:

$$\begin{aligned} D &= \text{Earth-Moon distance} \\ &= 3.84 \times 10^5 \text{ km} \end{aligned}$$

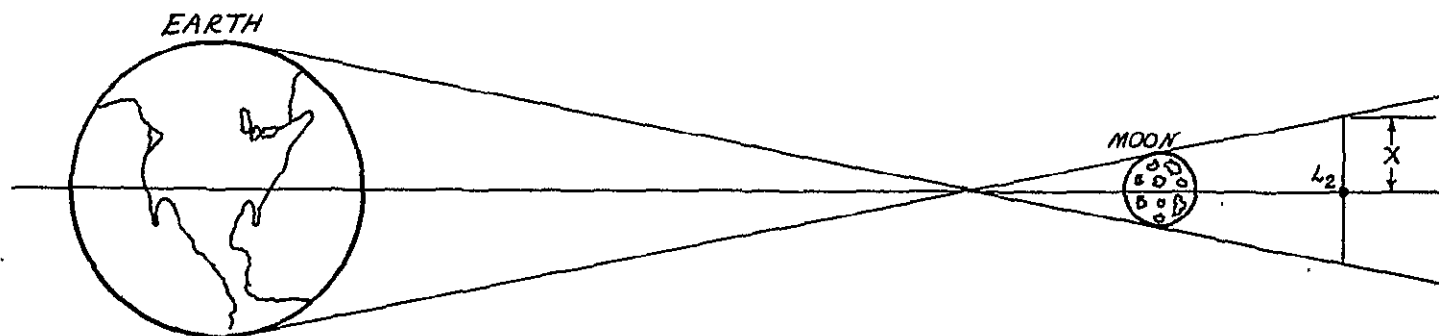


Figure B.2 Earth to L_2 Line of Sight

$$\begin{aligned}
d &= \text{Moon-}L_2 \text{ distance} \\
&= 6.45 \times 10^4 \text{ km} \\
D+d &= 4.48 \times 10^5 \text{ km} \\
R &= \text{Earth radius} \\
&= 6378 \text{ km} \\
r &= \text{Moon radius} \\
&= 1738 \text{ km}
\end{aligned}$$

From the simple geometry shown in Figure B.2,

$$\frac{X+R}{D+d} = \frac{R+r}{D} \quad (\text{B.5})$$

Solving for X,

$$X = \frac{d}{D} (R+r) + r \quad (\text{B.6})$$

Substituting the above values in (B.6), we get

$$X = 3117 \text{ km}$$

which is the minimum perpendicular distance of the satellite from L_2 .

B.4 EQUATIONS OF MOTION ABOUT THE L_2 LIBRATION POINT

In order to understand the motion of a body near L_2 , it is best to utilize a rotating coordinate system with its origin at the Earth - Moon center of mass. Let the X-axis point towards the Moon, the Z-axis in the

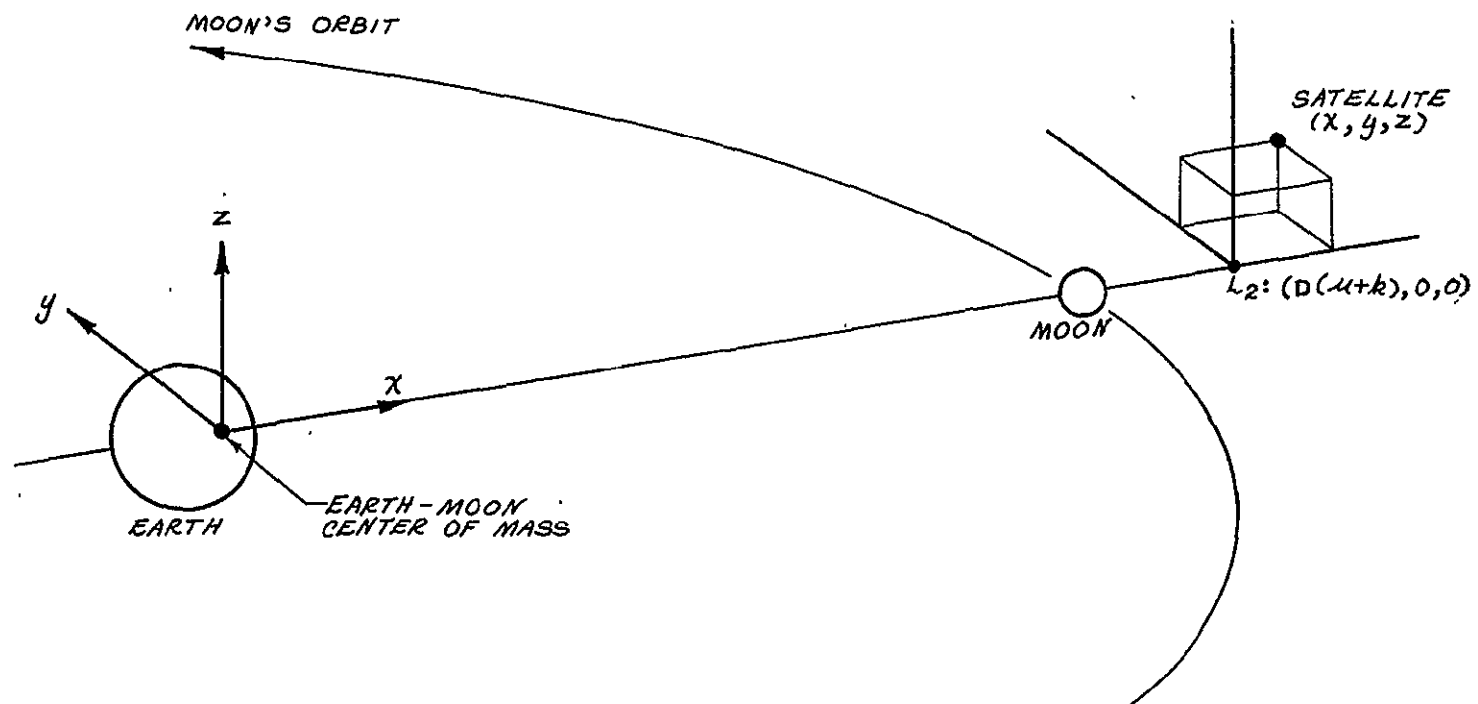


Figure B.3 Rotating Coordinate System for Equations of Motion

direction of the Moon's angular velocity vector, and the Y-axis in the direction of motion of the Moon. These three axes form a mutually right-handed coordinate system (see Figure B.3). The assumptions used here are:

- The Earth-Moon distance is constant.
- The angular velocity of the Earth-Moon line is constant.
- The displacement from L_2 is small (Reference 10).

The distance from the Earth-Moon center of mass to the Moon is $\left(\frac{M_e D}{M_e + M_m}\right)$ and the distance from the Moon to L_2 is kD . If the arbitrary position vector to a satellite relative to L_2 is given by

$$\underline{R} = X\underline{i} + Y\underline{j} + Z\underline{k} \quad (B.7)$$

then, relative to the coordinate origin, it is

$$\underline{r} = [D(u+k) + X]\underline{i} + Y\underline{j} + Z\underline{k} \quad (B.8)$$

where u and k are defined in Section B.2. Also, the velocity and acceleration vectors are

$$\dot{\underline{r}} = \dot{X}\underline{i} + \dot{Y}\underline{j} + \dot{Z}\underline{k} \quad (B.9a)$$

$$\underline{a} = \ddot{X}\underline{i} + \ddot{Y}\underline{j} + \ddot{Z}\underline{k} \quad (B.9b)$$

assuming D is a constant.

Using the angular velocity vector of the rotating coordinate system, we get

$$\underline{\omega} = \omega \underline{k} \quad (\text{B.10})$$

Thus, the acceleration of such a satellite in inertial space is

$$\underline{a}_I = \underline{a}_R + (2\underline{\omega} \times \dot{\underline{r}}) + (\dot{\underline{\omega}} \times \underline{r}) + (\underline{\omega} \times \underline{\omega} \times \underline{r}) \quad (\text{B.11})$$

For $\dot{\underline{\omega}} = 0$, (B.11) becomes

$$\begin{aligned} \underline{a}_I = & \left[\ddot{X} - 2\omega\dot{Y} - (D(u+k)+X)\omega^2 \right] \underline{i} \\ & + \left[\ddot{Y} + 2\omega\dot{X} - \omega^2 Y \right] \underline{j} + \ddot{Z} \underline{k} \end{aligned} \quad (\text{B.12})$$

If the respective vectors from the Earth to L_2 and the Moon to L_2 are

$$\underline{r}_1 = [D(1+k) + X] \underline{i} + Y \underline{j} + Z \underline{k} \quad (\text{B.13a})$$

$$\underline{r}_2 = (kD+X) \underline{i} + Y \underline{j} + Z \underline{k} \quad (\text{B.13b})$$

then the acceleration of a body near L_2 due to gravity is

$$\underline{a}_g = - \frac{GM_e}{|r_1|^3} \underline{r}_1 - \frac{GM_m}{|r_2|^3} \underline{r}_2 \quad (\text{B.14})$$

Using the general expansion

$$\frac{1}{(A+B)^3} = \frac{1}{A^3} - \frac{3B}{A^4} + \frac{6B^2}{A^5} - \frac{10B^3}{A^6} + \dots$$

and the fact that X, Y and Z are small compared to kD,
we can write

$$\begin{aligned} \frac{1}{|r_1|^3} \underline{r}_1 = & \left[\frac{1}{A_1^2} + \frac{X}{A_1^3} - \frac{3X}{A_1^3} - \frac{3X^2}{A_1^4} + \frac{6X^2}{A_1^4} + \dots \right] \underline{i} \\ & + \left[\frac{Y}{A_1^3} - \frac{3XY}{A_1^4} + \frac{6XY^2}{A_1^5} - \dots \right] \underline{j} \\ & + \left[\frac{Z}{A_1^3} - \frac{3XZ}{A_1^4} + \frac{6XZ^2}{A_1^5} - \dots \right] \underline{k} \end{aligned} \quad (B.15)$$

where $A_1 = D(1+k)$

A similar equation results for \underline{r}_2 when A_1 is replaced by $A_2 = kD$ in Equation (B.15).

Neglecting all but the linear terms of these expansions, and equating gravitational and centrifugal acceleration, we get

$$\ddot{X} - 2\omega\dot{Y} - [\omega^2 + 2K]X = \omega^2(u+k)D - \frac{GM_e}{(1+k^2)D^2} - \frac{GM_m}{k^2D^2} \quad (B.16a)$$

$$\ddot{Y} + 2\omega\dot{X} - [\omega^2 - K]Y = 0 \quad (B.16b)$$

$$\ddot{Z} + KZ = 0 \quad (B.16c)$$

where $K = \frac{GM_e}{A_1^3} + \frac{GM_m}{A_2^3}$

But according to (B.2), the right-hand side of (B.17a) must vanish. Thus, (B.16) represents the linearized equations of motion about L_2 , where (B.16a) and (B.16b) represent motion in the plane of the lunar orbit and are coupled. Their characteristic equation using operator notation and normalizing with respect to ω is

$$s^4 - (K-2)s^2 - (2K+1)(K-1) = 0 \quad (B.17)$$

There are four roots of (B.17): two imaginary and two real which are determined by

$$s = \pm \sqrt{\frac{K-2 \pm \sqrt{K(9K-8)}}{2}} \quad (B.18)$$

Thus, the free motion in the plane of the lunar orbit near the L_2 libration point is unstable with solutions:

$$X = P_X \sin \omega_1 t + Q_X \cos \omega_1 t + R_X \sinh \omega_2 t + S_X \cosh \omega_2 t \quad (B.19a)$$

$$Y = P_Y \sin \omega_1 t + Q_Y \cos \omega_1 t + R_Y \sinh \omega_2 t + S_Y \cosh \omega_2 t \quad (B.19b)$$

while the equation normal to the plane is simply

$$Z = P_Z \sin \omega_3 t + Q_Z \cos \omega_3 t \quad (B.20)$$

where $\omega_3 = \sqrt{K}$

Substituting the X and Y solutions into the equations of motion (Equations (B.16a) and (B.16b)) gives:

$$\begin{aligned} & \left\{ -\omega_1^2 [P_X \sin \omega_1 t + Q_X \cos \omega_1 t] \right. \\ & \quad + \omega_2^2 [R_X \sinh \omega_2 t + S_X \cosh \omega_2 t] \\ & - 2[\omega_1 (P_Y \cos \omega_1 t - Q_Y \sin \omega_1 t) \\ & \quad + \omega_2 (R_Y \cosh \omega_2 t + S_Y \sinh \omega_2 t)] \\ & - (2K+1) [P_X \sin \omega_1 t + Q_Y \cos \omega_1 t \\ & \quad \left. + R_X \sinh \omega_2 t + S_X \cosh \omega_2 t] \right\} = 0 \end{aligned} \quad (B.21a)$$

$$\begin{aligned} & \left\{ -\omega_1^2 [P_Y \sin \omega_1 t + Q_Y \cos \omega_1 t] \right. \\ & \quad + \omega_2^2 [R_Y \sinh \omega_2 t + S_Y \cosh \omega_2 t] \\ & + 2[\omega_1 (P_X \cos \omega_1 t - Q_X \sin \omega_1 t) \\ & \quad \left. + \omega_2 (R_X \cosh \omega_2 t + S_X \sinh \omega_2 t)] \right\} \end{aligned}$$

$$\begin{aligned}
& + (K-1) [P_Y \sin \omega_1 t + Q_Y \cos \omega_1 t \\
& \quad + R_Y \sinh \omega_2 t + S_Y \cosh \omega_2 t] \} = 0
\end{aligned}
\tag{B.21b}$$

Because the X and Y equations are coupled, they contain only four independent constants. Also, since the four general solutions for X and Y are linearly independent, the coefficients of each solution must vanish.

The following equations relating the coefficients may then be derived.

$$P_X = \frac{2\omega_1 Q_Y}{\omega_1^2 + (2K+1)} \quad P_Y = \frac{-2\omega_1 Q_X}{\omega_1^2 - (K-1)} \tag{B.22a}$$

$$Q_X = \frac{-2\omega_1 P_Y}{\omega_1^2 + (2K+1)} \quad Q_Y = \frac{2\omega_1 P_X}{\omega_1^2 - (K-1)} \tag{B.22b}$$

and

$$R_X = \frac{2\omega_2 S_Y}{\omega_2^2 - (2K+1)} \quad R_Y = \frac{-2\omega_2 S_X}{\omega_2^2 + (K-1)} \tag{B.23a}$$

$$S_X = \frac{2\omega_2 R_Y}{\omega_2^2 - (2K+1)} \quad S_Y = \frac{-2\omega_2 R_X}{\omega_2^2 + (K-1)} \tag{B.23b}$$

By establishing an initial state vector which excites only the periodic (ω_1) motion, the equations of satellite position with respect to time in the rotating coordinate system may be written as

$$X = P_X \sin \omega_1 t \quad (B.24a)$$

$$Y = Q_Y \cos \omega_1 t \quad (B.24b)$$

$$Z = P_Z \sin \omega_3 t \quad (B.24c)$$

where the motion amplitudes are arbitrary, but P_X and Q_Y are mutually dependent.

B.5 FREE MOTION IN THE VICINITY OF THE L_2 LIBRATION POINT

From Reference 11, it was found that

$$\omega_1 = .428 \text{ radians/day}$$

$$\omega_3 = .410 \text{ radians/day}$$

$$P_X = .343 Q_Y \quad (\text{from Equation (B.22a)})$$

Therefore, for a bounded orbit to exist in X and Y motion (the Z-axis motion is simple - harmonic and, therefore, bounded), an ellipse must be traced in the X-Y plane such that the X amplitude is .343 times the Y amplitude. The equation of such an ellipse is

$$r = Q_Y (1 - e \cos E) \quad (B.25)$$

where $e = .8823$

$E = \omega_1 t$, and is measured clockwise from the Y-axis
(Figure B.4)

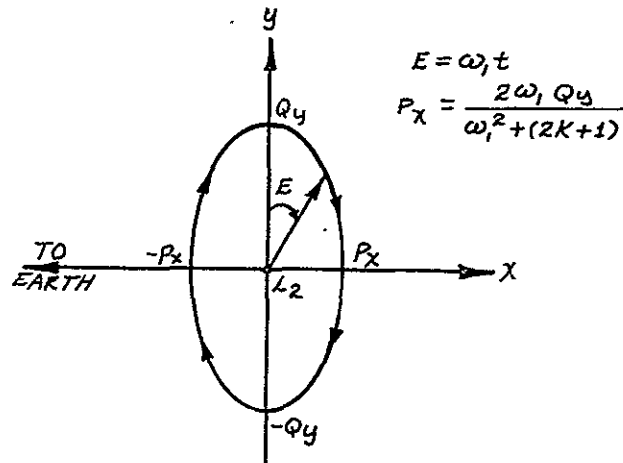


Figure B.4 Projection of Halo Orbit In X-Y Plane

The satellite in this X-Y motion is periodically occulted by the Moon even if Q_y is greater than 3117 km (Section B.3). Therefore, to establish continuous visual contact with the Earth, a Z-axis motion must also be established. But even if the Y and Z motions are started 90° out of phase (as suggested in Equations B.24), the difference in periods causes the orbit to appear as a Lissajous figure from Earth. Since this motion is also periodically occulted by the Moon, some type of period control is required. (Note that for equal Y and Z amplitudes ($Q_y = P_z$), the orbit plane is tilted 18.9 degrees with respect to the Z-axis as shown in Figure B.5).

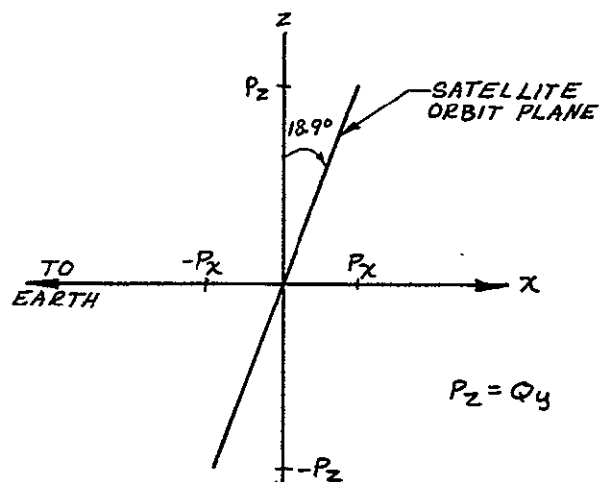


Figure B.5 Inclination of Satellite Halo Orbit

B.6 CONTROLLED MOTION IN THE VICINITY OF THE L_2 LIBRATION POINT

Since the period about the Z-axis is longer than the period about the Y-axis, it is proposed to artificially shorten the Z-axis period with periodic impulsive velocity changes. This is done most easily by reversing the excess Z-axis velocity when the halo orbit crosses the X-Y plane (see Figure B.6).

This Z-axis velocity change may be applied twice per orbit at every X-Z plane crossing (double Z-axis control) or only once per orbit (single axis control). Both of these methods are examined to determine yearly ΔV requirements.

The satellite's equations of motion are rewritten here for convenience.

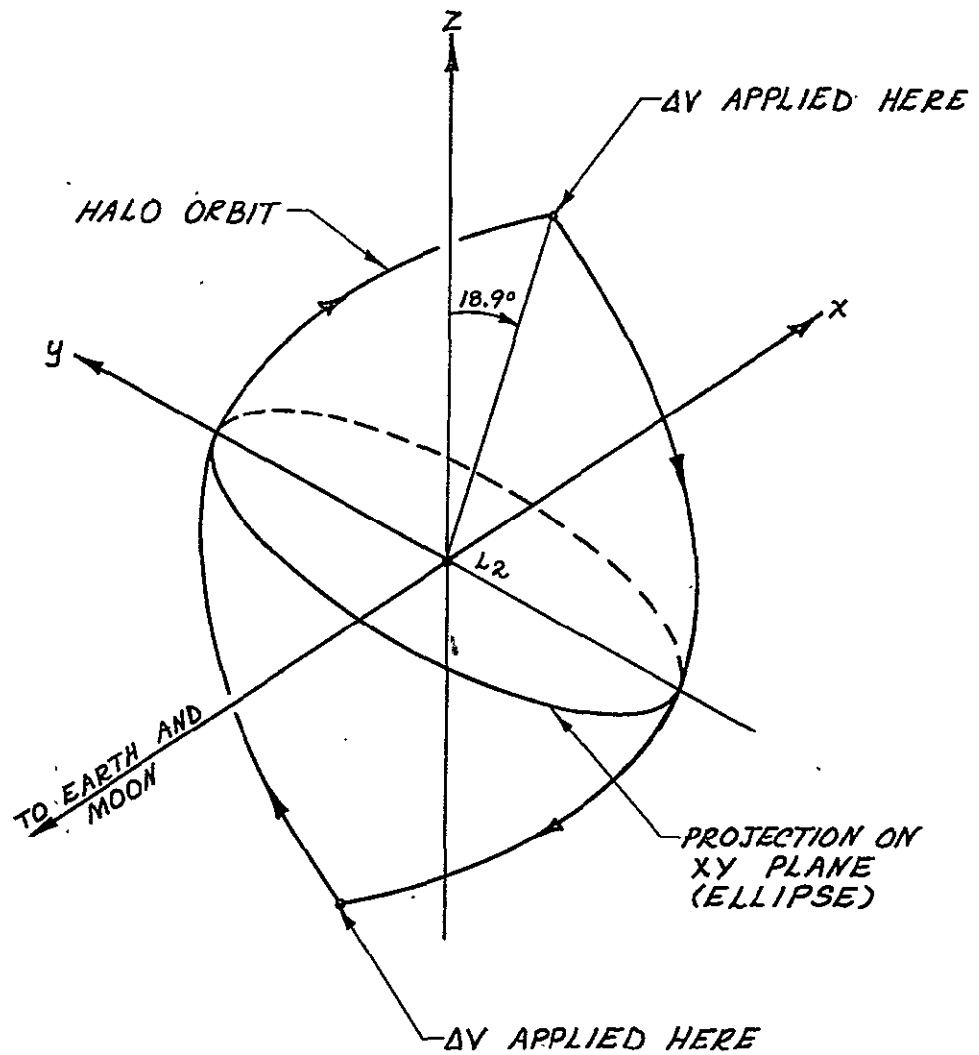


Figure B.6 Z-Axis Motion Period Control

$$X = P_X \sin \omega_1 t \quad \dot{X} = \omega_1 P_X \cos \omega_1 t \quad (\text{B.26a})$$

$$Y = Q_Y \cos \omega_1 t \quad \dot{Y} = -\omega_1 Q_Y \sin \omega_1 t \quad (\text{B.26b})$$

$$Z = P_Z \sin \omega_3 t \quad \dot{Z} = \omega_3 P_Z \cos \omega_3 t \quad (\text{B.26c})$$

where $\omega_1 = .428$ radians/day

$\omega_3 = .410$ radians/day

Therefore, the periods become

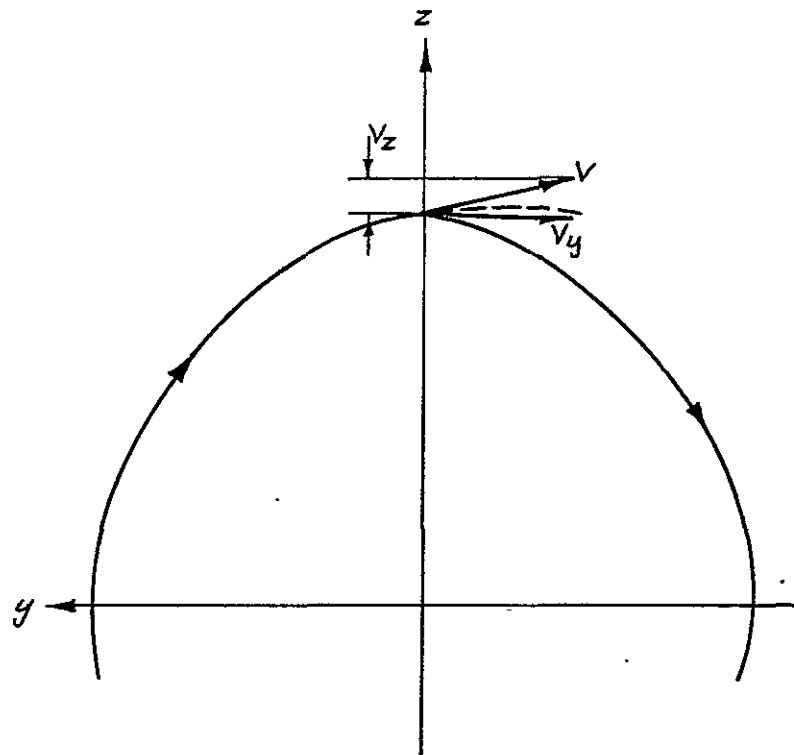
$$T_1 = \frac{2\pi}{\omega_1} = 14.66 \text{ days} \quad (\text{B.27a})$$

$$T_3 = \frac{2\pi}{\omega_3} = 15.30 \text{ days} \quad (\text{B.27b})$$

Assuming that the satellite is in a controlled halo orbit with $P_Z = Q_Y$, the point $t = 0$ may be taken when the orbit crosses the positive Y-axis. One quarter orbit later, ($t = 3.67$ days) the excess Z-axis velocity is (Figure B.7)

$$\begin{aligned} \dot{Z} &= (.410) (3500) \cos .410t \\ &= 1435 \cos 86.2^\circ \\ &= 95.1 \text{ km/day} = 3.62 \text{ ft/sec} \end{aligned} \quad (\text{B.28})$$

Since there are 25 halo orbits/year, and each ΔV must be $2(3.62)$ ft/sec, the total ΔV required is 362 ft/sec. Note that this ΔV requirement increases linearly with the Z-axis amplitude (P_Z).



-----ORBIT CONTINUATION
WITHOUT ΔV
 ΔV FOR CONTINUING
HALO ORBIT = $2 V_z$

Figure B.7 Halo Orbit With Double Z-Axis Control

Another stationkeeping scheme utilizes a Z-axis. ΔV only once per orbit (14.66 days). This method proves to be more complex than double axis control, since omitting a ΔV causes a position error at the next X-Z plane crossing (see Figure B.8, point A). The halo orbit crosses the X-Z plane with a Z amplitude of

$$\begin{aligned} \text{Z-axis amplitude} \\ \text{of halo orbit} &= 3500 \sin 86.2^\circ & (B.29) \\ &= 3485 \text{ km} \end{aligned}$$

Point A has a Z-axis coordinate of

$$\begin{aligned} \text{Z-axis amplitude} \\ \text{of point A} &= 3500 \sin 79.6^\circ & (B.30) \\ &= 3440 \text{ km} \end{aligned}$$

Thus, the position error after one orbit is about 45 km. Even though this distance is small when compared with the orbit radius, the ΔV can be applied a short time later (Figure B.8, point B) and the position error will no longer exist.

To find the actual crossing point of the two orbits, it must be realized that the Y-axis motions of these two orbits are the same. The problem is then to find the point at which the Z-axis components are equal. After one orbit without velocity changes, the Z-axis

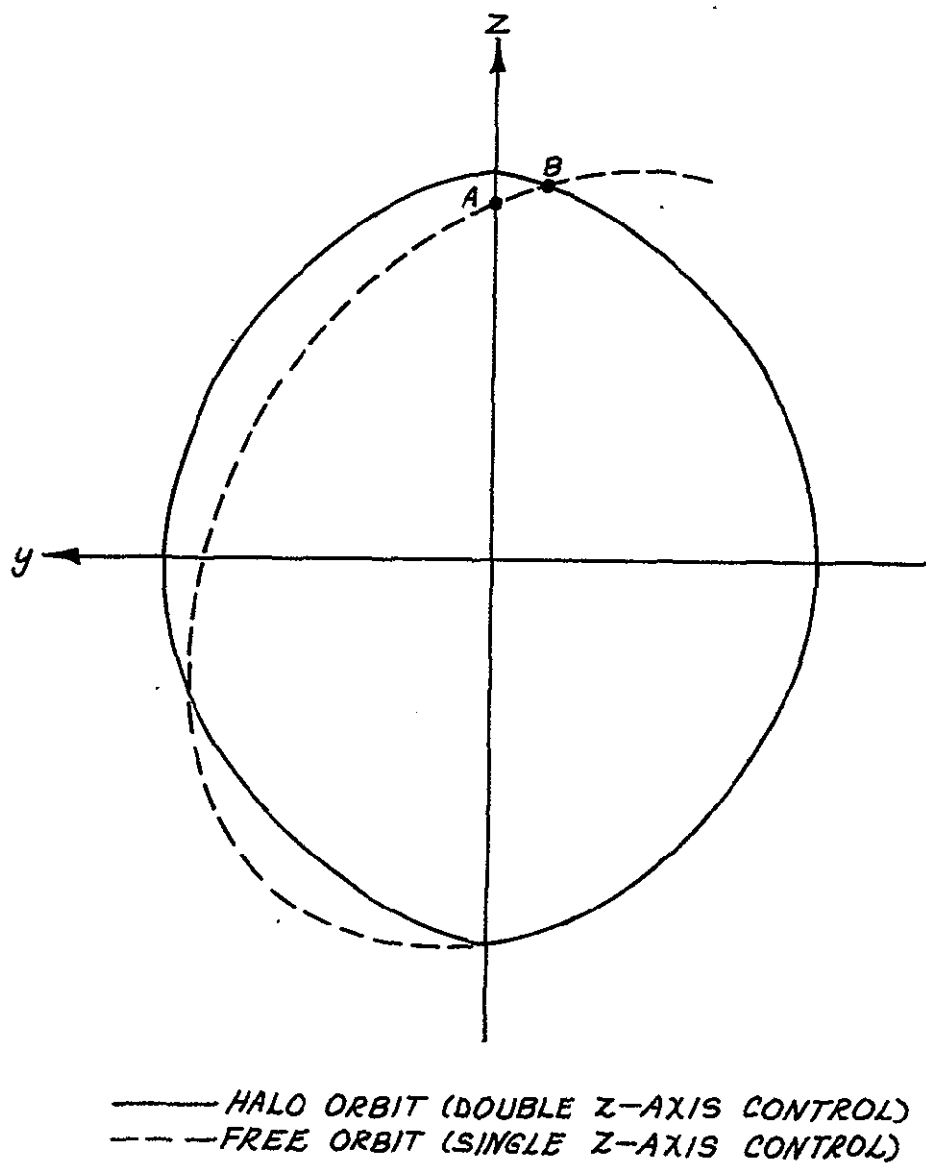


Figure B.8 Halo Orbit Single Z-Axis Control

motion lags that of the previous orbit by $4(3.8^\circ) = 15.2^\circ$, and, likewise, the Z-axis motion which initially led the Y-axis motion by 93.8° (solid line in Figure B.8), only leads by 78.6° after one orbit (dotted line in Figure B.8). It can be seen from Figure B.9 that the Z-axis components will be equal at a time

$$t = \frac{3.8^\circ}{\omega_3 (57.3)} = .162 \text{ days} = 3.88 \text{ hours} \quad (\text{B.31})$$

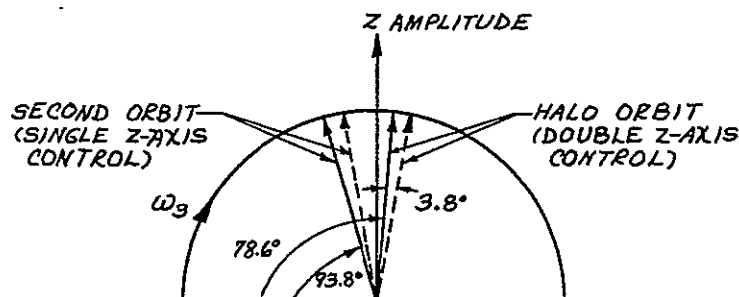


Figure B.9 Phasor Representation of Z-Amplitude For Single Vs Double Z-Axis Control

after crossing the X-Z plane. At this time, the Z-axis velocity is

$$\begin{aligned} \text{Z-axis velocity} \\ \text{at time 3.88 hours} &= .410(3500) \cos 83.6^\circ \end{aligned}$$

$$= 192 \text{ km/day} = 8.45 \text{ ft/sec.}$$

This implies an annual ΔV requirement of 423 ft/sec.

B.7 PERIODIC AND NONLINEAR PERTURBATION EFFECTS

The halo orbit analysis thus far has ignored deviations from the linearized equations of motion due to the nonlinear terms of the gravity field series expansion. Also, the restricted three body problem neglects complexities in the motion of L_2 and perturbation forces acting on a satellite in the vicinity of L_2 .

Four major effects will be discussed. They are due to:

- Eccentricity of the Moon's orbit
- Solar gravity
- Nonlinear terms in the equations of motion
- Errors in halo orbit initiation resulting in excitement of the non-periodic terms in the X and Y equations of motion.

Deviations from the nominal halo orbit due to lunar gravitational anomalies (mass concentration) are not discussed since:

- L_2 is nearly on the lunar sphere of influence and any such effects would be minimal

- Very little is presently known concerning the anomalies.

Lunar orbit eccentricity causes a periodic deviation of a satellite from a nominal halo orbit path. This is due to the variation of the L_2 to system center of mass distance (it depends on the distance separating the primary bodies as shown in Section B.2). The magnitude of these excursions is about 10 per cent of the halo orbit amplitude. Solar gravity causes a similar perturbation, but its magnitude is only about 1.2 per cent of the halo amplitude. Nonlinear terms in the gravity field expansion, when included in the equations of motion, cause small changes in the position of L_2 and both the in- and out-of-plane periods of the halo orbit.

The principal effect of the second order terms is to shift the center of the halo orbit toward the Moon by a distance proportional to the square of the orbit amplitude. For a 3500 kilometer orbit, the change is about 90 kilometers. A third order solution shows that the X-Y period of the orbit is increased and the Z-axis period decreased, again by an amount proportional to the square of the halo orbit amplitude. However, these changes are small, since the increase is about 2.5 minutes and the decrease is about 11.5 minutes.

Reference 5 includes results of a halo orbit simulation in which errors in initial conditions are introduced along with the other perturbations and effects which are discussed here. It was found that the stationkeeping cost was not significantly higher than that predicted by the linearized equations of motion for Z-axis period control.

All stationkeeping costs for one year are estimated to be 25 ft/sec-year, exclusive of period control requirements (Reference 11).

APPENDIX C

LUNAR ORBIT DYNAMICS

C.1 PLANAR RELATIONSHIPS

The following discussion ignores variations in the angles in inclination of the Earth's equatorial plane and the lunar orbit plane with respect to the plane of the ecliptic (i.e., all values are mean values), and planar precession rates are assumed to be constant.

Figure C.1 shows the normals to the planes pertinent to this problem. The Earth's equator makes an angle of $23^{\circ}27'$ with the ecliptic. The vernal equinox rotates in inertial space once in every 25,725 years (Reference 12) and, hence, is considered stationary. The plane of the lunar orbit is inclined $5^{\circ}09'$ to the ecliptic and the longitude of the ascending node rotates once in every 6,798 days (18.6 years). The vernal equinox and ascending node of the lunar orbit plane are aligned in July, 1970. The limits and variation of the angle between the lunar orbit plane and the equatorial plane are discussed in the next section. The vector normal to the plane of a satellite with a given inclination rotates around

τ - VERNAL EQUINOX
 N_{EC} - NORMAL TO THE ECLIPTIC
 N_{EQ} - NORMAL TO THE EARTH'S EQUATOR
 N_{LO} - NORMAL TO LUNAR ORBIT PLANE
 N_S - NORMAL TO EARTH'S PARKING ORBIT PLANE
 i - INCLINATION OF SATELLITE ORBITS ($i=28^\circ 28'$
 FOR A DUE EAST CAPE KENNEDY LAUNCH)

ANGLES BETWEEN VECTORS

$N_{EC} \angle N_{EQ}$	$23^\circ 27'$
$N_{EC} \angle N_{LO}$	$5^\circ 09'$
$N_{EQ} \angle N_S$	i

N_S AND N_{LO} ROTATE IN
 THE DIRECTIONS SHOWN
 WITH PERIODS OF:
 N_S - 24 HOURS
 N_{LO} - 18.6 YEARS

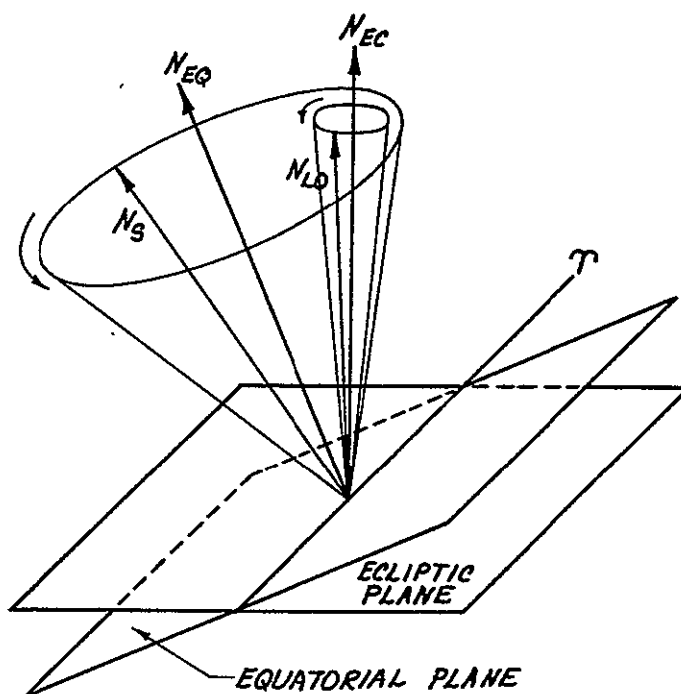


Figure C.1 Planar Relationship.

the Earth's spin axis in inertial space once every 24 hours. (The inclination for a due East launch from Cape Kennedy is $28^{\circ}28'$).

The angle between the trans- L_2 trajectory (assuming no plane change from Earth parking orbit and a due East launch) and the lunar orbit plane varies from $08'$ to $57^{\circ}04'$.

C.2 LUNAR ORBIT PLANE MOTION

To find the angle between the normal to the Earth's equator and the normal to the Moon's orbit plane, consider the spherical triangle formed by these two vectors and the normal to the ecliptic, where they intersect a unit sphere (Figure C.2). From geometry, it is noticed that

$$A = \omega(t - t_0) \quad (C.1)$$

where ω = angular velocity of the Moon's ascending node on the ecliptic plane

$$= \frac{360 \text{ degrees}}{18.6 \text{ days}}$$

$$= 19.4 \text{ degrees/day}$$

t_0 = initial time, taken to be July, 1970

<u>VECTOR</u>	<u>NORMAL TO</u>
N_{EC}	ECLIPTIC
N_{EQ}	EQUATOR
N_{LO}	LUNAR ORBIT

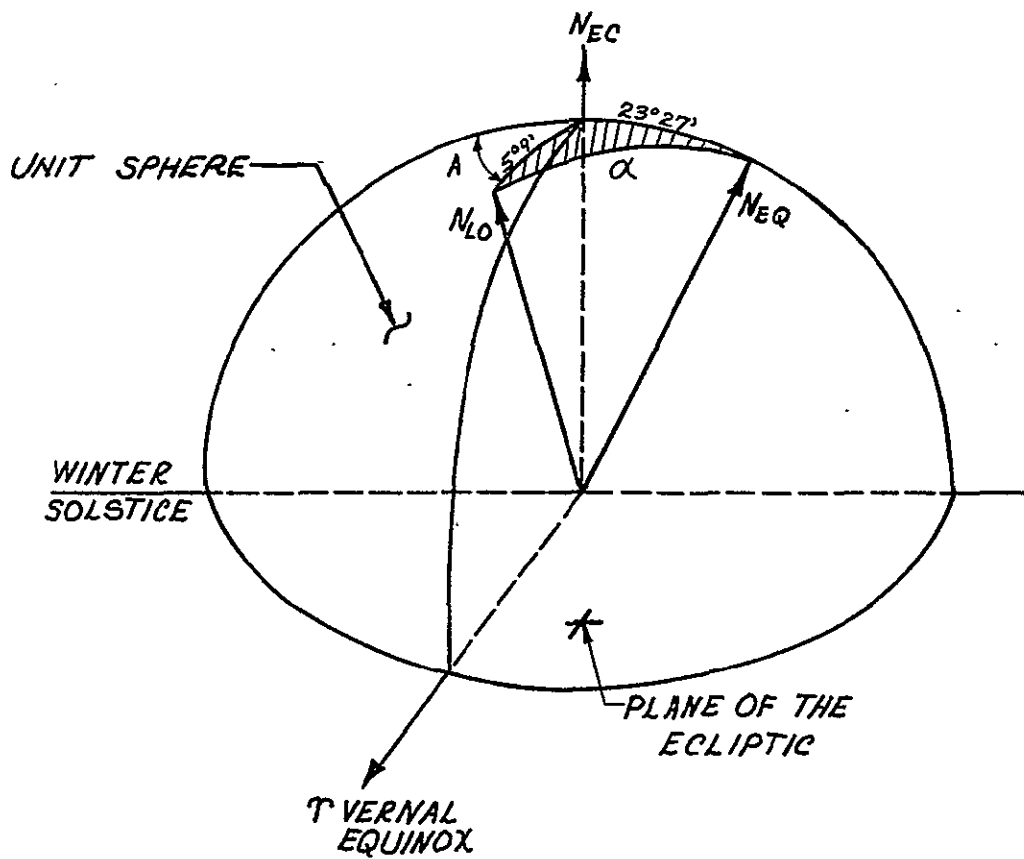


Figure C.2 Rotation of the Lunar Orbit Plane

Standard relationships of spherical triangles gives

$$\begin{aligned}\cos\alpha &= (\cos 5^{\circ}09')(\cos 23^{\circ}27') \\ &\quad + (\sin 5^{\circ}09')(\sin 23^{\circ}27')(\cos (180^{\circ}-A))\end{aligned}$$

or evaluating the functions

$$\cos\alpha = .912 + 0.03565\cos(180^{\circ}-A)$$

where A is determined at any time after July, 1970. For example, January, 1974 gives a value of A = 70.7 degrees for an $\alpha = 26^{\circ}$ (Section 4.1).

APPENDIX D

TRAJECTORY ANALYSIS

D.1 DESCRIPTION OF COMPUTER PROGRAM

A digital simulation program (written in Fortran IV) and an IBM 360/65 computer were used to obtain the results presented in this appendix. The Earth, Moon, and LCS are the only bodies considered in this simulation, and the LCS is assumed to be massless (i.e., the restricted three body problem).

An idealized model of the Earth-Moon system was chosen, since a specific launch date is not proposed. An inertial coordinate system with its origin fixed at the Earth-Moon center of mass was employed, with the Earth and Moon moving in circular orbits about the origin. Cowell's method of direct integration of acceleration and velocity was employed. The integration scheme was a variable step Adams-Moulton routine with error criteria and integration step size limits specified by the user (Reference 13).

The values of the constants used in the program were:

Earth radius	6378 km
--------------	---------

Moon radius	1738 km
Earth-Moon distance	384405 km
Moon- L_2 distance	64516 km
Ratio of Earth mass to Moon mass	81.31
Angular velocity of the Earth-Moon line	.00958212 rad/hr

To facilitate problem initiations and to decrease sensitivity to small changes, it was decided to run the simulation backwards: to start the LCS from L_2 and attempt to achieve a perigee of 100 nm in Earth orbit. Thus, all of the results presented are referenced to time equals zero at L_2 .

D.2 LUNAR ORBIT PLANE TRAJECTORY

In Chapter IV, it is noted that a Cape Kennedy launch results in an out-of-plane trajectory. However, to decrease the number of variables for an initial analysis, an in-plane study was conducted.

A small velocity change at L_2 is desired because short thruster firings result in small velocity errors. Also, in order to decrease its tangential velocity (backwards trajectory), the LCS must fly across the far-side of the Moon. Because of these two constraints, the velocity vector at L_2 must have:

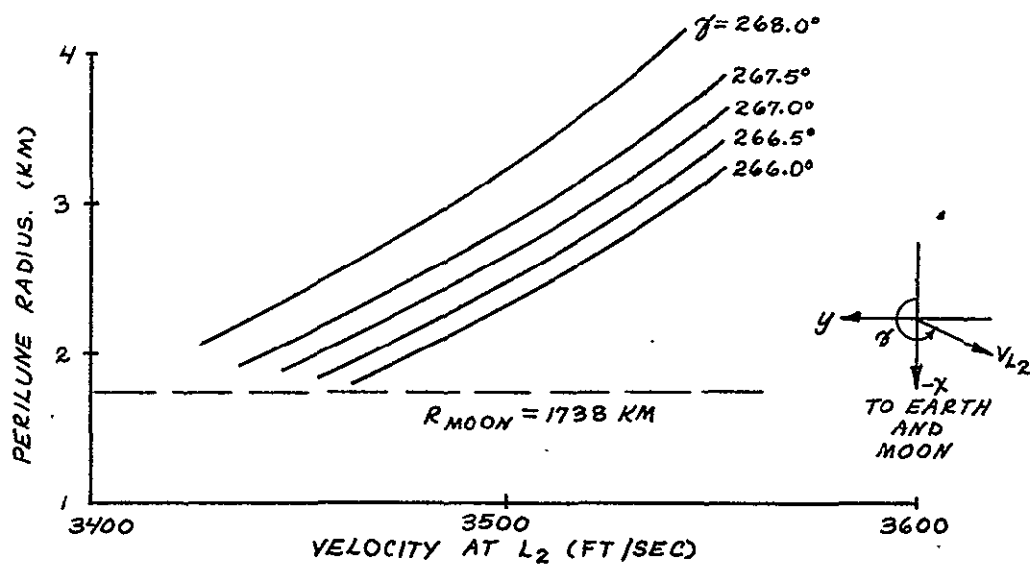
- a magnitude nearly equal to that needed
- to be stationary at L_2
- a direction nearly perpendicular to the Earth-Moon line

The magnitude and direction of the velocity vector were changed parametrically, and the results of this study are summarized by Figure D.1. In addition, at perilune the angle between the Earth-Moon line and the Moon-LCS line varied from about 41° to 56° and the velocity relative to the Moon changed from 5300 ft/sec to 7500 ft/sec.

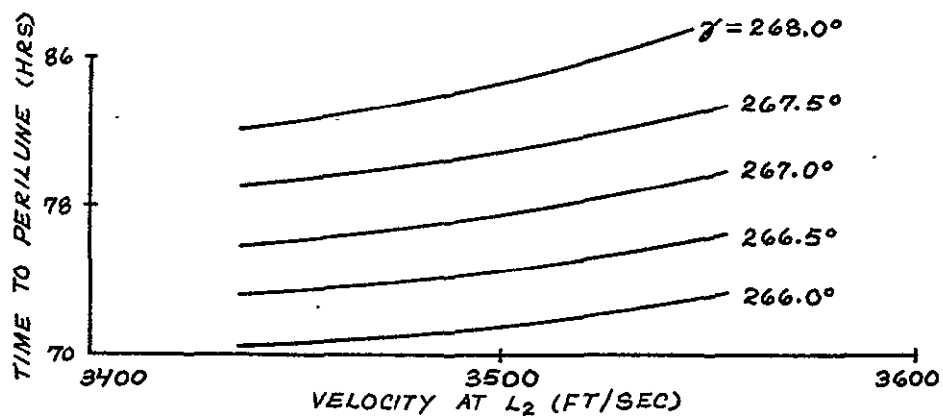
A velocity change is most effective (in terms of energy change) when performed while the satellite is at its maximum velocity. So, to escape the lunar sphere of influence and start the fall to Earth, an impulsive velocity increase was initiated at perilune. The resulting trajectory from L_2 to perigee takes approximately nine days.

The results for a particular trajectory are shown in Figures D.2 and D.3. The data for this trajectory are:

Velocity at L_2	3442.59 ft/sec
Velocity change at L_2	472.41 ft/sec
Flight path angle (γ) at L_2	267.2 degrees
Time of flight to perilune	77.3 hours



(a)



(b)

Figure D.1 In-Plane L_2 To Moon Trajectory Results

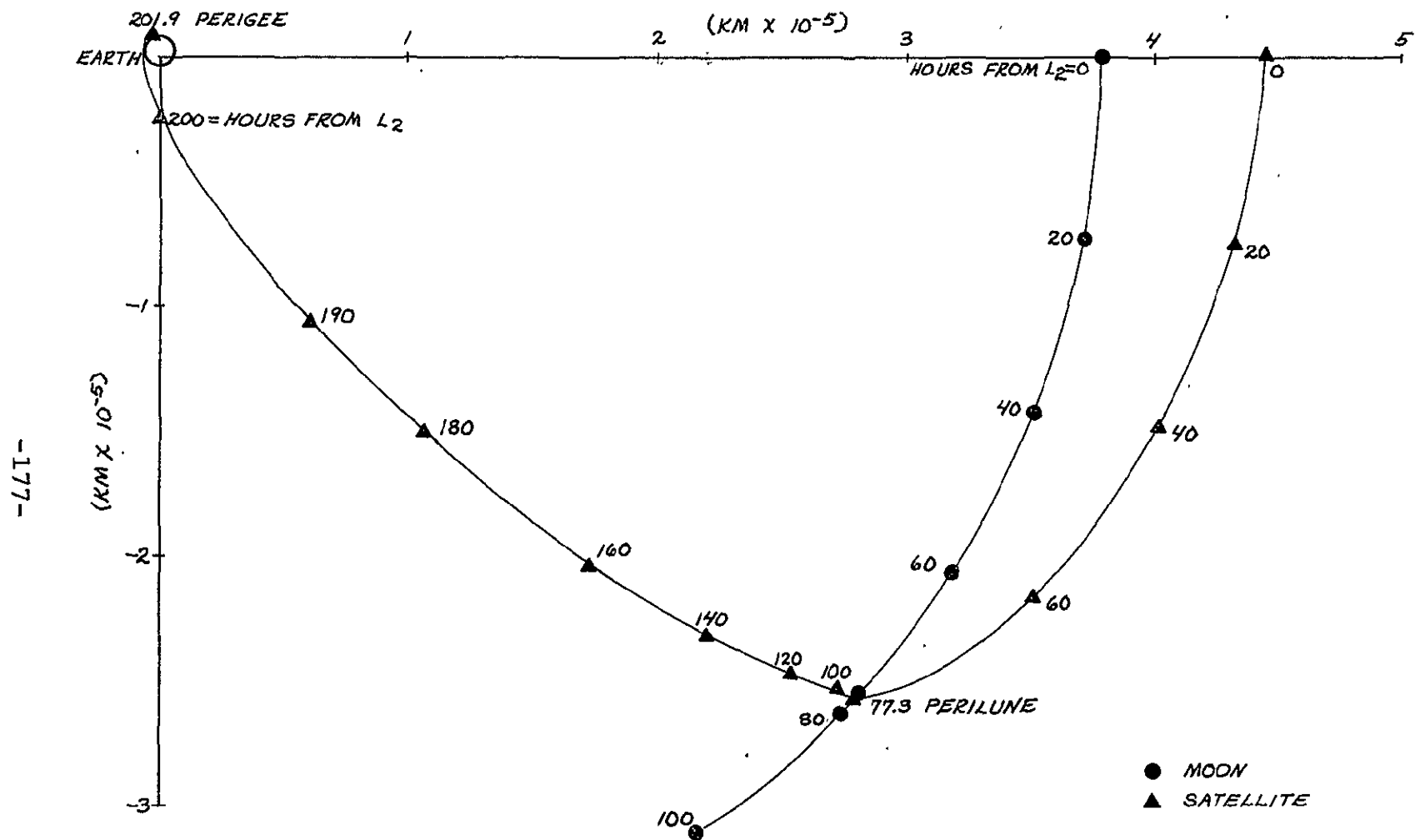


Figure D.2 Example of In-Plane Trajectory

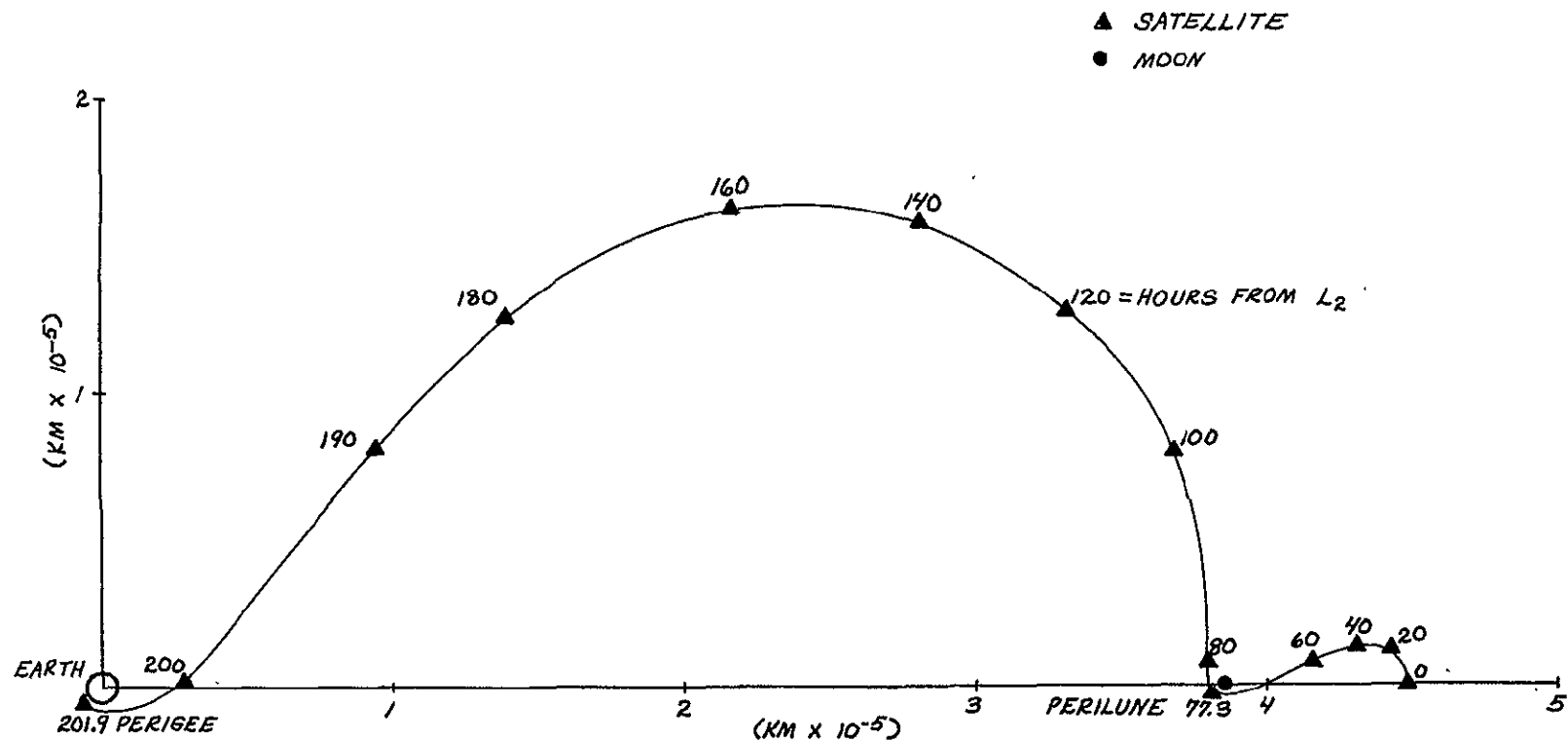


Figure D.3 In-Plane Trajectory In Rotating Coordinate System

Perilune radius	1823.0 km
Velocity change at	
perilune	688.06 ft/sec
Right ascension	
(measured from Earth-	
Moon line at perilune)	48.24 degrees
Time of flight to	201.9 hours or
perigee	8.41 days

The variation in these numbers for other trajectories is about five per cent.

D.3 OUT-OF-PLANE TRAJECTORY

There are two major reasons for performing an out-of-plane analysis:

- The trajectory must be inclined to the lunar orbit plane at perigee so that a plane change from Earth parking orbit is not required.
- The LCS must be in view of the Earth at halo orbit insertion. The best way to achieve this is to enter the orbit at a point directly above L_2 , since the Y-axis velocity change required for insertion is a minimum (Figure D.4).

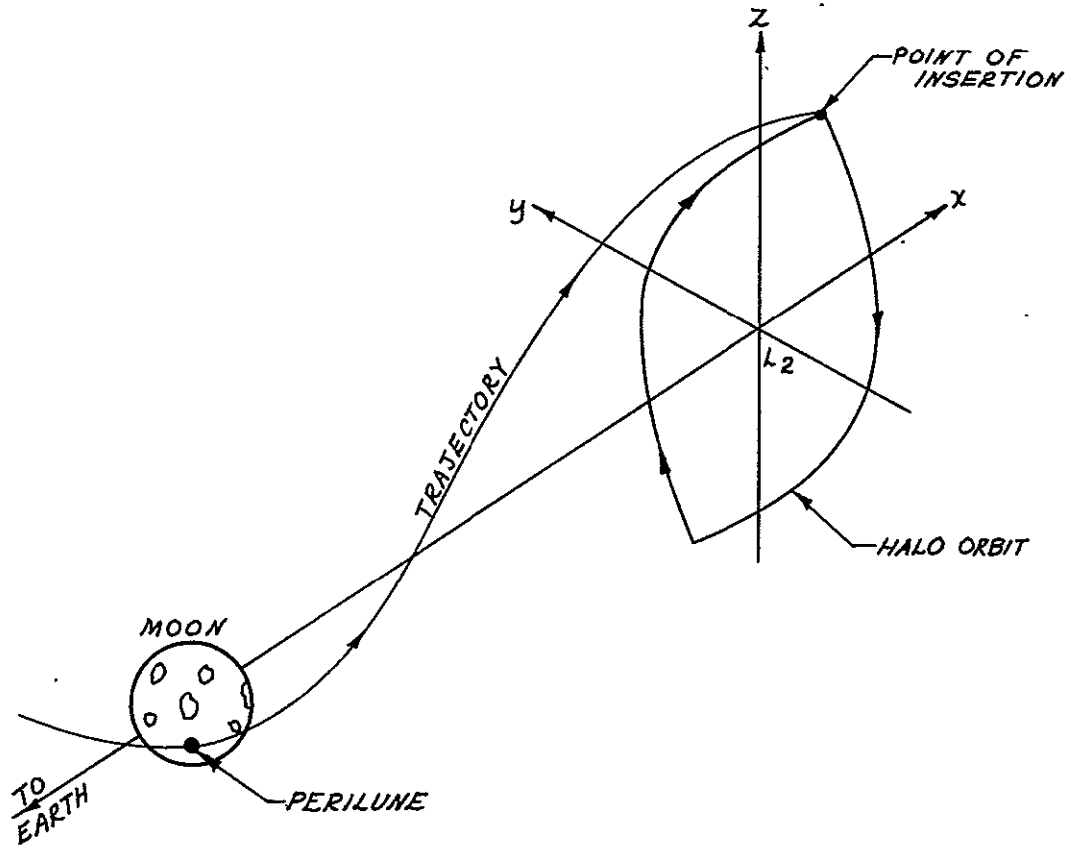


Figure D.4 Trajectory From Perilune
To Halo Orbit Insertion

Again, it was found that there is little variation from the numbers presented in the previous section. An increase in ΔV requirements of about 15 ft/sec are expected at L_2 and about 40 ft/sec at perilune. Times of flight increase slightly and a wide range of inclinations at the Earth are achievable (Reference 5).

Since these trajectories must be very precise, provision should be made for up to 70 ft/sec of midcourse

correction. Also, the perilune burn should be made in less than 10 minutes in order to maintain the validity of the impulse model.

D.4 DIRECT TRANSFER TRAJECTORY

A Hohmann transfer ellipse with (i) pericenter on an Earth parking orbit at an altitude of 100 nm, (ii) apocenter at L_2 , and (iii) a massless Moon, gives a good approximation of the ΔV required for a direct trajectory to L_2 . The following equation

$$v^2 = \mu \left(\frac{2}{r} - \frac{1}{a} \right) \quad (D.1)$$

where v = local circular velocity (ft/sec)

$$\mu = GM_E = 1.407 \times 10^{16} \text{ ft}^3/\text{sec}^2$$

r = distance from the center of Earth (ft)

a = semi-major axis of orbit (ft)

gives a local circular velocity for a 100 nautical mile orbit of (where $a = r$)

$$v = \left(\frac{1.407 \times 10^{16}}{2.12 \times 10^7} \right)^{1/2} = 25,800 \text{ ft/sec}$$

Velocity at pericenter of the transfer ellipse is

$$v = [1.407 \times 10^{16} \left(\frac{2}{2.12 \times 10^7} - \frac{1}{1.49 \times 10^9} \right)]^{1/2}$$

$$= 36,200 \text{ ft/sec}$$

for a ΔV to inject into the Hohmann transfer of 10,400 feet per second. Velocity at apocenter of the transfer ellipse is

$$v = [1.407 \times 10^{16} \left(\frac{2}{1.47 \times 10^7} - \frac{2}{1.49 \times 10^9} \right)]^{1/2}$$

$$= 500 \text{ ft/sec}$$

But the velocity of the L_2 point is about 3880 feet per second, so at L_2 the ΔV is 3380 feet per second. When the Moon is included in the analysis, a ΔV of 4030 feet per second is required (Reference 5). Because of this high velocity change requirement, a direct transfer trajectory is considered to be unfeasible.

APPENDIX E

POWER SUBSYSTEM CALCULATIONS

E.1 SOLAR PANEL AREA

The total surface area of the LCS solar panels is determined according to the maximum power requirements of the satellite and the effective output of the solar cells after an operational lifetime of four years.

The power output of the 2 x 2 centimeter N/P 2 ohm-centimeter cells being used on the LCS is given by

$$\text{Power output} = (S) (F_1) (F_2) (F_3) (F_4) (F_5) (F_6) (F_7) (F_8) \quad (\text{E.1})$$

where. S = solar intensity

$$= 1400 \text{ watts/meters}^2$$

F_1 = cell efficiency

$$= .105$$

F_2 = temperature factor

$$= .93$$

F_3 = coverglass filter

$$= .90$$

F_4 = UV degradation

= .95

F_5 = manufacturing allowance

= .98

F_6 = micrometeorite losses

= .98

F_7 = solar constant variation

= .97

F_8 = orientation losses

= .99

Multiplying these factors, the cell power output becomes

Power output = 110 watts/meter²

= .0109 watts/cell

The cells are connected in series in order to obtain the required 35 volts (this is five volts more than is actually necessary for the operation of the LCS subsystem because a loss of five volts was estimated through transmission lines, diodes, and regulators; Section 6.3.4). Thus, the number of cells in series is

$$\text{No. of cells}_{\text{series}} = \frac{\text{Required voltage output of cells}}{\text{Voltage output per cell}}$$

(E.2)

$$= \frac{35.0 \text{ volts}}{.380 \text{ volts/cell}}$$

= 93 cells in series

The cells are connected in parallel in order to obtain the required current. The required cell output power is

$$\begin{aligned} \text{Required power} \\ \text{output of cells} &= \frac{\text{Operational power requirements}}{\text{Converter efficiency}} \end{aligned} \quad (\text{E.3})$$

$$= \frac{471 \text{ watts}}{.85}$$

= 553 watts required from cells

The required current is determined by

$$\begin{aligned} \text{Required current} \\ \text{output of cells} &= \frac{\text{Required power output of cells}}{\text{Required voltage output of cells}} \end{aligned} \quad (\text{E.4})$$

$$= \frac{553 \text{ watts}}{35 \text{ volts}}$$

= 15.8 amps required

Thus, the number of cells in parallel is

$$\begin{aligned} \text{No. of cells}_{\text{parallel}} &= \\ &= \frac{\text{Required current output of cells}}{\text{Current output per cell}} \end{aligned} \quad (\text{E.5})$$

$$= \frac{15.8 \text{ amps}}{.0985 \text{ amps/cell}}$$

= 160 cells in parallel.

Now to determine the total surface area of the solar cells, consider that each of the satellite's two panels contain 80 columns of cells, where each column is comprised of 93 cells in series to generate the required voltage, and the columns are connected in parallel to obtain the required current. Since the dimensions of one cell is 2 x 2 centimeters, the surface area of cells per panel is

$$\begin{aligned} \text{Cell surface area} &= \left\{ (\text{No. of cells}_{\text{series}}) \right. \\ &\quad \left. (\text{No. of cells}_{\text{parallel}}) (\text{Area/cell}) \right\} \\ &\quad (E.6) \end{aligned}$$

$$\begin{aligned} &= (93) (80) (4\text{cm}^2/\text{cell}) \\ &= 29,760 \text{ cm}^2 \text{ per panel.} \end{aligned}$$

Considering a packing density of .85 and a hinge area of 2.5 ft², the actual area of each solar panel is

$$\begin{aligned} \text{Solar panel area} &= \frac{\text{Cell surface area}}{\text{Packing factor}} + \text{Hinge area} \\ &\quad (E.7) \end{aligned}$$

$$\begin{aligned} &= \frac{29,760}{.85} + 2160 \\ &= 37,172 \text{ cm}^2 \\ &= 40.0 \text{ ft}^2 \text{ per panel.} \end{aligned}$$

E.2 BATTERY CAPACITY

The total battery capacity of the LCS is determined by the amount of power which must be provided during a given period of time. Thus, the battery must supply electrical power for emergency LCS operations which requires 471 watts for 1.75 hours.

The battery cells are connected in series to provide the required LCS voltage of 30 volts DC. Therefore, the number of cells in series is

$$\begin{aligned}\text{No. of cell}_{\text{series}} &= \frac{\text{Required LCS operating voltage}}{\text{Voltage output per cell}} \\ &= \frac{30.0 \text{ volts}}{1.28 \text{ volts/cell}} \\ &= 24 \text{ cells in series}\end{aligned}\tag{E.8}$$

The required supplied battery power rating is given by

$$\begin{aligned}\text{Supplied power rating} &= \left\{ \begin{array}{l} \text{Operational power requirement} \\ \text{(Period of Output)} \end{array} \right\} \\ &= (471 \text{ watts})(1.75 \text{ hours}) \\ &= 824 \text{ watt-hours}\end{aligned}\tag{E.9}$$

Allowing for 25% deterioration of the battery during four years of operation and assuming a 90% depth of discharge during emergency operation, the required power rating is

$$\text{Required power rating} = \left\{ \begin{array}{l} \text{(Supplied power rating)} \\ \text{(Depth of discharge)} \\ \text{(1 - Deterioration Allowance)} \end{array} \right\}$$

(E.10)

$$= (824 \text{ watt-hours}) (.90) (1-.25)$$

$$= 1260 \text{ watt-hours}$$

The total current output of the battery for 1.75 hours is .

$$\text{Total current output rating} =$$

$$\frac{\text{Required power rating}}{\text{Required LCS operating voltage}} \quad (\text{E.11})$$

$$= \frac{1260 \text{ watt-hours}}{30 \text{ volts}}$$

$$= 42 \text{ amp-hours}$$

The cells are connected in parallel in order to obtain the total current output rating of 42 amp-hours. Therefore, the number of cells in parallel is

$$\text{No. of cells}_{\text{parallel}} = \frac{\text{Total current output rating}}{\text{Power output per cell}}$$

(E.12)

$$= \frac{42 \text{ amp-hours}}{6 \text{ amp-hours/cell}}$$

$$= 7 \text{ cells in parallel}$$

Thus, there are 24 cells in series comprising one bank with a power output of 6 amp-hours per bank. By connecting 7 banks in parallel (which generates the same current as 7 cells in parallel), the total current power rating of 42 amp-hours is obtained. The total number of cells is,

$$\begin{aligned} \text{Total number of cells} &= \left\{ (\text{No. of cells}_{\text{series}}) \right. \\ &\quad \left. (\text{No. of cells parallel}) \right\} \\ &\hspace{15em} (\text{E.13}) \\ &= (24 \text{ cells})(7 \text{ cells}) \\ &= 168 \text{ cells} \end{aligned}$$

Since each cell has a weight of .5 pounds, the total weight of the battery is,

$$\begin{aligned} \text{Total battery weight} &= \left\{ (\text{Total No. of cells}) \right. \\ &\quad \left. (\text{Weight per cell}) \right\} \\ &\hspace{15em} (\text{E.14}) \\ &= (168 \text{ cells})(.5 \text{ pounds/cell}) \\ &= 84 \text{ pounds} \end{aligned}$$

During eclipse periods, the battery will have a depth of discharge of only 75% and must supply 251 watts of power. Thus, the duration of operation is

Duration of operation =
during eclipse

$$\frac{(\text{Supplied power rating}) (\text{Depth of discharge})}{(\text{Operational power requirement})}$$

(E.15)

$$= \frac{(824 \text{ watt-hours}) (.75)}{(251 \text{ watts})}$$

$$= 2.75 \text{ hours}$$

which is the maximum possible duration of an eclipse.

APPENDIX F

TABLES OF PHYSICAL DATA OF THE SATELLITE

F.1 LAUNCH VEHICLE

The complete specifications for the proposed launch vehicle are the following:

STAGE	SPECIFIC IMPULSE (sec)	THRUST (lb)	BURN TIME (sec)	WEIGHT (lb)
<hr/> 1st Stage				
DSV-2L-1B	285	170,000	218	153,867
9-CASTOR-I	274	486,000	40	79,803
(Combined)	(282)	(656,000)	(218)	(233,670)
2nd Stage				
AJ10-118F	296	9,450	324	11,895
3rd Stage				
TE-364-4	Specifications not available			

The third stage, powered by a Thiokol TE-364-4, is currently under development. This is simply a TE-364 with additional propellant (2100 pounds as opposed to 1440 pounds). The total weight at launch, less fairing and spacecraft, is 247,837 pounds.

F.2 WEIGHT, SIZE, AND MOMENTS OF INERTIA

The letter designations in Table F.1 refer to the tables in Figures F.1 and F.2 to describe the weight, size, and moments of inertia of the LCS equipment. The folded configuration of the satellite inside the fairing of the Delta launch vehicle is shown in Figure F.3.

F.3 CALCULATION OF CENTER OF MASS AND CENTER OF PRESSURE

The data and calculation of the center of mass and center of pressure of the LCS are shown in Tables F.2 and F.3. Since the satellite is symmetrical about its roll axis, the station in these tables refers to the distance of each LCS component along the roll axis from the aft end of the satellite (which is opposite the high gain antenna). Solar pressure torque is assumed to affect the yaw axis motion of the satellite also because the LCS is roll axis symmetric and is traveling approximately in the plane of the ecliptic.

F.4 THRUSTER EQUIPMENT

A monopropellant (hydrazine) system is chosen to provide the necessary thrust for (i) Z-axis period control, (ii) midcourse corrections during the Earth-to- L_2 trajectory, and (iii) stationkeeping and attitude control. This system is very simple and reliable, in addition to

Table F.1

WEIGHT, SIZE, AND MOMENTS OF INERTIA

COMPONENT	DESIGNATION FIG. F.1 AND F.2	SIZE (in)	WT/ITEM (lbs)	NUMBER REQUIRED	TOTAL WEIGHT (lbs)	MOMENTS OF INERTIA (slug-ft ²)		
						ROLL	PITCH	YAW
Communication Package	A	12x18x18	55.0	1	55	0.64	0.49	0.49
Travelling Wave Tube Amplifiers	B	6x6x18	6.5	2	13	0.46	3.24	3.40
Guidance and Control	C	6x6x9	20.0	1	20	1.00	2.49	2.50
Moon Sensor Electronics	D	6x6x6	3.0	1	3	0.056	0.37	0.37
Canopus Sensors	E	6x6x9	12.0	2	24	3.83	1.72	1.71
Batteries	F	6x6x6	21.0	4	84	1.79	2.56	2.56
Gyros	G	6x6x9	3.0	3	9	0.25	0.31	0.078
Momentum Wheel Package	H	9x9x9	30.0	1	30	0.087	0.087	0.087
Computer	I	6x6x9	12.0	1	12	0.142	0.149	0.0198
Solar Panel Drive Motors	J	9 dia x 9	2.0	8	16	1.42	1.42	1.15

Table F.1
CONTINUED

COMPONENT	DESIGNATION FIG. F.1 AND F.2	SIZE (in)	WT/ITEM (lbs)	NUMBER REQUIRED	TOTAL WEIGHT (lbs)	MOMENTS OF INERTIA (slug-ft ²)		
						ROLL	PITCH	YAW
Solar Panels	K	60x96	50.0	2	100	176.0* (16.54**)	180.0*	89.7
Hydrazine Fuel Tanks (Loaded)	L	14 dia (sphere)	60.0	4	240	15.9	4.76	4.76
Nitrogen Pressuriza- tion Tanks (Loaded)	M	8 dia (sphere)	5.0	2	10	0.50	0.014	0.71
Midcourse Correction Thruster	N	6 dia x 8 + Nozzle	3.0	1	3	0.0029	0.049	0.049
Antenna and Moon Sensor	O	12 dia (parabolic)	21.0	1	21	8.16 (0.37**)	5.56	5.56
Steerable Feed Drive	P	6x6x6	10.0	1	10	0.013	1.25	1.25
Power Converter	Q	6x6x9	20.0	1	20	1.00	2.49	2.50

Table F.1
CONTINUED

COMPONENT	DESIGNATION FIG. F.1 AND F.2	SIZE (in)	WT/ITEM (lbs)	NUMBER REQUIRED	TOTAL WEIGHT (lbs)	MOMENTS OF INERTIA (slug-ft ²)		
						ROLL	PITCH	YAW
Structures & Thermal			145.0	1	145	18.0	11.0	11.0
Subtotal					815	229.25	217.96	128.06
			11% Growth Factor		90			
Totals					905	229.25 (62.0**)	217.96	128.06

* Panels are in orientation shown in Figure G.1.

** Roll moments of inertia for folded configuration shown in Figure G.3.

Table F.2

CENTER OF MASS DATA OF THE LCS EQUIPMENT

UNFOLDED CONFIGURATION			
COMPONENT	STATION (in)	WT (lb)	TORQUE (in-lb)
Communication	36.0	55	1980.0
TWT	42.0	13	546.0
G&C	42.0	20	840.0
Moon Sensor Electronics	42.0	3	126.0
Canopus Sensors	3.0	24	72.0
Batteries	39.0	36	1405.0
	3.0	48	144.0
Gyros	21.0	6	126.0
	28.5	3	85.5
Momentum Wheels	21.0	30	630.0
Computer	21.0	12	252.0
Solar Panel Drive Motors	4.5	16	72.0
Solar Panels	3.0	100	300.0
Hydrazine Fuel Tanks	21.0	240	5040.0
Nitrogen Pressurization Tanks	5.0	10	50.0
Midcourse Correction Thrusters	3.0	3	9.0
Antenna and Moon Sensors	54.0	21	1134.0
Steerable Feed Drive	42.0	10	420.0
Power Converter	42.0	20	840.0

Table F.2
CONTINUED

COMPONENT	STATION (in)	WT (lb)	TORQUE (in-lb)
Subtotal		670	14071.5
Structures and Thermal		145	3045.0
Total		815	17116.5
Center of mass = $\frac{17116.5 \text{ in-lbs}}{815.0 \text{ lbs}} = 21 \text{ inches from the aft end of the satellite.}$			

FOLDED CONFIGURATION			
COMPONENT	STATION (in)	WT (lb)	TORQUE (in-lb)
Antenna	70.0	21	1470.0
Panels	46.0	100	4600.0
Remaining subsystems from unfolded configuration		694	15682.5
Total		815	21752.5
Center of mass = $\frac{21752.5 \text{ in-lb}}{815.5 \text{ lbs}} = 26.6 \text{ inches from the aft end of the satellite.}$			

Table F.3

CENTER OF PRESSURE DATA OF THE LCS

SECTION	STATION (ft)	AREA (ft ²)	AREA x STATION (ft ² -ft)
1	2.0	8.0	16.0
2	2.75	4.5	9.4
3	3.75	1.5	5.6
Antenna	4.5	6.0	27.0
Solar Panels	0.25	80.0	20.0
Totals		100.0	72.0
Center of pressure = $\frac{72 \text{ ft}^2\text{-ft}}{100.0 \text{ ft}^2} = 0.72 \text{ feet} = 8.65 \text{ inches}$ from the aft end of the satellite.			

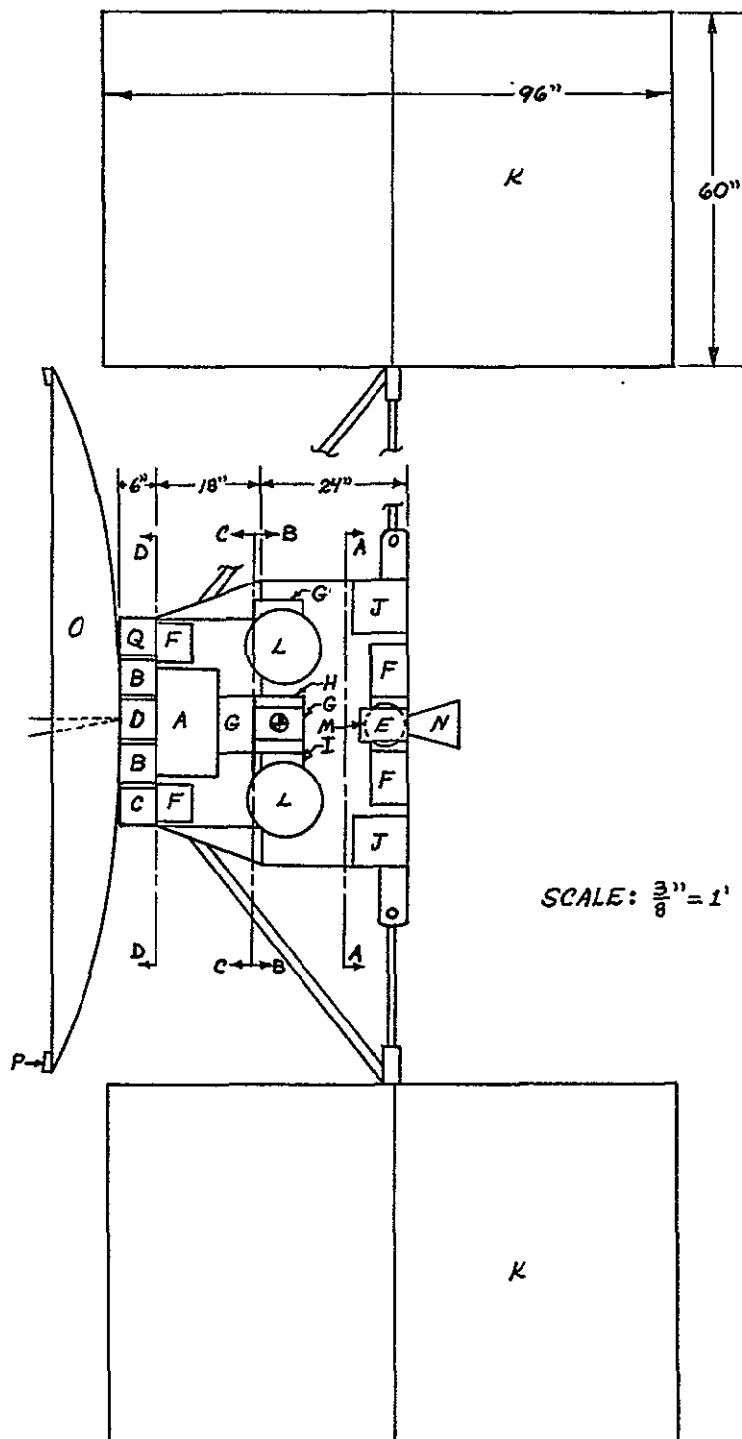


Figure F.1 Equipment Placement

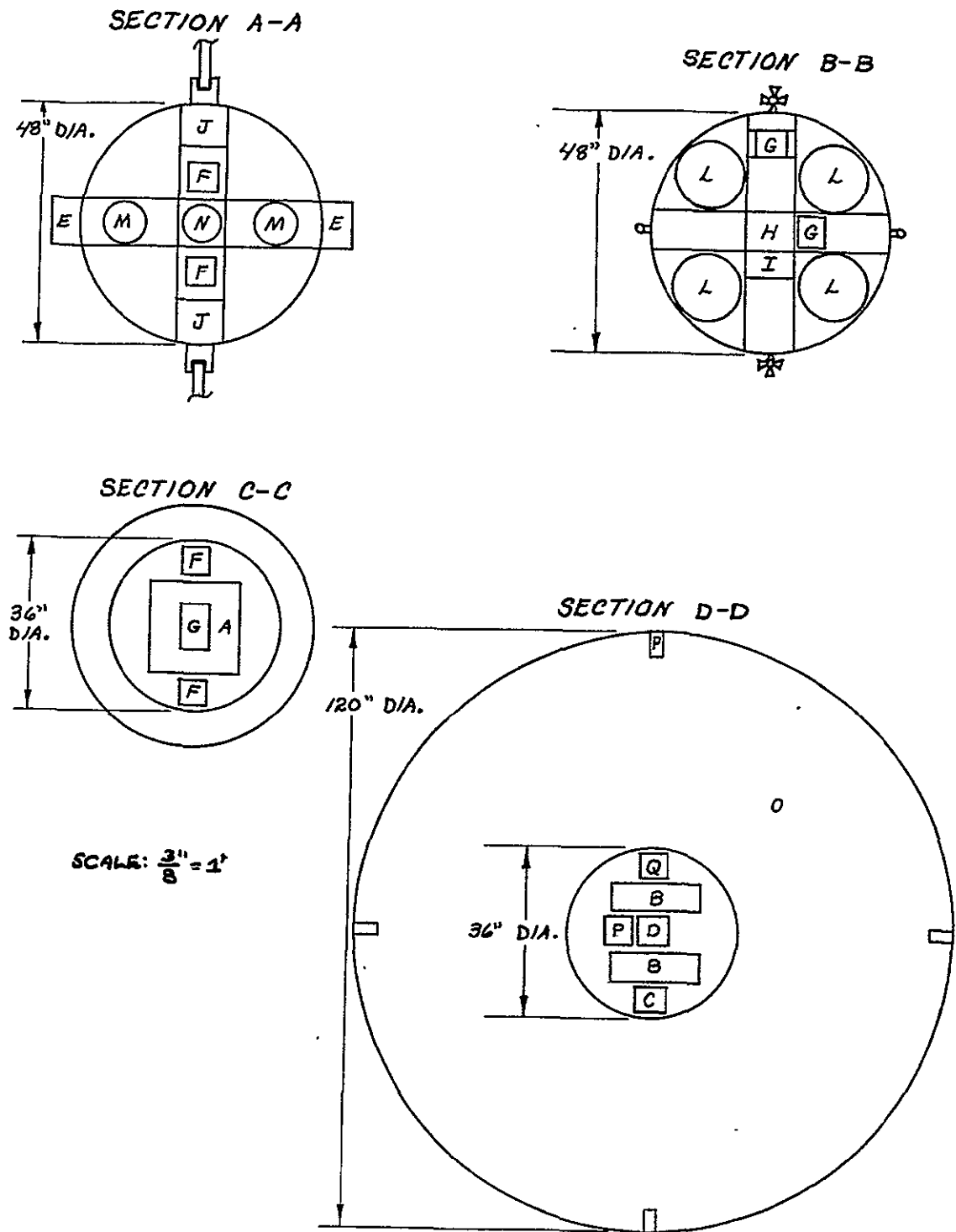


Figure F.2 Equipment Placement

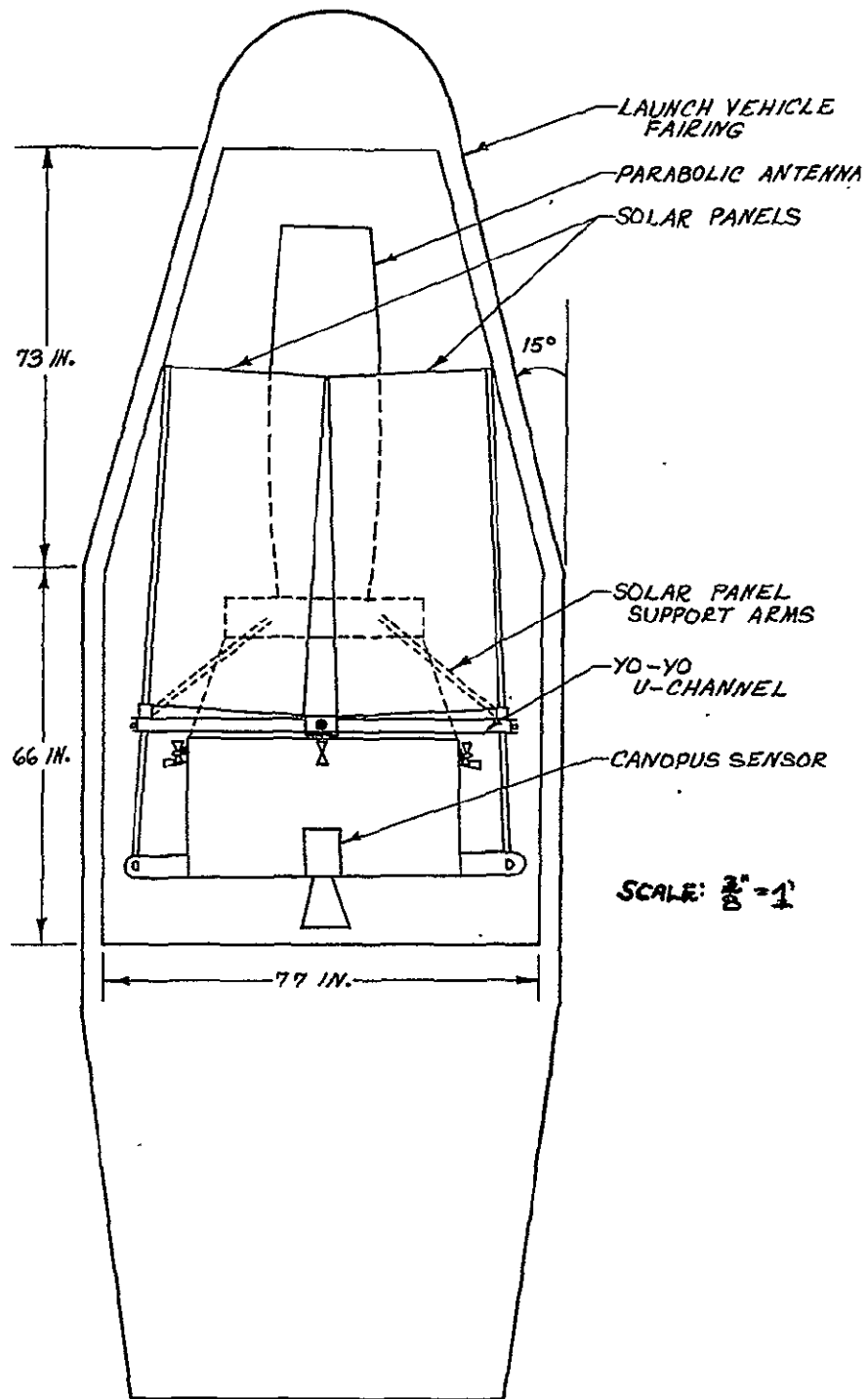


Figure F.3 LCS Inside Fairing of Delta Vehicle

being available in a wide range of thruster sizes.

Figure F.4 is a schematic of the thruster system proposed for the LCS.

Three sizes of thrusters are employed on the LCS: a large thruster for midcourse corrections, perilune, and halo orbit insertion burns; two intermediate size thrusters for Z-axis period control; and twelve smaller thrusters for attitude control and stationkeeping.

To determine the thrust level of the large thruster, one must consider the constraint that the perilune burn is to be performed within a ten minute (600 second) period (Section D.3). Given a 905 pound satellite and a 700 ft/second velocity change, the minimum required thrust is

$$T = \frac{(905 \text{ lb})(700 \text{ ft/sec})}{(600 \text{ sec})(32.2 \text{ ft/sec}^2)}$$
$$= 32.8 \text{ lbs of thrust required}$$

Using a round figure of 35 pounds, the total impulse and fuel weight requirements for this thruster are estimated. For an initial LCS weight of 905 pounds and total midcourse velocity corrections of 70 ft/sec, the required impulse is

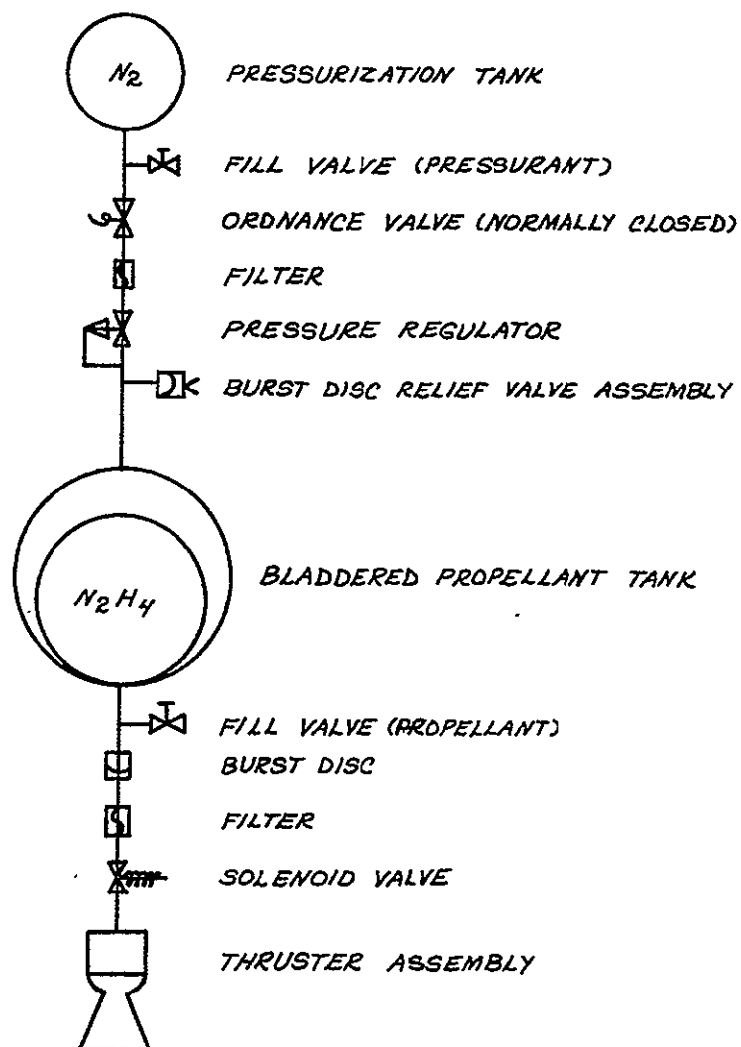


Figure F.4 Hydrazine Thruster System

$$I_T = \frac{(905 \text{ lb})(70 \text{ ft/sec})}{(32.2 \text{ ft/sec}^2)}$$

$$= 1966 \text{ lb-sec required impulse}$$

The time to perform the midcourse correction burns is determined by dividing the impulse by the thrust level.

$$t = \frac{I_T}{T} = \frac{1966 \text{ lb-sec}}{35 \text{ lb}}$$

$$= 57.2 \text{ seconds to perform midcourse correction burns}$$

Since hydrazine has a specific impulse (I_{sp}) of 220 seconds, the fuel flow rate is

$$\dot{w} = \frac{T}{I_{sp}} = \frac{35 \text{ lb}}{220 \text{ sec}}$$

$$= .159 \text{ lb/sec fuel flow rate}$$

and the amount of fuel consumed by these burns is

$$w = (.159 \text{ lb/sec})(57.2 \text{ sec})$$

$$= 9.1 \text{ lbs of fuel consumed}$$

The LCS weighs 895.9 pounds after these burns and the same procedure is followed to estimate the fuel consumed

during the perilune and halo orbit insertion burns. The results of these calculations are summarized in Table F.4.

Table F.4

LCS FUEL CONSUMPTION

BURN	ΔV (ft/sec)	SPECIFIC THRUST IMPULSE (lb-sec)	THRUST LEVEL (lb)	BURN TIME (sec)	FUEL CONSUMED (lb)	LCS WEIGHT*
Midcourse Correction	70	1966	35	57.2	9.1	895.9
Perilune	700	19500	35	557.0	88.5	807.4
Halo Insertion	500	12500	35	358.0	56.9	750.5
Z-axis Control	<u>362</u>	<u>8450</u>	2	338.0**	<u>38.4</u>	722.1
Total	1632	42416			192.9	

*905 pounds initial weight

**Each of 25 burns during the four year lifetime.

Note, that if one-pound thrusters are employed for Z-axis period control, it takes less than six minutes to perform each burn. Therefore, specifying a fuel weight of 215 pounds allows extra fuel for attitude control and the stationkeeping burns. The thrust levels for the twelve small thrusters is approximately .1 pound.

Hydrazine has a density of 63 lb/ft³, so four 14-inch diameter spherical tanks are sufficient for 215 pounds of fuel. Assuming the tanks, plumbing, and valves weigh 25 pounds, the total system weight is 240 pounds.

REFERENCES

1. Schmid, P. E., Lunar Far-Side Communication Satellites, NASA TN D-4509, June, 1968.
2. Godfrey, R. D., Coffman, J. W., and Burr, P. T., Lunar Backside Communications Study, NASA Goddard Space Flight Center Report S-830-69-509, November, 1969.
3. Arndt, G. D., Batson, B. H., and Navosad, S. W., "An Analysis of the Telecommunications Performance of A Lunar Relay Satellite System," International Communications Conference Proceedings, June, 1969, pp. 7-21 to 7-27.
4. Vonbun, F. O., A Hummingbird for the L₂ Lunar Libration Point, NASA TN D-4468, April, 1968.
5. Final Report for Lunar Libration Point Flight Dynamics Study, Contract NAS 5-11551, General Electric Company, Valley Forge Space Center, May-November, 1968.
6. Hood, B. H. and Moorehead, R. W., ed., A Communications Performance Evaluation for the Reference Lunar Landing Mission, NASA Manned Space Flight Center Report EB69-2004 (U), January, 1969.
7. ALSEP Data Management Plan, NASA Goddard Space Flight Center Report X-834-69-209, May, 1969.

8. Hatcher, N. M., A Survey of Sensors for Spacecraft,
NASA SP-145, 1967.
9. Project MISSAC, University of Michigan, Ann Arbor,
Michigan, April, 1968.
10. Farquhar, R. W., "Lunar Communications with Libration-
Point Satellites," Journal of Spacecraft, Vol. 4,
No. 10, pp. 1383-1384, October, 1967.
11. Farquhar, R. W., The Control and Use of Libration-
Point Satellites, Stanford University, No. 350,
July, 1968.
12. Battin, R. H., Astronautical Guidance, New York,
McGraw-Hill Book Co., 1964.
13. Sheehan, J., "Differential Equation Solver Package,"
Raytheon Co., Space and Information Division,
Sudbury, Mass., October, 1966.

BIBLIOGRAPHY

1. Baker, R. H., Astronomy, Princeton, N. J., D. Van Nostrand Co., Inc., 1959.
2. Balakrishnan, A. U., Space Communications, New York, McGraw-Hill Book Co., 1963.
3. Bauer, P., Batteries for Space Power Systems, NASA SP-172, 1968.
4. Bowditch, N., American Practical Navigator, U. S. Navy Hydrographic Office, 1962.
5. Corliss, W. R., Scientific Satellites, NASA SP-133, 1967.
6. "Delta Payload Planners Guide," McDonnell-Douglas Company, Western Division, April, 1969.
7. Duncombe, R. L. and Szebehely, V. G., ed., Methods in Astrodynamics and Celestial Mechanics, Vol. 17, Academic Press, 1966.
8. Farquhar, R. W., "Future Missions for Libration-Point Satellites," Aeronautics and Astronautics, May, 1969, pp. 52-56.
9. Hood, B. H., "Command and Service Module Unified S-Band System," Proceedings of the Apollo Unified S-Band Technical Conference, Goddard Space Flight Center, July 14-15, 1965.

10. Krassner, G. N. and Michaels, J. V., Introduction to Space Communication Systems, New York, McGraw-Hill Book Co., 1964.
11. Kuykendall, W., "Lunar Excursion Module Unified S-Band System," Proceedings of the Apollo Unified S-Band Technical Conference, Goddard Space Flight Center, July 14-15, 1965.
12. Mariner-Mars 1964, Final Project Report, Jet Propulsion Laboratory, NASA Office of Technology Utilization, 1967.
13. Rudaux, L. and DeVaucouleurs, G., Larousse Encyclopedia of Astronomy, Prometheus Press, New York, 1959.
14. Schmid, P. E., The Feasibility of a Direct Relay of Apollo Spacecraft Data Via a Communication Satellite, NASA TN D-4048, August, 1967.
15. Showman, R. D., et al., Simple Processors of Star Tracker Commands for Stabilizing an Inertially Oriented Satellite, NASA TN-D-4490, 1968.
16. Sims, G. D. and Stephenson, I. M., Microwave Tubes and Semiconductor Devices, London, Blackie and Son, 1963.
17. Szebehely, V. G., Theory of Orbits, Academic Press, 1967.

18. The American Ephemeris and Nautical Almanac for the Year 1969, U. S. Naval Observatory, U. S. Government Printing Office, 1967.
19. "TRW Space Data," TRW Systems Group, Redondo Beach, California, 1967.
20. Wrigley, W., Hollister, W.M., and Denhard, W.G., Gyroscopic Theory, Design, and Instrumentation, Cambridge, Massachusetts, MIT Press, 1969.